

AD-A151 749

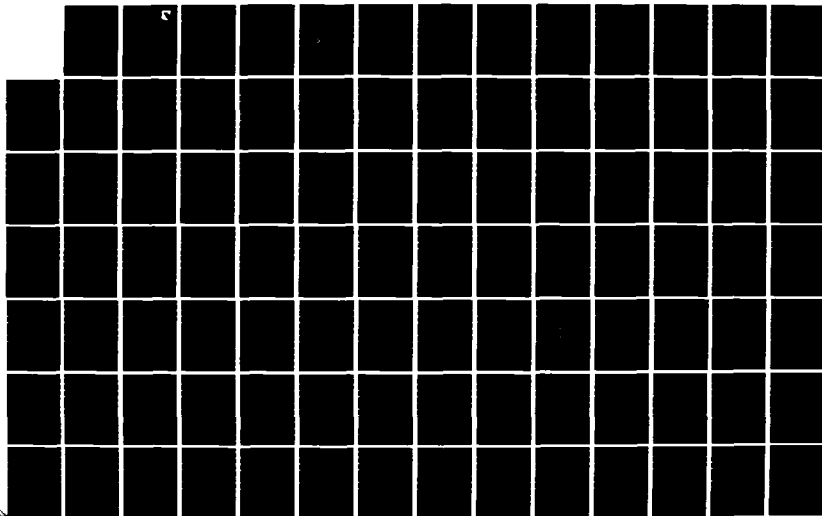
PRELIMINARY DESIGN OF A LIMB RESTRAINT EVALUATOR(U)
SYSTEMS RESEARCH LABS INC DAYTON OH R P WHITE ET AL.
DEC 84 AFAMRL-TR-84-042 F33615-81-C-0500

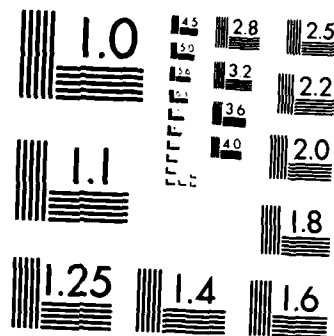
1/2

UNCLASSIFIED

F/G 6/7

NL





MICROCOPY RESOLUTION TEST CHART
NATIONAL BUREAU OF STANDARDS 1963-A

AFAMRL-TR-84-042



PRELIMINARY DESIGN OF A LIMB RESTRAINT EVALUATOR

RICHARD P. WHITE, JR.
THOMAS W. GUSTIN
MICHAEL C. TYLER

SYSTEM RESEARCH LABORATORIES, INC.
2800 Indian Ripple Road
Dayton, Ohio 45440

DECEMBER 1984

DTIC
ELECTE
MAR 27 1985
B

Approved for public release; distribution unlimited.

DTIC FILE COPY

AIR FORCE AEROSPACE MEDICAL RESEARCH LABORATORY
AEROSPACE MEDICAL DIVISION
AIR FORCE SYSTEMS COMMAND
WRIGHT-PATTERSON AIR FORCE BASE, OHIO 45433

85 03 12 105

NOTICES

When US Government drawings, specifications, or other data are used for any purpose other than a definitely related Government procurement operation, the Government thereby incurs no responsibility nor any obligation whatsoever, and the fact that the Government may have formulated, furnished, or in any way supplied the said drawings, specifications, or other data, is not to be regarded by implication or otherwise, as in any manner licensing the holder or any other person or corporation, or conveying any rights or permission to manufacture, use, or sell any patented invention that may in any way be related thereto.

Please do not request copies of this report from Air Force Aerospace Medical Research Laboratory. Additional copies may be purchased from:

National Technical Information Service
5285 Port Royal Road
Springfield, Virginia 22161

Federal Government agencies and their contractors registered with Defense Technical Information Center should direct requests for copies of this report to:

Defense Technical Information Center
Cameron Station
Alexandria, Virginia 22314

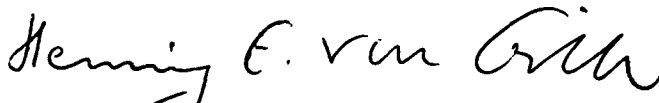
TECHNICAL REVIEW AND APPROVAL

AFAMRL-TR-84-042

This report has been reviewed by the Office of Public Affairs (PA) and is releasable to the National Technical Information Service (NTIS). At NTIS, it will be available to the general public, including foreign nations.

This technical report has been reviewed and is approved for publication.

FOR THE COMMANDER



HENNING E. VON GIERKE, Dr. Ing
Director
Biodynamics and Bioengineering Division
Air Force Aerospace Medical Research Laboratory

UNCLASSIFIED

SECURITY CLASSIFICATION OF THIS PAGE

REPORT DOCUMENTATION PAGE

1a. REPORT SECURITY CLASSIFICATION Unclassified			1b. RESTRICTIVE MARKINGS		
2a. SECURITY CLASSIFICATION AUTHORITY			3. DISTRIBUTION/AVAILABILITY OF REPORT Approved for public release, distribution unlimited.		
2b. DECLASSIFICATION/DOWNGRADING SCHEDULE			5. MONITORING ORGANIZATION REPORT NUMBER(S)		
4. PERFORMING ORGANIZATION REPORT NUMBER(S) AFAMRL-TR-84-042			7a. NAME OF MONITORING ORGANIZATION Aerospace Medical Research Laboratory		
6a. NAME OF PERFORMING ORGANIZATION Systems Research Laboratories, Inc.		6b. OFFICE SYMBOL (If applicable)	7b. ADDRESS (City, State and ZIP Code) AMD, AFSC, Wright-Patterson AFB Ohio 45433		
6c. ADDRESS (City, State and ZIP Code) 2800 Indian Ripple Road Dayton, Ohio 45440		9. PROCUREMENT INSTRUMENT IDENTIFICATION NUMBER F33615-81-C-0500			
8a. NAME OF FUNDING/SPONSORING ORGANIZATION Life Support System Program Office		8b. OFFICE SYMBOL (If applicable) ASD/AES	10. SOURCE OF FUNDING NOS.		
8c. ADDRESS (City, State and ZIP Code) Wright-Patterson Air Force Base, Ohio 45433		PROGRAM ELEMENT NO. 64706F 62202F	PROJECT NO. 412A 7231	TASK NO. A0269 00	WORK UNIT NO. 01
11. TITLE (Include Security Classification) PRELIMINARY DESIGN OF A LIMB RESTRAINT EVALUATOR (U)					
12. PERSONAL AUTHOR(S) Richard P. White, Jr., Thomas W. Gustin, and Michael C. Tyler					
13a. TYPE OF REPORT Final		13b. TIME COVERED FROM _____ TO _____		14. DATE OF REPORT (Yr., Mo., Day) December 1984	
15. PAGE COUNT 128					
16. SUPPLEMENTARY NOTATION					
17. COSATI CODES			18. SUBJECT TERMS (Continue on reverse if necessary and identify by block number)		
FIELD	GROUP	SUB. GR.	Ejection Escape Systems, Test Manikins.		
			Ejection Seat Restraint Systems, Test Instrumentation.		
			Limb Restraint Anthropomorphic Dummies, Ejection Injuries.		
19. ABSTRACT (Continue on reverse if necessary and identify by block number) Limb restraint devices are needed to prevent limb flail injuries during emergency ejection from aircraft at the higher dynamic pressures. Various active limb restraint devices are now being investigated and developed. While human subjects can be used to conduct many of the human factors evaluations of the proposed restraint systems, there is no means of evaluating the effectiveness of the proposed restraint systems during rocket sled or in-flight ejection tests. This report summarizes the results of mechanical and instrumentation design studies conducted to formulate the preliminary design of a system to measure the effectiveness of various limb restraint systems during wind tunnel, rocket sled, or laboratory tests. The system is to be integrated into an anthropometric test dummy designated the Limb Restraint Evaluator (LRE).					
20. DISTRIBUTION/AVAILABILITY OF ABSTRACT UNCLASSIFIED/UNLIMITED <input checked="" type="checkbox"/> SAME AS RPT. <input type="checkbox"/> DTIC USERS <input type="checkbox"/>			21. ABSTRACT SECURITY CLASSIFICATION Unclassified		
22a. NAME OF RESPONSIBLE INDIVIDUAL JAMES W. BRINKLEY			22b. TELEPHONE NUMBER (Include Area Code) (513) 255-3931		22c. OFFICE SYMBOL AFAMRL/BBP

Mechanical design considerations include anthropometry, joint articulation, structural strength, the usability of available commercial components, and sensor selection and placement. The instrumentation will have a total capability of 96 channels of data, including 52 LRE parameters involving limb joint rotation, knee joint loads, forces and moments developed at the neck and forearm, and torso accelerations. The system will also be capable of recording data from up to 26 transducers mounted on the ejection seat. The test data can either be stored on-board the system or telemetered to ground stations.

The major conclusion is that a successful limb restraint evaluator can be designed and constructed, using current state-of-the-art techniques and many existing components from anthropomorphic dummies, to survive the extreme environmental conditions to which it will be exposed, and to accurately evaluate the effectiveness of various limb restraint devices in preventing limb flailing during aircraft ejections.

DTIC
ELECTE
MAR 27 1985

Accession For

NTIS	GPA&I	<input checked="" type="checkbox"/>
ERIC	TR	<input type="checkbox"/>
Other		<input type="checkbox"/>

Submit to

by

to

Library Codes

and/or

Special

A-1

SUMMARY

Ejection systems have been very useful in providing a means for crewmembers to escape from disabled higher performance aircraft. Nevertheless, injuries and fatalities remain a problem when the ejections are initiated at high airspeeds. Many injuries result from the flailing of limbs which occurs when the body is subjected to large forces and moments when encountering the high windblast conditions associated with ejections. While some mechanisms have been used to help prevent or reduce flail injuries, important work related to the development of improved limb restraint devices continues. In conjunction with these development efforts, there is a need for a system to evaluate the effectiveness of limb restraint equipment during tests. This evaluation system must possess certain properties: (1) an accurate simulation of the anthropometric characteristics of human limbs and joint motion so that representative aerodynamic forces and moments can be developed, (2) a high degree of structural strength and durability to withstand these loads at high airspeeds and prevent damage to the system, and (3) a comprehensive data acquisition capability to acquire, process, store, and transmit meaningful test data from a large number and variety of sensors. It is desired that a system with these properties be incorporated into a manikin designated the Limb Restraint Evaluator (LRE). This report presents the results of preliminary design studies related to the development of the LRE.

Results of the preliminary design studies are presented in two sections pertaining to the mechanical and the instrumentation systems, respectively. The mechanical system description contains discussions of general requirements, anthropometry, existing data bases, and a rationale for the estimation of anticipated loads that must be accounted for in the mechanical design. The estimated magnitudes of forces and moments that are expected to occur at various parts of the body are presented for three airspeed conditions: 500, 600, and 700 KEAS. A conceptual mechanical design is presented which includes specialized mechanical extremities, with realistically articulated joints, attached to modified, commercially available torso components; the proposed general locations of instrumentation system elements; the synthesis of specialized new manikin parts and existing vendor supplied parts to form the LRE structure and the types of mechanical articulation

proposed for each joint. The mechanical system description concludes with a discussion of sensor selection and placement considerations in order to obtain the necessary restraint system evaluation data.

The proposed instrumentation system is described in considerable detail. In general, the system will be capable of handling 96 channels of data and processing the data for both on-board storage and transmission to ground receivers via telemetry. Fifty-two parameters of desired LRE data are noted. There are provisions for 26 additional parameters of ejection seat data; thus, 18 channels of data remain available. The instrumentation system description addresses sensor functions, signal conditioning and processing, data storage, and the telemetry capability. Power and memory requirements are noted, and the component selection analyses are discussed. Auxiliary equipment needed to support the LRE instrumentation system is also described. The preliminary design is presented to the level of components, block diagrams and, in some cases, the board level.

The major conclusion produced by the studies was that an effective LRE can be designed and fabricated, using state-of-the-art techniques and some components available in existing anthropometric dummies, that will survive the extreme environmental conditions associated with ejections and acquire pertinent data to evaluate the operational effectiveness of limb restraint equipment. Other conclusions relate to the following specific capabilities:

- Dummy body extremities will approximate the anthropometric properties of large male flying personnel.
- Extremity joints will be articulated and the range of motion will have mechanical limits.
- Fifty-two channels of LRE data will be sensed, processed, stored, and telemetered.
- LRE data measured will include limb joint rotation angles; loads applied to the knee joints; forces and moments developed at the neck by the helmet and head; and forearm and torso accelerations.
- The LRE will be structurally capable of withstanding loads generated by airspeeds up to 700 KEAS.

PREFACE

The investigations described in this report were conducted under Air Force Contract F33615-81-C-0500, Task 82-24, "Limb Restraint Evaluator Conceptual Design Study." The investigations were conducted by Systems Research Laboratories, Inc. (SRL), 2800 Indian Ripple Road, Dayton, Ohio.

Mr. Richard P. White, Jr. was responsible for the mechanical design, and Mr. Michael C. Tyler and Mr. Thomas W. Gustin developed the instrumentation design. Mr. J. Tieber of SRL was program manager of the support contract.

The Air Force Contract Technical Monitor was Mr. R. Rasmussen of the Modeling and Analysis Branch, and the Task Monitors were Captain Michael P. Connors and Mr. James W. Brinkley of the Biomechanical Protection Branch, Biodynamics and Bioengineering Division of the Air Force Aerospace Medical Research Laboratory (AFAMRL).

Funding for the preliminary design of the instrumentation and dummy extremities was provided by the Life Support System Program Office of the Aeronautical Systems Division (ASD/AEL) under Program Element 64706F, Project 412A, Task A0269. The preliminary design of the head/neck balance was funded by the AFAMRL under Program Element 62202F, Project 7231, Task 0001.

GLOSSARY

BAUD	Bits Per Second (for this system)
BIØ-L	Bi-Phase-Level (split phase)
BNE	Branch if Not Equal Instruction
Byte	8 Bits
CCITT	Comite Consultatif International Telephonique et Telegraphique
CMMR	Common-Mode Rejection
CMOS	Complementary Metal Oxide Semiconductors
CMP	Compare Instruction
DAC	Digital-to-Analog Converter
DB##	Test Condition, Decrement and Branch ## Instruction
DC	Direct Current
DF	Drag Force
DIP	Dual In-Line Package
DRAM	Dynamic Random Access Memory
EEPROM	Electrically Erasable Programmable Read-Only Memory
EIA	Electrical Industry Association
EPROM	Erasable Programmable Read-Only Memory
ϵ	Strain
FET	Field Effect Transistors
GARD	Grumman Alderson Research Dummy
GPiA	General Purpose Interface Adaptor
GPiB	General Purpose Interface Bus
HP-IB	Hewlett-Packard Interface Bus

GLOSSARY (continued)

IC	Integrated Circuit
IEEE	Institute of Electrical and Electronic Engineers
I/O	Input/Output
IRIG	Inter-Range Instrumentation Group
KBIT	= 1024 Bits
KBYTES	= 1024 Bytes
KEAS	Knots Equivalent Airspeed
KIAS	Knots Indicated Airspeed
LF	Lift Force
LRE	Limb Restraint Evaluator
LSB	Least Significant Bit
LSI	Large Scale Integrated (circuit)
M_N	Mach Number
MOV	Move Data Instruction
MSI	Medium Scale Integrated (circuit)
MUX	Multiplexer
NHTSA	National Highway Traffic Safety Agency
NRZ-L	Non-Return-to-Zero-Level
PCM	Pulse Code Modulator
PLA	Programmable Logic Array
PM	Pitch Moment
POT	Potentiometer
PROM	Programmable Read Only Memory
POT	Potentiometer

GLOSSARY (continued)

q	Dynamic Pressure (due to airstream velocity)
RAM	Random Access Memory
RFQ	Request For Quotation
RM	Roll Moment
SF	Side Force
SRAM	Static Random Access Memory
SSI	Small Scale Integrated (circuit)
TTL	Transistor-Transistor Logic
UART	Universal Asynchronous Receiver Transmitter
VLSI	Very Large Scale Integrated (circuit)
YM	Yaw Moment

TABLE OF CONTENTS

<u>Section</u>	<u>Page</u>
1 INTRODUCTION	12
2 TECHNICAL DISCUSSION	15
MECHANICAL SYSTEM	15
Background	15
Escape System Technology Overview	15
Anthropomorphic Dummy Status	17
Escape System Loads	18
LRE Design Considerations	21
Human Body Simulation Parameters	21
Performance Parameters Measurement	27
Estimated Loads	
Conceptual Mechanical Design	40
Limb and Joint Design	42
Application of Existing Components	47
Head/Neck Balance System	53
LRE Load Measurement System	58
Data Acquisition System	61
INSTRUMENTATION	63
System Description	63
Data Sensing	68
Data Capture	73
Supporting Investigations	83
Data Capture	83
Filtering	85
Memory Errors	93
System Conceptual Design	94
Data Sensing	94
Data Capture	104
LRE Power Supply	117
Auxiliary Equipment	118

TABLE OF CONTENTS (continued)

<u>Section</u>		<u>Page</u>
3	CONCLUSIONS	123
	REFERENCES	125

Reference Publication 1024 (1978) was utilized as a guideline for the duplication of human body dimensional characteristics. Early in the investigation it was decided that the 95th percentile of USAF male flying personnel was the approximate size that should be considered in conceptual design studies. In addition to the guidance gained from data in NASA Reference Publication 1024 (1978), dimensional data regressed from the 95th, 97th, and 99th percentile personnel for knee height, sitting, biacromial breadth, sitting height, and head breadth were also considered in the design study to estimate fabrication cost. Table 1 presents the data developed by Dr. K. W. Kennedy, Air Force Aerospace Medical Research Laboratory, using the regression analysis. Also presented in the table, for the dimensions that could be compared, are the dimensions of a commercially available (comm) 95th percentile anthropomorphic dummy, as well as the percent that these dimensions varied from the 99th percentile person.

Weight, Inertia, Center of Gravity Characteristics. The duplication of weight, inertia, and center of gravity (CG) characteristics of the body components is necessary if the dynamic response of various body segments to the accelerations and aerodynamic forces developed during ejection is to be properly duplicated.

McConville and Churchill (1980) and Clauser, McConville, and Young (1969) were used to obtain guidelines for the mass characteristics of the human body. Again, the 95th percentile human was used as the reference body size. In addition to the data in McConville and Churchill (1980) and Clauser, McConville, and Young (1969), the data presented in Table 2 were also utilized. The data presented in Table 2 were developed using the same type of regression analyses used for Table 1.

in these reports had little direct application to the LRE design studies since the pilot was in a fixed stowed position for ejection. However, the measured variation of the forces with Mach number and position relative to the cockpit was very useful in determining the time variation of loads during ejection as a function of Mach number.

Although the results of the various investigations were not directly applicable to the conceptual design of the LRE, they did provide background information on the effects of various aerodynamics and mechanical parameters of importance during ejection from high-speed aircraft.

LRE Design Considerations

As previously discussed, the pilot is subjected to accelerations and time-varying aerodynamic flow fields during ejection, resulting in forces which may cause violent motions of the body and limbs. While the normal seat harness limits body motion, the limbs are generally not restrained and flailing can occur. In order to use the LRE to evaluate the effectiveness of various limb restraint devices in preventing limb flail, the dynamic response characteristics of the human limbs and the degree to which they are affected by the dynamic motions of the body must be duplicated. The proper duplication of these dynamic motions requires realistic simulation of the mass, inertia, and dimensional characteristics of the human body, as well as an accurate simulation of the rotational characteristics of limb joints. The investigations conducted to establish requirements for the various component simulations will be presented in the following paragraphs.

Human Body Simulation Parameters

- Dimensional Characteristics

A realistic simulation of human dimensional characteristics, both linear and cross-sectional, is very important to the generation of accurate aerodynamic forces. If these characteristics are not properly duplicated for each body segment, the aerodynamic forces and moments developed by the various body segments would not be representative of the real-life environment. NASA

strain gauge beams which measured the side and rearward force generated by the hand gripping the D ring. The results of the tests reported in this reference indicated that the leg and arm dislodgement forces were strongly affected by the pitch and yaw angle of the seat with respect to the air-stream. While the data quantified to some degree the effect of seat pitch and yaw on limb dislodgement forces, the measurements were again for limbs in the "stowed" position for ejection and, thus, provided no insight as to the loads that might be developed at maximum joint extension during flail.

In addition to the above noted measurements, the pressure distributions as well as the forces and moments developed by a standard Air Force helmet were measured over a range of pitch and yaw angles. The data for the helmet were obtained for the basic helmet and also the helmet with various devices to reduce the loads. The results of the investigation were useful for the LRE conceptual design studies in that they quantified the variation of the forces and moments with pitch and yaw angle.

The test results in Payne, Inc. (1975c), extended the range of pitch and yaw angles of the test results reported in Payne, Inc. (1975b), on limb dislodgement forces during ejection. Payne, Inc. (1976), reported tests conducted to measure the lift forces developed by the hand and leg when in the "stowed" position for ejection. The data were obtained with the same ACES II seat utilized in Payne, Inc. (1975b), and Payne, Inc. (1975c). However, the D ring instrumentation was modified to measure the lift forces instead of the drag and side forces. Again, since all data represented limb dislodgement forces with the limbs in the stowed position for ejection, the data could not be used in the LRE conceptual design studies because this position would not reflect the worst-case loading conditions.

Newhouse, Payne, and Brown (1980) and Payne, Inc. (1980), reported a test program to measure the limb dislodgement forces over a Mach number range of 0.4 to 1.2 and determine the effect of the aircraft/pilot-seat aerodynamic interactions on these forces. The measurements were made on a highly instrumented one-half scale model of a 50th percentile pilot sitting in a scaled ACES II seat. Data were obtained for various seat/pilot ejection positions with respect to a simulated F-16 nose section. The data presented

pilot/seat combination at various locations with respect to a simulated F-16 cockpit. A brief review of the data from the above-noted documents will be presented to indicate the data base available for use in accomplishing the LRE conceptual design.

Payne (1974b) presented measurements obtained during a wind tunnel test to explore the magnitude of the knee separation forces as well as the forces developed at the D ring due to airloads on the arms. Load measurements obtained at speeds up to 160 feet/second were used to evaluate the effects of seat modifications and D ring location on the forces developed at the knee and by the arm. In support of a tractor rocket egress system for pilots, data were also obtained on human subjects with a minimum amount of clothing, loose fitting flight suits, and tight fitting clothing to determine the effect of clothing on the forces developed by the body. While the data obtained were not directly applicable for use in the conceptual design of the LRE, the report documented a 24 percent increase in the force coefficient due to clothing, which was useful in estimating a suitable drag coefficient for use in the design study.

Payne, Inc. (1975a), reported an effort conducted to collect and correlate all available data on the aerodynamic forces acting on the human body. It was noted that the data available were very sparse and generally not in a useful form. The majority of the data presented were obtained in the 1950 time period and reported in Schmitt (1954). That basic data set was compared with limited data obtained with anthropomorphic dummies in wind tunnels and during free falls. While the data were not directly useful in the LRE conceptual design studies, they did provide some additional information on the effects of clothing on the forces developed by the human body.

Payne, Inc. (1975b), summarized the results that were obtained in a low-speed wind tunnel to evaluate the effect of seat yaw and pitch angle on the forces tending to separate the pilot's legs and break the pilot's grip when he assumed the limbs are in the "stowed" position for ejection. The leg separation forces were measured by strain gauge beams calibrated to measure the rearward and outward force at the foot as well as the outward force at the knee. The loads developed by the arms were also determined by means of

While the load-carrying capabilities of available components are not known, it is believed that the upper thorax, pelvis, head, feet, hands, and flesh coverings for a 95th percentile dummy could be utilized effectively to construct the LRE.

In addition to the investigations conducted to evaluate the availability of commercial components, pertinent investigations conducted to improve the dynamic response characteristics of anthropomorphic dummies were also reviewed. Notable among the efforts reviewed was a research program conducted for the Air Force Aerospace Medical Research Laboratory (AFAMRL) in 1971 to develop a dynamic simulation of a human for use in testing aircraft escape-systems (Payne and Band, 1971). While this effort produced an anthropomorphic dummy (Dynamic Dan) that simulated the dynamic characteristics of the spine, neck, internal organs, and major extremity joints, it did not contain provisions for limb motion measurement or space for instrumentation electronics.

On the basis of the review, it was concluded that while some commercially available body parts could be used in the LRE, suitable limbs would have to be designed and constructed to provide integral instrumentation and adequate dynamic representation of the limbs for flail investigations.

Escape System Loads

As previously noted, research to support the development of effective limb restraint systems has increased significantly in the last decade. The research area associated with determining the aerodynamic loads that can be developed at various components of the human body has received considerable attention. While some investigations have been conducted with human subjects in low speed wind tunnels, additional testing has been accomplished at higher speeds with anthropomorphic dummies and with instrumented scale models of the human body seated in an ejection seat. Payne (1974b); Payne, Inc. (1975a,b,c, 1976, 1980); Schmitt (1954); and Newhouse, Payne, and Brown (1980) summarized investigations conducted at low speeds with human subjects while Newhouse, Payne, and Brown (1980) and Payne, Inc. (1980), presented data obtained in a transonic wind tunnel with a one-half scale model of a

Anthropomorphic Dummy Status

The use of anthropomorphic dummies for escape system testing by the U.S. Military services began in the 1940s; but due to limited knowledge of human kinematic and dynamic response, the first generation of dummies was extremely crude. With the development of aircraft ejection seats with rocket catapults, a more sophisticated dummy was developed for testing the stability of man-seat combination ejections. An example of a dummy developed for this type of testing is the Grumman Alderson Research Dummy (GARD). The GARD dummy, still in limited production, is designed to duplicate the center of gravity location and moment of inertia of the seated male. While the GARD dummy is designed to contain instrumentation to measure and telemeter many parameters of ejection seat performance and man/seat interface loadings, it was not designed to measure parameters critical to the evaluation of limb flail protection equipment.

Passage of the Highway Safety Act in the middle 1950s provided the impetus for the development of anthropomorphic dummies having more representative body biodynamic characteristics. On the basis of this Act, it was decided that dummies developed to test compliance with the Federal Motor Vehicle Safety Standard 208 must be realistic and have repeatable measuring instruments. A dummy was developed to meet these objectives, and a set of specifications was developed to ensure compliance with the testing standards. To meet those specifications, General Motors developed the GM Hybrid II dummy, which was designated by the NHTSA as the Part 572 Dummy. Although General Motors has improved the dynamic response of the Part 572 Dummy in their Hybrid III dummy, it still does not provide the biofidelity required for dynamic limb response testing. Because of the requirement that all automotive companies and component manufacturers must meet the NHTSA safety standards, a number of companies started to manufacture test dummies to the Part 572 specification.

Notable among these organizations are Humanoid Systems of Carson, California, and Alderson Research Laboratories of Stamford, Connecticut. Components of existing dummies obtained from these companies will be utilized for the LRE.

3. Crew requirements for mobility, restraint, external vision, physiological stress control, comfort, and appearance.

When consideration is given to developing a universal system for different aircraft as well, the ability to satisfy the previously noted constraints becomes much more difficult.

Although advanced restraint systems are not as yet universally incorporated, a concentrated effort is being undertaken to develop effective limb restraint devices to prevent limb flail injury during ejection at high flight speeds. Preliminary investigations of various limb restraint devices that are compatible with the F-15 and F-16 aircraft are summarized in Cummings and Dasata (1979). Rockwell International (1980) presents an evaluation of six different limb restraint devices which have shown promise: (1) arm straps, (2) deployable sleeves, (3) leg straps, (4) G-suit restraints, (5) arm length sleeves dooned at ingress, and (6) net-epaulet arm restraints.

On the basis of the studies and evaluations conducted during these investigations, the best devices appear to be the net-epaulet restraints and the G-suit modification. The net-epaulet concept involves a passive lateral restraint net developed by an active retracting strap loop which breaks out of an epaulet-like keeper on the shoulder and contracts down over the forearm and thigh.

The G-suit modification involves load spreading devices sewn to the backside of the thigh and calf sections of the garment. During ingress, a retraction strap is attached to these devices so that after strap retraction, the legs will be held within the upper and lower leg guards.

The development effort of these candidate systems or their modifications is continuing, and air worthiness verifications of the systems must be undertaken in the future to evaluate their effectiveness in an operational environment. The conceptual design of the LRE presented in this report was undertaken as an initial step to provide a means by which the effectiveness of restraint systems can be realistically evaluated.

Section 2

TECHNICAL DISCUSSION

MECHANICAL SYSTEM

Background

Escape System Technology Overview

The problem of windblast induced injuries and fatalities during high speed seat ejection has been recognized for more than two decades. Statistical studies of injuries that occurred during noncombat ejection from U.S. Air Force, U.S. Navy, and RAF aircraft from 1964 to 1970 (Payne and Hawker, 1974) indicated that the probability of limb flail injuries increased very rapidly above 400 KIAS. For example, at 400 KIAS the probability of flail injury was only 20 percent, and the probability had risen to approximately 50 percent at 500 KIAS and to greater than 85 percent at 600 KIAS. As the operational speed of aircraft increased over the past 20 years and, thus, the probability of flail injury, research and development to provide a means of projecting the pilot from flail injuries during ejection also increased. The investigations followed a number of different approaches which included: (1) theoretical analyses and wind tunnel tests to determine the aerodynamic forces applied to the human body during ejection (Payne, 1974a, 1974b; Payne, Inc., 1975b; Hawker and Fuller, 1975, 1976; Schneck, 1978), (2) anatomical studies of injuries and potential injuries during ejection, and (3) a number of design programs related to escape systems and windblast protection device studies (Phillips et al., 1973; Stencil Aero Engineering Corp., 1979; Cummings and Dasata, 1979). Despite these numerous investigations, equipment to provide limb flail protection is not, as yet, widely implemented. It is not difficult to understand the problem of developing an universal solution to windblast injury when one considers the various interacting design considerations which must be addressed:

1. The escape environment.
2. The structural functional characteristics of the escape system.

The purpose of the effort documented in this report was to conduct a preliminary design study that would yield an LRE design to satisfy the above noted requirements. The study involved two major areas of investigation as discussed in the body of this report. These were preliminary designs of the LRE structure and mechanical system, and the instrumentation and data acquisition system. The study involved, in both cases, a review of available data; analysis of performance requirements; investigation of available products, components, or capabilities; evaluation of trade-off factors; and judgmental decisions to identify optimal design approaches.

Potential risk areas were also considered in assessing the overall feasibility of designing and fabricating suitable LRE devices.

concern that limb flail injuries will occur at higher speeds. Approaches to the resolution of this potential problem are being addressed through the Active Limb Restraint Program which is an ongoing activity of the Life Support System Program Office (SPO) of the Aeronautical Systems Division.

In conjunction with the development of potential limb restraint devices, a means to evaluate these systems must also be developed. Human subjects can be used to evaluate such factors as crewmember mobility, external vision, comfort, donning, egress procedures, and even the limb capture characteristics of new equipment. However, a valid evaluation must go beyond these measures and incorporate a means for the objective assessment of equipment performance in a windblast environment as realistically similar to that of an actual ejection as possible. This environment can be investigated to varying degrees either in a high speed wind tunnel or during blast tests. More realistic evaluations involve test ejections of seats with limb restraint equipment from high speed rocket propelled sleds or flight test aircraft.

In order to accomplish these objective evaluations of limb restraint equipment in a realistic environment, an evaluation system is needed. This device must possess the characteristics of the human body to the degree that the ejecting crewmember is adequately simulated for the evaluation, and it must also incorporate a means of quantitatively measuring specific evaluation parameters. To properly simulate the human body, a Limb Restraint Evaluator (LRE) must reflect the dimensions, mass, and dynamic response characteristics of crewmember limbs. In order to obtain the data needed to evaluate the comparative effectiveness of various restraint systems, instrumentation must be provided to measure the motion of the body and limbs as well as the loads applied to critical areas of the body. The information sensed must also be processed for internal storage and/or transmission to an external receiver. Finally, sufficient data channel capacity must be provided in order to accommodate changes or growth in data requirements as development efforts proceed.

Section 1

INTRODUCTION

As the performance of combat aircraft increased during the World War II era, escape from disabled aircraft became increasingly more difficult and likely to cause crewmember injury. Since that period, development and implementation of ejection seat systems has resulted in a significant reduction in the amount of injuries and fatalities that might otherwise have occurred during operations involving higher performance aircraft. Nevertheless, injuries and fatalities during ejections continue to be a problem, especially when ejections occur at the high speeds associated with modern aircraft operations. The high speeds introduce extreme windblast forces during ejection, which can cause injuries as a result of limb flailing, the largely uncontrollable motion of limbs in high velocity, turbulent airflow conditions. Limb flailing is caused by large aerodynamic forces and moments acting on limb segments of the ejecting crewmember encountering the windblast environment. The injuries due to limb flailing can be generally attributed to two factors: injury to extremity joints which occurs when the limits of joint motion are attained and excessive force is applied, and injury caused by unrestrained impact of limb segments with the seat structure.

It is reasonable to consider the feasibility of using protective equipment to reduce the frequency and severity of injuries of this nature. Until recently, few U.S. Air Force aircraft were equipped with windblast protection devices. However, among aircraft currently operating there are two exceptions, the F-4 and SR-71 aircraft which are fitted with leg restraints. These devices are categorized as "active" restraint equipment since crewmember actions are required to don them. The "passive" approach is generally desirable in that crewmember actions are not required. The leg side panels, which are part of the ACES II ejection system found in the A-10, F-15, and F-16 aircraft, are examples of this approach. Proper restraint operation of this equipment does, however, depend on effective seat directional stability.

While current operational experience at ejection speeds up to about 450 knots has demonstrated the effectiveness of the ACES II system, there is

LIST OF TABLES

<u>Table</u>		<u>Page</u>
1	LIMB RESTRAINT EVALUATION DEVICE: ANTHROPOMORPHIC DESIGN CRITERIA	23
2	WEIGHT, VOLUME, AND CENTER OF MASS OF BODY SEGMENTS	25
3	MAXIMUM ESTIMATED LIMB FORCES IN RESTRAINED POSITION (PITCH = 0 DEGREES, YAW = 0 DEGREES)	32
4	MAXIMUM ESTIMATED HELMET FORCES AND MOMENTS	40
5	LRE MEASUREMENT SYSTEM	64
6	PULSE CODE MODULATION SYSTEMS, GENERAL SPECIFICATIONS	103
7	POWER REQUIREMENTS	117
8	MAJOR COMPONENTS OF POWER UNIT	122

LIST OF ILLUSTRATIONS (continued)

<u>Figure</u>		<u>Page</u>
25	On-Board Computer System Block Diagram	78
26	Typical LRE Internal Power System	81
27	Aliasing Error versus Sample Rate	87
28	Percent Error versus Frequency	90
29	Four-Point Interpolation Example	92
30	Temperature Measurement Circuit	97
31	Typical Potentiometer Signal Conditioning	99
32	Typical Bilevel-to-Analog	100
33	Typical Low-Level Signal Conditioning Circuit	101
34	Typical LRE Computer System Processor Board Block Diagram	107
35	DRAM Controller Board	109
36	DRAM Array Board	111
37	PCM Decoder, Serial-to-Parallel Converter	113
38	PCM Decoder, Status Registers	114
39	Typical Communications Board	116
40	Schematic of Power Unit	121

LIST OF ILLUSTRATIONS

<u>Figure</u>		<u>Page</u>
1	Effect of Reaction Points on Bending Moment Distribution	29
2	Maximum Joint Loads: (a) 500 KEAS, (b) 600 KEAS, (c) 700 KEAS	35
3	LRE Conceptual Design Assembly	41
4	LRE Internal Structure	43
5	Modular Joint Design	44
6	Details of Joint Design	46
7	Limits of Joint Rotation	48
8	Body Internal Structure	49
9	Flesh Covering	52
10	Breakaway Hand Concept	54
11	Six-Component Head/Neck Balance	56
12	Coupled Balance Matrix	57
13	Uncoupled Balance Matrix	59
14	Instrumentation for Load Measurement	60
15	Load Measurement System for Knee	62
16	Instrumentation Placement	65
17	Block Diagram of LRE and Support Electronic Systems	67
18	Typical High-Level "Potentiometer Sensor	69
19	Typical High-Level "Bilevel" Sensor	69
20	Typical Low-Level "Bridge" Circuit	71
21	Typical Pulse Code Modulation System	72
22	Typical Skull Antenna (for 790 MHz to 847 MHz Range)	74
23	Typical Telemetry System (Record and Playback)	76
24	Typical NRZ-L and BIØ-L Waveforms	77

TABLE 1. LIMB RESTRAINT EVALUATION DEVICE: ANTHROPOMORPHIC DESIGN
CRITERIA (Regressed from 95th, 97th, and 99th Percentile)

	95% Comm	95%*	97%*	99%*	Maximum % Difference 95% Comm/99%
<u>Knee Height, Sitting</u>	<u>23.3</u>	<u>23.6</u>	<u>23.9</u>	<u>24.4 in.</u>	<u>4.7</u>
	Subsample				
	Comm 95%	\bar{X} 95%	\bar{X} 97%	\bar{X} 99%	
Weight	200.8	193.1	196.1	202.4	0.8
Height	73.1	73.1	74.1	75.1	2.7
Cervicale Height	--	63.3	63.9	64.9	--
Acromiale Height	--	60.5	61.1	62.1	--
Suprasternale Height	--	60.4	61.0	62.0	--
Nipple Height	--	53.9	54.5	55.3	--
Waist Height	--	44.7	45.2	46.1	--
Iliocristale Height	--	45.9	46.5	47.3	--
Trochanterion Height	--	39.6	40.1	40.9	--
Patella Height (Top)	--	22.3	22.6	23.1	--
Knee Circ. Height	--	21.1	21.4	21.8	--
Calf Height	--	15.2	15.4	15.8	--
Ankle Height	--	5.8	5.8	5.9	--
Popliteal Height, S.	18.5	18.5	18.8	19.2	3.8
Buttock Knee, L.	25.5	25.2	25.4	25.8	1.2
Buttock Popliteal, L.	--	21.0	21.3	21.6	--
Shoulder Elbow, L.	15.7	15.0	15.2	15.4	2.0
Acromion Radiale	--	13.8	13.9	14.2	--
Elbow Wrist, L.	--	12.5	12.7	12.9	--
Radiale Stylion	--	11.3	11.4	11.6	--
Elbow-Grip, L.	--	14.7	14.8	15.1	--
Thumb Tip Reach	--	33.4	33.8	34.3	--
Waist Breadth	--	12.7	12.9	13.0	--
Bicristale Breadth	--	11.5	11.6	11.7	--
Hip Breadth	--	14.4	14.5	14.7	--
Hip Breadth, S.	16.2	15.5	15.6	15.8	2.5
Knee Circ.	--	15.9	16.0	16.2	--
Knee Circ., S.	--	16.2	16.3	16.5	--
Ankle Circ.	--	9.1	9.2	9.2	--
Scye Circ.	--	19.7	19.9	20.1	--
Wrist Circ.	--	7.1	7.2	7.2	--

TABLE 1. LIMB RESTRAINT EVALUATION DEVICE: ANTHROPOMORPHIC DESIGN
CRITERIA (Regressed from 95th, 97th, and 99th Percentile)
(continued)

	95% Comm	95%*	97%*	99%*	Maximum % Difference 95% Comm/99%
<u>Biacromial Breadth</u>	<u>--</u>	<u>17.2</u>	<u>17.5</u>	<u>17.8 in.</u>	<u>--</u>
	Subsample				
	Comm 95%	\bar{X} 95%	\bar{X} 97%	\bar{X} 99%	
Bideloid Breadth	19.4	20.0	20.2	20.6	6.2
Chest Breadth	13.8	13.5	13.6	13.8	0.0
Neck Circ., Max.	--	15.5	15.6	15.7	--
Shoulder Circ.	--	48.4	48.7	49.3	--
Chest Circ., Scye	43.7	42.0	42.4	42.9	1.9
Chest Circ.	--	40.4	40.7	41.2	--
Buttock Circ.	--	40.0	40.3	40.6	--
Buttock Circ., S.	47.5	43.7	44.0	44.4	7.0
Upper Thigh Circ.	--	24.0	24.2	24.4	--
Upper Thigh Circ., S.	--	23.6	23.8	24.0	--
Calf Circ.	--	15.1	15.2	15.4	--
Biceps Circ., Ext.	--	12.6	12.7	12.8	--
Elbow Circ., Ext.	--	11.2	11.3	11.4	--
Forearm Circ.	--	11.4	11.5	11.6	--
<u>Sitting Height</u>	<u>38.0</u>	<u>33.8</u>	<u>34.0</u>	<u>34.5 in.</u>	<u>10.0</u>
	Subsample				
	Comm 95%	\bar{X} 95%	\bar{X} 97%	\bar{X} 99%	
Eye Height, S.	--	33.8	34.0	34.5	--
Mid-Shoulder Height, S.	27.6	27.0	27.3	27.6	0.0
Acromiale Height, S.	--	25.6	25.8	26.2	--
<u>Head Breadth</u>	<u>6.1</u>	<u>6.5</u>	<u>6.6</u>	<u>6.7 in.</u>	<u>9.8</u>
	Subsample				
	Comm 95%	\bar{X} 95%	\bar{X} 97%	\bar{X} 99%	
Head Circumference	23.4	23.1	23.2	23.3	0.1
Bigonial Breadth	--	4.8	4.8	4.8	--

*Population percentile values.

TABLE 2. WEIGHT, VOLUME, AND CENTER OF MASS OF BODY SEGMENTS

<u>Head and Trunk</u>			
Weight	95th% Test Device	= 49.45 kg	(109.0 lbs)
	97th%	= 50.41 kg	(111.2 lbs)
	99th%	= 52.09 kg	(114.9 lbs)
Volume	95th% Test Device	= 45.80 l	(2795 cu.in.)
	97th%	= 46.75 l	(2853 cu.in.)
	99th%	= 48.16 l	(2939 cu.in.)
CM from Top of Head	95th% Test Device	= 48.4 cm	(19.0 in.)
	97th%	= 48.5 cm	(19.1 in.)
	99th%	= 48.6 cm	(19.1 in.)
<u>Head</u>			
Weight	95th% Test Device	= 5.016 kg	(11.06 lbs)
	97th%	= 5.063 kg	(11.16 lbs)
	99th%	= 5.156 kg	(11.37 lbs)
Volume	95th% Test Device	= 4.807 l	(293.3 cu.in.)
	97th%	= 4.858 l	(296.5 cu.in.)
	99th%	= 4.948 l	(301.9 cu.in.)
CM from Top of Head	95th% Test Device	= 12.0 cm	(4.7 in.)
	97th%	= 12.0 cm	(4.7 in.)
	99th%	= 12.2 cm	(4.8 in.)
CM from Back of Head	95th% Test Device	= 8.0 cm	(3.1 in.)
	97th%	= 7.9 cm	(3.1 in.)
	99th%	= 7.9 cm	(3.1 in.)
<u>Thigh</u>			
Weight	95th% Test Device	= 9.822 kg	(21.66 lbs)
	97th%	= 10.00 kg	(22.05 lbs)
	99th%	= 10.13 kg	(22.34 lbs)
Volume	95th% Test Device	= 9.578 kg	(584.5 cu.in.)
	97th%	= 9.762 kg	(595.7 cu.in.)
	99th%	= 10.06 kg	(613.6 cu.in.)
CM from Trochanterion	95th% Test Device	= 10.2 cm	(7.5 in.)
	97th%	= 19.5 cm	(7.7 in.)
	99th%	= 20.0 cm	(7.9 in.)
CM from Anterior Aspect (0.595 x AP at CM level) - 0.956 = cm			

TABLE 2. WEIGHT, VOLUME, AND CENTER OF MASS OF BODY SEGMENTS
(continued)

<u>Leg and Foot</u>			
Weight	95th% Test Device	=	5.150 kg (11.36 lbs)
	97th%	=	5.240 kg (11.55 lbs)
	99th%	=	5.392 kg (11.89 lbs)
Volume	95th% Test Device	=	4.833 l (294.9 cu.in.)
	97th%	=	4.935 l (301.1 cu.in.)
	99th%	=	5.072 l (309.5 cu.in.)
CM from Tibiale	95th% Test Device	=	22.0 cm (8.7 in.)
	97th%	=	22.3 cm (8.8 in.)
	99th%	=	22.6 cm (8.9 in.)
CM from Anterior Aspect (0.539 x AP at CM Level) - 1.731 = cm			
<u>Arm</u>			
Weight	95th% Test Device	=	2.298 kg (5.077 lbs)
	97th%	=	2.356 kg (5.196 lbs)
	99th%	=	2.436 kg (5.372 lbs)
Volume	95th% Test Device	=	2.294 l (140.0 cu.in.)
	97th%	=	2.355 l (143.7 cu.in.)
	99th%	=	2.443 l (149.1 cu.in.)
CM from Acromiale	95th% Test Device	=	16.77 cm (6.6 in.)
	97th%	=	17.11 cm (6.7 in.)
	99th%	=	17.16 cm (6.8 in.)
CM from Anterior Aspect (0.444 x AP CM Level) + 0.665 = cm			
<u>Forearm and Hand</u>			
Weight	95th% Test Device	=	1.809 kg (3.989 lbs)
	97th%	=	1.839 kg (4.055 lbs)
	99th%	=	1.907 kg (4.204 lbs)
Volume	95th% Test Device	=	1.669 l (101.9 cu.in.)
	97th%	=	1.700 l (103.8 cu.in.)
	99th%	=	1.756 l (107.2 cu.in.)
CM from Radiale	95th% Test Device	=	17.66 cm (6.95 in.)
	97th%	=	17.77 cm (7.00 in.)
	99th%	=	17.96 cm (7.07 in.)
CM from Anterior Aspect (0.890 x AP at CM Level) - 2.355 = cm			

Joint Characteristics. Duplication of the degrees of freedom at the various body joints, as well as the limits of joint travel, is important if the motions of various body segments and the manner in which the loads are transmitted across these joints is to be duplicated. Engin (1979, 1981) and Grood, Noyes, and Butler (1978) were reviewed to define the degrees of freedom at various body joints and the manner in which rotations are achieved. Data presented in NASA Reference 1024 (1978) were utilized to define the free motion limits of the various body joints.

Long Bones. Evans (1957, 1973), Reilly and Burstein (1975), Burstein, Frankel, Reilly (1972), and Hight (1981) were reviewed to understand how the limb structural loads are resisted and transmitted by the long bones. The long bones of the LRE should be designed to react and transmit loads that far exceed those which the human bones can tolerate. This is necessary in order to help ensure the structural integrity of the LRE during actual ejection testing at high dynamic pressures.

Duplication of Hand Grip Forces. While the effects of muscular forces were neglected for all other joints within the human body, the muscular forces associated with the hand grip must be duplicated. This duplication of the hand grip force is necessary to properly simulate the time at which the hand is pulled away from the D ring. The time at which arm flail is no longer prevented by the grip of the hand on the D ring is a significant parameter in the design of an effective arm restraint device since it will be necessary to properly evaluate the effect of the restraint's deployment time on its effectiveness. Horner and Hawker (1973) was reviewed to establish a realistic range of hand grip forces that should be considered for duplication.

Performance Parameters Measurement

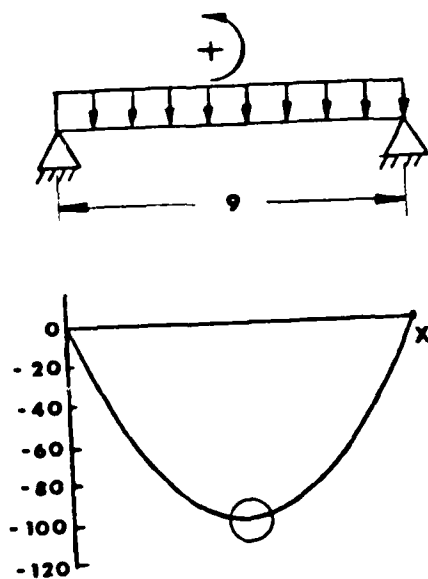
In order to provide the capability to evaluate the effectiveness of one limb restraint versus another, it was originally desired to measure the following parameters:

1. The angular displacement of the various degrees of freedom at the shoulder, elbow, hip, and knee joints.
2. Three axes of possible flail accelerations of the forearms.
3. The loads developed at the joints when limits of rotation are attained.
4. The bending moments and tension and compression forces in the long bones of the upper and lower arms and legs.

In addition to these measurements associated with limb flail, a system for measuring the forces and moments developed in the neck from the aerodynamic and inertial loads of the head and the helmet was also desired.

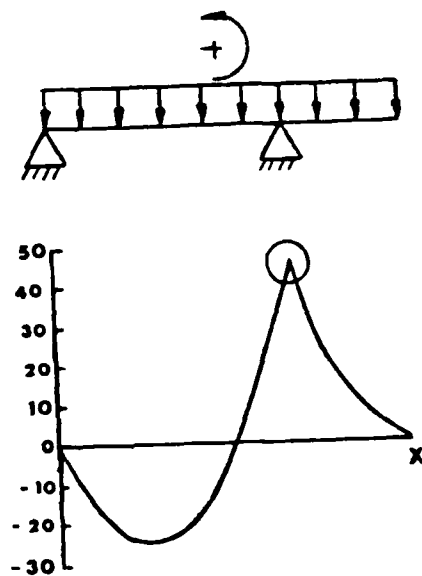
While there is no difficulty associated with defining appropriate transducers to record the desired data, there was concern regarding the number of instrumentation channels required to handle all the desired data. Measurement of the bending moments in the long bones provides an example of the possible problem. The purpose of the measurement is to obtain data to determine if the limb restraint system might allow the development of loads and moments sufficient to fracture the bones. The problem associated with making suitable measurements to conduct such an evaluation is illustrated in Figure 1. These examples illustrate the changes in the forearm moment distribution due to different points of limb restraint application. The example at the top left is a simplification of the forearm with restraints at both ends (elbow restraints and hand on D ring). As might be expected, the maximum moment occurs halfway between the supports (4.5 inches).

The example at the top right of Figure 1 is the case with the wrist and elbow restrained and the fist clenched. It is noted that the location of the maximum moment is different than that of the first example. The two cases at the bottom of Figure 1 are for the hand in an open position, which creates more aerodynamic forces than the clenched fist. As can be seen from the examples given in Figure 1, location of the maximum moment depends on



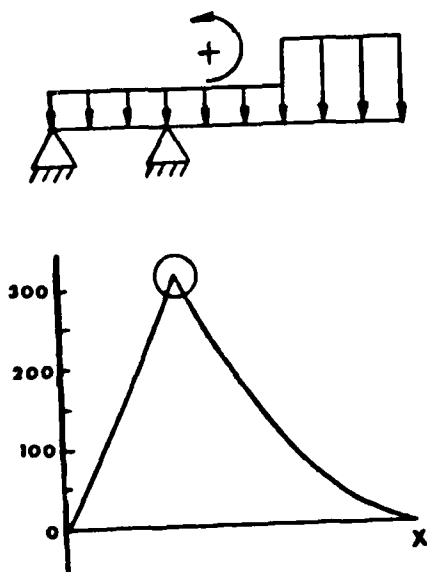
$$x(\text{FOR } M_{\text{MAX}}) = 4.5$$

$$M_{\text{MAX}} = 101$$



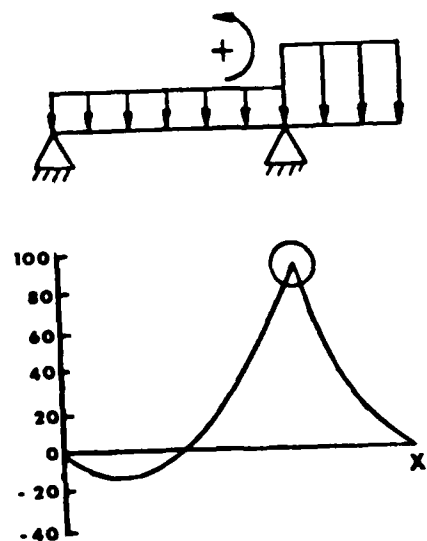
$$x(\text{FOR } M_{\text{MAX}}) = 6.0$$

$$M_{\text{MAX}} = 45$$



$$x(\text{FOR } M_{\text{MAX}}) = 3.0$$

$$M_{\text{MAX}} = 315$$



$$x(\text{FOR } M_{\text{MAX}}) = 6.0$$

$$M_{\text{MAX}} = 90$$

Figure 1. Effect of Reaction Points on Bending Moment Distribution

where the limb restraint system reacts to the applied aerodynamic loadings. Thus, to satisfy the intent of determining if a moment sufficient to break a bone is developed, a large number of strain gauges would have to be used to measure the entire moment distribution. It is estimated that at least four gauge sets would have to be used along the length of each long bone. Thus, to measure the bending moment distribution in two planes and the tension-compression forces for the long bones in the arms and legs, many (approximately 70) channels of strain gauge data would be needed.

Further, since little data exist on the strength of the long bones, the data would not be immediately useful in an evaluation comparing limb restraint stress levels. Therefore, the design will incorporate provisions for including measurement of the moments in the long bones at a future date.

However, since data on knee joint strengths are presently available, instrumentation will be included to measure loads developed at the knee joints after they have reached full rotation.

Estimated Loads

Estimation of the aerodynamic loads that might be applied to the LRE during ejection was difficult due to the lack of a complete data base. As noted in the section in which the available data were reviewed, the majority of the reported data were obtained for a pilot whose limbs were in the "stowed" position for ejection. Payne (1974b), however, did present data at low speeds for a number of human subjects suspended perpendicular to the wind-stream in a wind tunnel. A notable result was that the effect of flight clothing could increase the drag of various body components by 25 percent and the total drag of a human or dummy by as much as 40 percent over that measured when a flight suit was not worn. Newhouse, Payne, and Brown (1980) and Payne, Inc. (1980), presented data for a rigid half-scale model of a 50th percentile person tested over a Mach number range of $0.40 < M_N < 1.2$ at various vertical locations with respect to a simulated F-16 cockpit. The data presented in Newhouse, Payne, and Brown (1980) and Payne, Inc. (1980), showed a very strong influence of Mach number and flow distortions caused by the proximity of the seat/pilot to the cockpit fuselage during ejection.

Since an estimation of the loads that might be experienced by the LRE at high free stream velocities in the vicinity of an open cockpit was desired, the data in Newhouse, Payne, and Brown (1980) and Payne, Inc. (1980), were utilized to estimate the maximum loads that the LRE might encounter during ejection in the "stowed" position. Since the half-scale model of the crew-member had a smooth surface similar to a naked man, the force coefficients derived from Newhouse, Payne, and Brown (1980) and Payne, Inc. (1980), were increased by 1.4, as suggested in Payne (1974b), to account for the increase in the force that might be caused by a flight suit. Using either the plots or the equations describing the maximum force coefficient for the various limb segments presented in Payne, Inc. (1980), the forces on the arms and legs were estimated for the LRE in the "stowed" position ejecting from the basic aircraft configuration. Table 3 presents the forces estimated for the arms and legs at three values of the free stream dynamic pressure. As noted from the results shown in Table 3, all forces increased with dynamic pressure as might be expected, except for the side force on the lower leg. This was caused by a rapid drop-off in the force coefficient with Mach number as the free stream dynamic pressure increased from 1220 to 1700 pounds/feet². The forces tabulated for the side and normal forces developed by the lower arms reflect the constant coefficient reported for this limb in Payne, Inc. (1980).

The forces developed by the hand and feet were estimated using the data in Payne, Inc. (1980), in conjunction with data presented in Payne (1975b). In Payne (1975b) the knee and foot were strapped to strain gauge beams to measure the drag and side force loadings at these points. In addition, the hands gripped an instrumented D ring calibrated to measure the side force and drag force reacted by the hands. These tests were conducted at relatively low speeds, $V < 200$ feet/second, and resulted in force data non-dimensionalized by the free stream dynamic pressures that could be utilized to estimate the forces that might be developed by the foot and hand forces in the "stowed" position during ejection.

TABLE 3. MAXIMUM ESTIMATED LIMB FORCES IN RESTRAINED POSITION (PITCH = 0 DEGREES, YAW = 0 DEGREES)

Limb	Free Stream Dynamic Pressure (lbs/ft ²)		
	700	1220	1700
Upper Arm			
Side Force	3030	3720	5300
Axial or Normal Force	2040	5060	9520
Lower Arm			
Side Force	100	175	245
Axial or Normal Force	100	175	245
Upper Leg			
Side Force	790	1375	1915
Axial or Normal Force	315	515	575
Lower Leg			
Side Force	180	225	190
Axial or Normal Force	290	500	695
Foot			
Side Force	30	5	70
Axial or Normal Force	110	190	265
Hand			
Side Force	55	95	130
Axial or Normal Force	55	95	130

Since the loads measured by the foot strain gauge balance were due to the foot as well as the load developed by a portion of the lower leg, a means of extracting just the foot force from the total force had to be determined. If it is assumed that one-half of the lower leg force was reacted by the

knee balance and the other half by the foot balance, the following relationship can be expressed:

Measured force at foot balance = foot force + $1/2$ lower leg force.

Using the measured force coefficients from Payne, Inc. (1975b), and the appropriate lower leg forces tabulated in Table 3, the foot drag and side forces listed in Table 3 were estimated. A similar technique was used to estimate the side forces developed by the hands. The axial forces developed by the hands were assumed to be the same as the side forces.

While the loads in Table 3 yielded a set of limb loads that could be used in the conceptual design study for the LRE in the "stowed" position for ejection, they gave no information as to the loadings that might be experienced by the limbs during flail when the joints reach their limits of free motion. Since there are no known data that could be drawn upon to develop a data base to design the LRE for the maximum flail loadings across the joints, a means of estimating these loadings was devised. The manner by which these loadings were estimated is described in the following paragraphs.

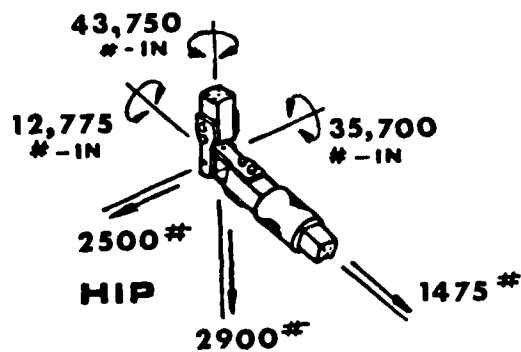
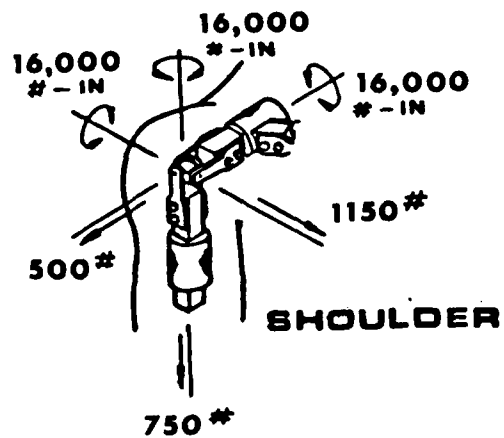
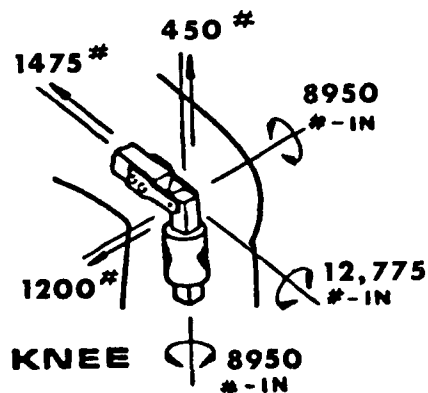
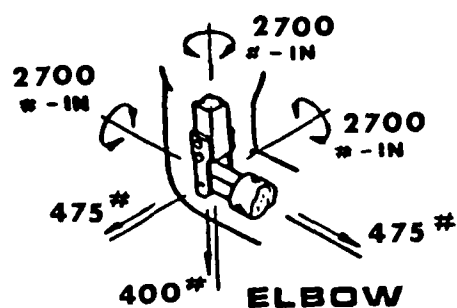
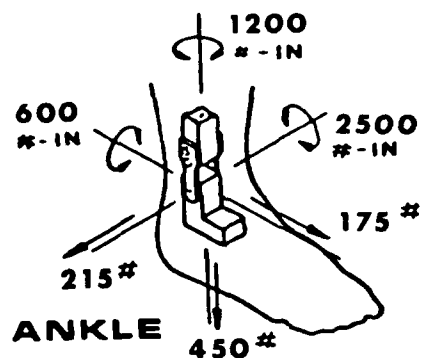
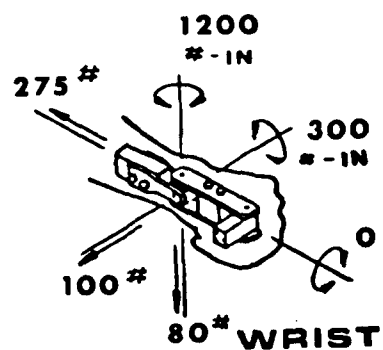
The technique developed to estimate loads was based on the following basic assumptions:

1. The maximum loads that can be developed by any given limb will be experienced when the limb is perpendicular to the airstream.
2. The probability that the limbs will end up perpendicular to the aircraft is 100 percent.
3. The drag coefficient used to calculate the applied aerodynamic force is that associated with separated flow on circular rods perpendicular to the airstream.
4. The cross-sectional characteristics of the limbs may be represented by circular cylinders having a constant diameter.

The drag coefficient used for the limbs was that presented in Hoerner (1965) for circular rods tested at Reynolds numbers above transition. At the Mach number of interest, 0.95, the measured drag coefficient reported in Hoerner (1965) is approximately 2.0. Since the increase in drag due to clothing is probably due to flapping of the material, it is reasonable to also apply the 1.4 factor to the drag coefficient which yields an estimated drag coefficient of 2.8. While it is believed that using a drag coefficient of 2.8 is conservative, it was used in all of the calculations reported herein to obtain a conservative set of loadings for use in the LRE design.

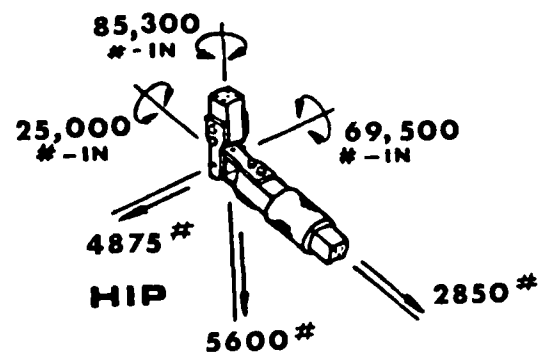
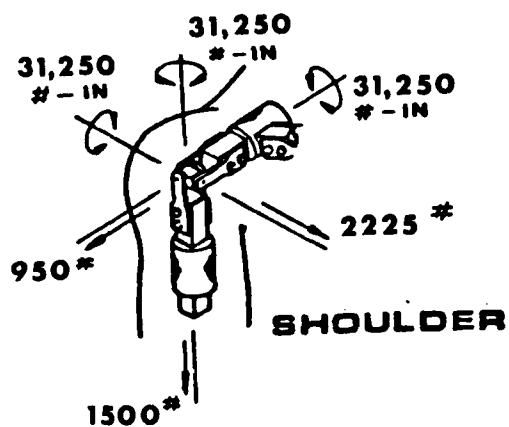
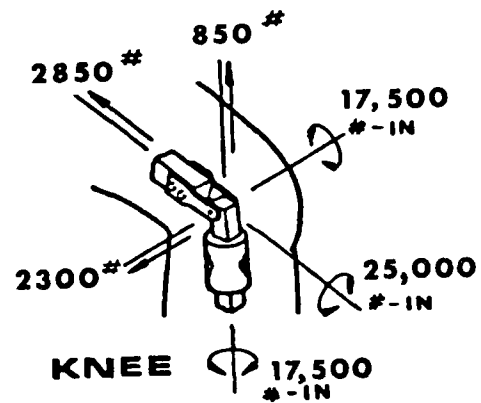
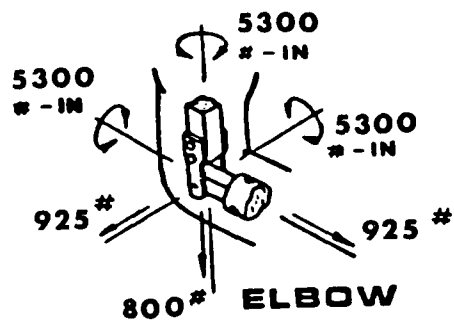
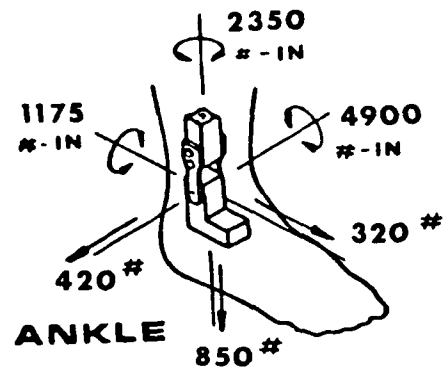
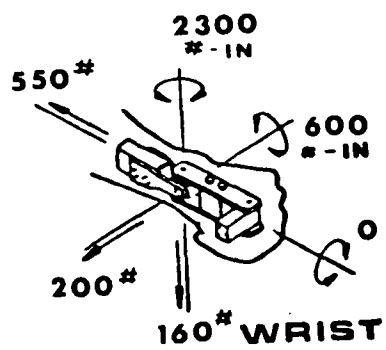
The diameter of the circular cylinder representing the various limb segments was determined by using the average of the circumferential dimensions reported in NASA Reference Publication 1024 (1978) for the 95th percentile anthropomorphic representation of the human body. The segment lengths of the various limbs were those developed by Dr. K. W. Kennedy, of the Air Force Aerospace Medical Research Laboratory, for the 95th percentile human body.

The maximum shears and moments calculated at each of the joints of interest for the design of the LRE using the approach described above are presented in Figure 2 for airspeeds of 500, 600, and 700 KEAS. As can be seen from the results presented, the estimated maximum loads are rather large particularly at the shoulder and hip joints. The conditions at which the shoulder and hip loads were estimated will be described briefly so that the assumptions involved are understood. The moments at the shoulder joint were calculated assuming the elbow joint was locked and the arm was a continuous circular cylinder. The moment about the vertical shoulder axis was calculated assuming the arm, in its extended locked position, had flailed 100 degrees to approximately a horizontal position and the body was positioned perpendicular to the airstream. The moment about the lateral shoulder axis was estimated by assuming the shoulder locked in extension, and the seat at a +30 degree pitch altitude. The moment about the longitudinal shoulder axis was estimated assuming the arm had rotated 100 degrees upward at the shoulder and the seat had yawed 90 degrees and rolled 110 degrees.



(a) 500 KEAS

Figure 2. Maximum Joint Loads



(b) 600 KEAS

Figure 2. Maximum Joint Loads (continued)

weldment while the pelvic unit is an aluminum casting. The butyl lumbar spine, normally used in anthropomorphic dummies to connect the thorax and pelvic units, is replaced by a mechanical spine which incorporates the same modular joint design to be used in the limbs. This was done for two reasons: (1) design of the spine to carry the applied loads, and (2) the ability to provide three degrees of torso rotations about known pivot points. Rotary position transducers will be utilized to measure the rotations about each of the axes. This approach in representing the lumbar spine will permit, in the future, a computer program to be written utilizing the output signals from all the motion transducers to reconstruct the position of all limbs with respect to the pelvic location as a function of time. This potential capability could be a significant factor in the development and evaluation of limb restraint systems.

Also indicated in Figure 8 is the manner in which the special LRE limbs will mate with the existing components. While the attachments of the arms to the thorax unit are straightforward, the connection of the upper leg to the pelvic unit may require a different approach than that indicated. It would be desirable to attach the upper legs to the existing stub units that are connected to the pelvic unit through a ball and socket. The trouble anticipated with the existing ball and socket approach will be in providing the means to limit and measure motions about two orthogonal axes. If a suitable means of accomplishing this cannot be found early in the detail design phase, the existing stub units and the ball and socket will be replaced by a double universal joint of the modular design.

It was determined during conversations with the manufacturers of anthropomorphic dummies that the load-carrying capabilities of the head, upper thorax, and pelvic units were not known. While these units have been used successfully in automobile crash tests, the structural integrity of the units for ejection testing must be determined. Therefore, early in the detail design phase, the load-carrying capability of the head, upper thorax, and pelvic units must be obtained, instrumented, and loaded with representative forces and moments to determine the stresses at critical locations.

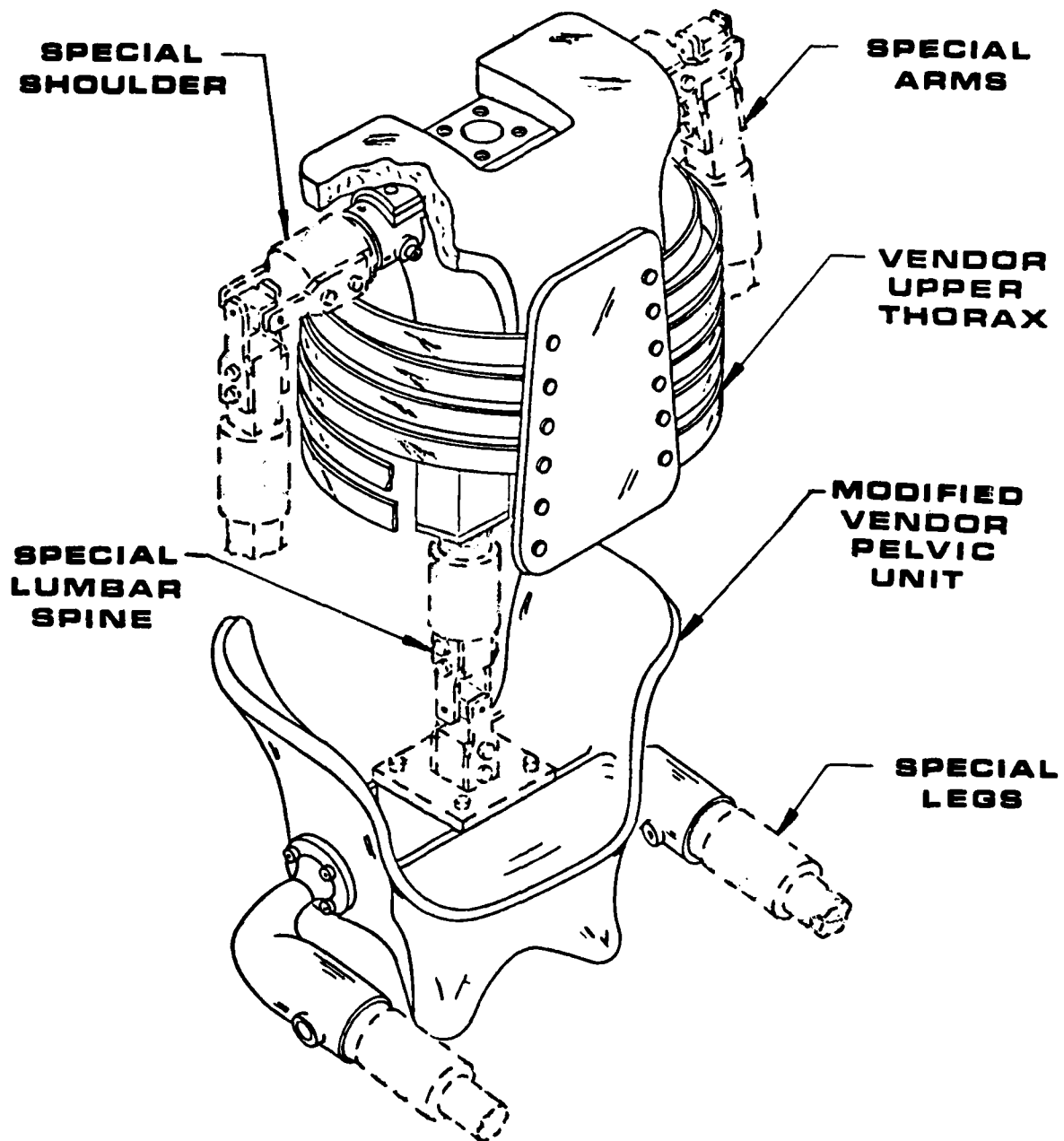


Figure 8. Body Internal Structure

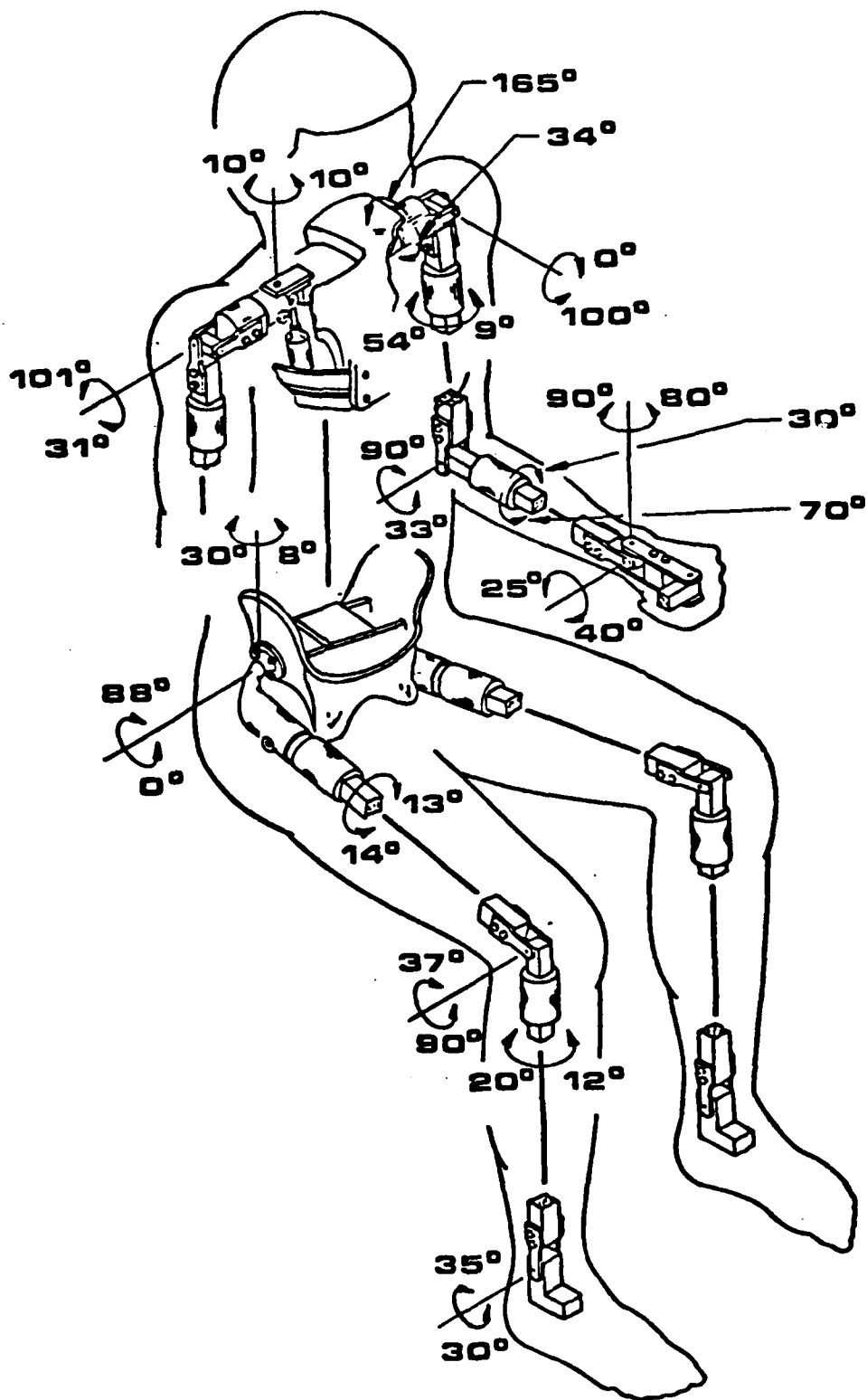


Figure 7. Limits of Joint Rotation

The universal joint illustrated at the bottom of Figure 6 is a simple adaptation of a conventional double universal joint in common use for years. A double universal joint is shown (rotation about two axes 90 degrees to each other) and a single universal would only have rotation about a single axis. As is indicated in the sketch, there is a rotary transducer located on each axis of the universal joint to measure the angular rotation about its axis. Unlike a rotary joint, bushings will be utilized instead of angular contact bearings to provide the interface between rotating and stationary parts.

The limits of motion that will be allowed at each of the joints are shown in Figure 7. It is noted that the limits of motion are less than those attainable with the human body. The motion limits allowed are those which, statistically, will limit human injury to less than 5 percent. It is believed that there will be no problems in providing suitable stops to ensure these limits. The manner in which these limits will be achieved is discussed in a later section of this report.

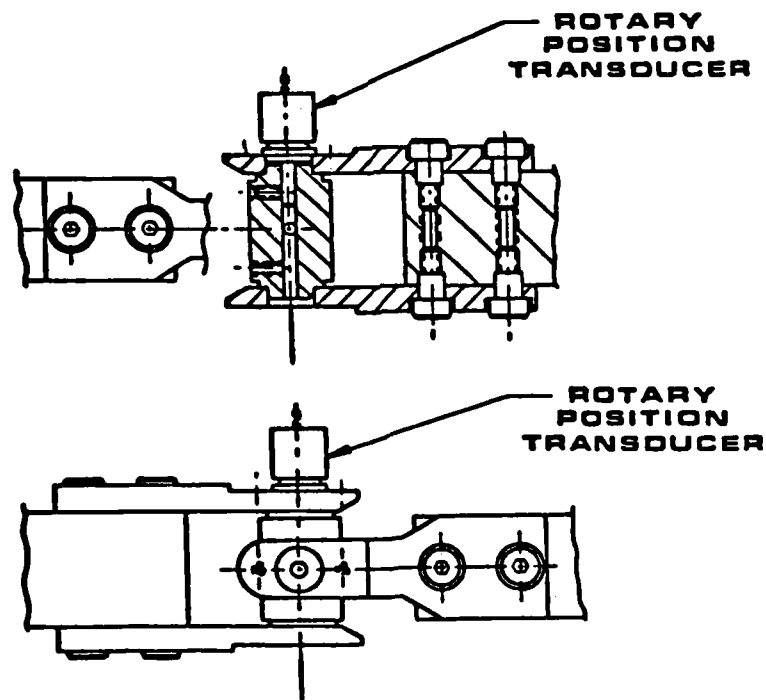
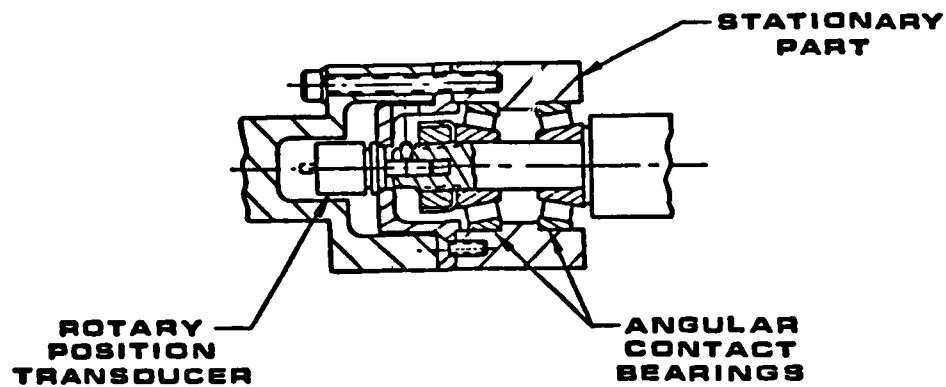
Application of Existing Components

As previously emphasized, the use of components available from existing anthropomorphic dummy designs has been maximized in the conceptual design of the LRE. The components that are suitable are the skull, upper thorax assembly, pelvic unit, hands, feet, and the flesh covering. While some of these components can be used directly, others may require modifications to satisfy LRE requirements. The use of each of the available components in the design of the LRE will be discussed in the following paragraphs.

It is believed that the skull and feet can be used without modification. Both of these components are available in the 95th percentile size. The skull is an aluminum casting having the proper weight characteristics. The feet are vinyl moldings, having a steel insert for rigidity and to provide a means of pivoting the foot about a single axis of the ankle with appropriate angular stops.

Figure 8 shows the use of existing pelvic and upper thorax assemblies for the required duplication of the LRE torso. The upper thorax unit is a steel

TYPICAL ROTARY JOINT



TYPICAL UNIVERSAL JOINT

Figure 6. Details of Joint Design

Figure 5, limb motions are generated by the mechanical joints as indicated below:

<u>Limb Motion</u>	<u>Mechanical Joint</u>
Wrist Flexion - Extension	Universal
Wrist Adduction - Abduction	Universal
Forearm Supination - Pronation	Rotary
Elbow Flexion	Universal
Shoulder Lateral - Medial Rotation	Rotary
Shoulder Extension - Flexion	Rotary
Shoulder Adduction - Abduction	Universal
Shoulder Vertical Rotation	Universal
Ankle Flexion - Extension	Rotary
Knee Medial - Lateral Rotation	Rotary
Knee Flexion	Universal
Hip Lateral - Medial Rotation	Rotary
Hip Adduction - Abduction	Ball and Socket
Hip Flexion	Ball and Socket

As noted above, the hip adduction-abduction and flexion motions will be represented by the existing ball and socket joint of the vendor-supplied pelvic unit. However, if a convenient way cannot be devised for limiting the motions as well as measuring the angular rotations, the ball and socket will be replaced with one of the modular universal joints.

Details of both the rotary and universal joints are presented in Figure 6. As can be seen from the cross-sectional sketch of the rotary joint, the stationary and rotating parts are connected through a pair of angular contact bearings that are preloaded by means of threaded bolts. At the end of the rotating shaft, a rotary potentiometer is attached to measure the angular rotation.

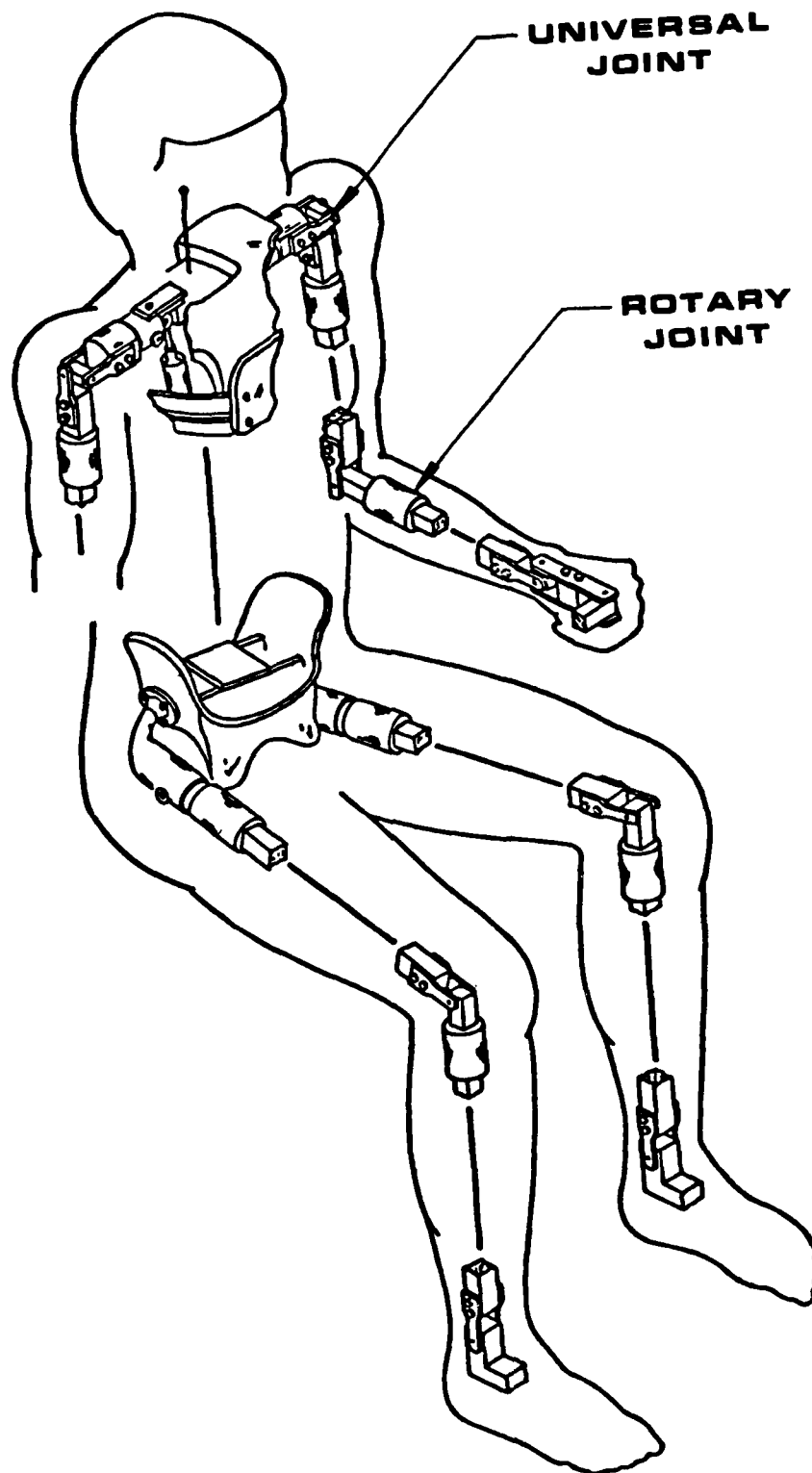


Figure 5. Modular Joint Design

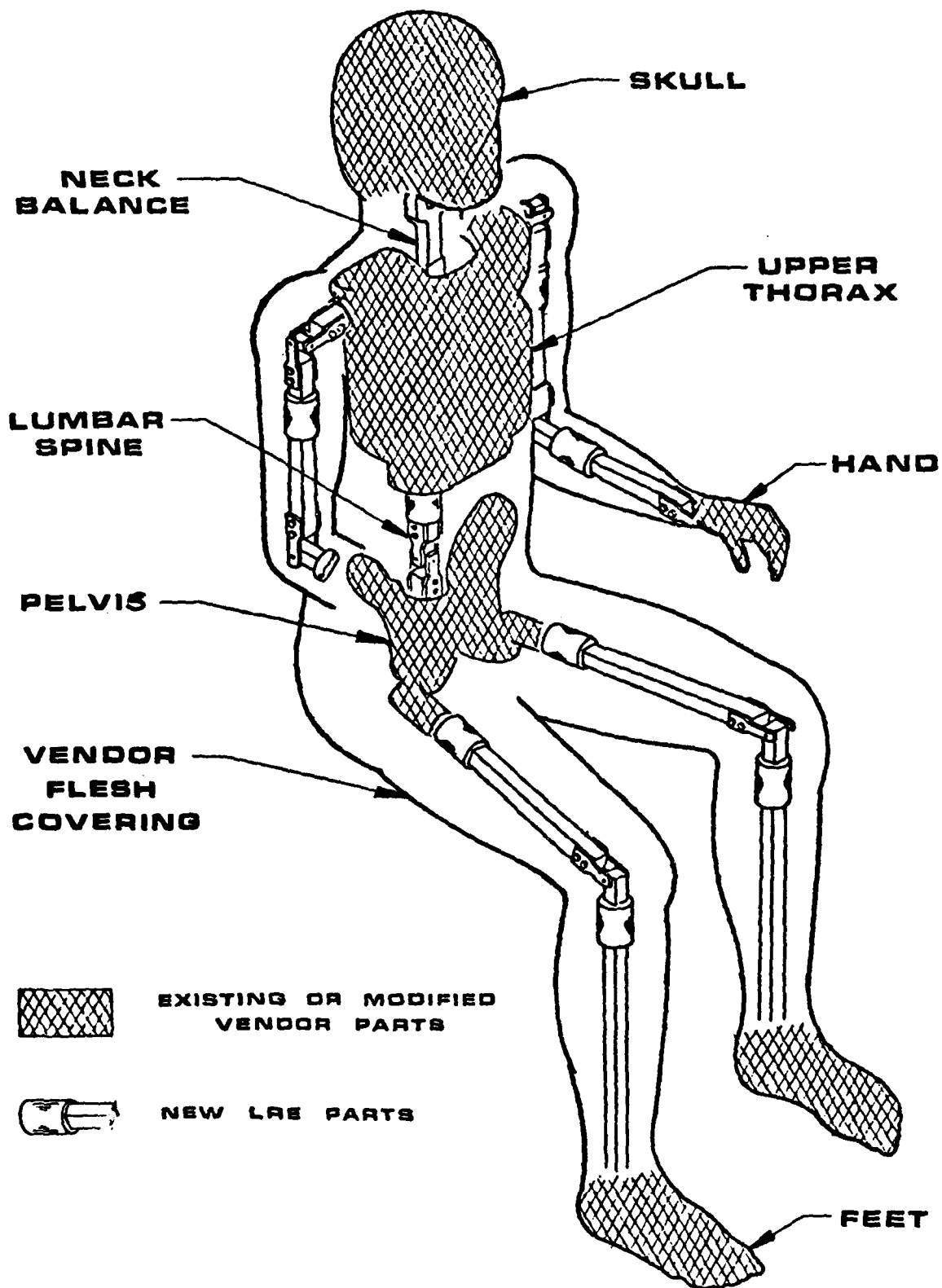


Figure 4. LRE Internal Structure

- Torso rotations
- Measurement of all joint rotation angles
- Measurement of the loads applied to the knee
- Measurement of helmet loads
- Instrumentation/telemetry package for 52 data parameters

Basically, the design utilizes existing parts for simulating the head/torso/pelvic regions, and limbs specifically designed to duplicate limb flail motions. Figure 4 indicates the areas in which existing assemblies and new assemblies will be utilized to construct the LRE. The skull and pelvic units are aluminum castings, while the upper thorax assembly is a steel weldment. The hands and feet are fabricated of vinyl with a steel insert. The vinyl flesh covering will be a modified version of a standard 95th percentile size covering. As noted in Figure 4, the feet and hands are connected to the body unit through specifically designed limb/joint assemblies.

The pelvic unit is connected to the upper thorax assembly through a special lumbar spine and the skull is attached to the thorax by means of a six-component balance. The following sections will describe in detail the conceptual design of the various subsystems of the LRE.

Limb and Joint Design

The limb and joint conceptual design to provide the degrees of freedom at the various joints is presented in Figure 5. The long bone limbs connecting the joints will be hollow beams having either a rectangular or circular cross-section. The joints are of a modular design utilizing a universal joint, a rotary joint, or a combination of these joints to duplicate the degrees of freedom at the various limb articulation points. Referring to

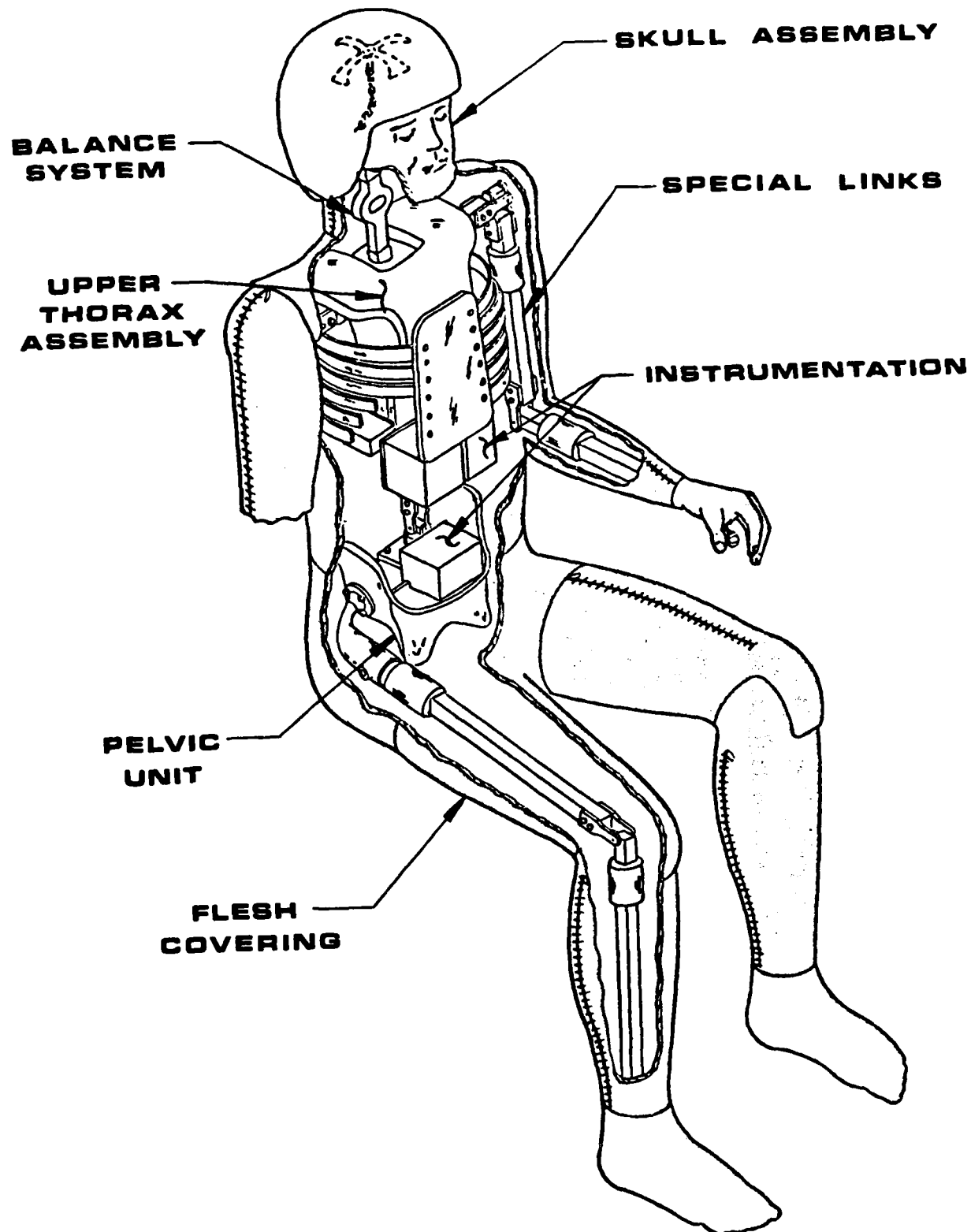
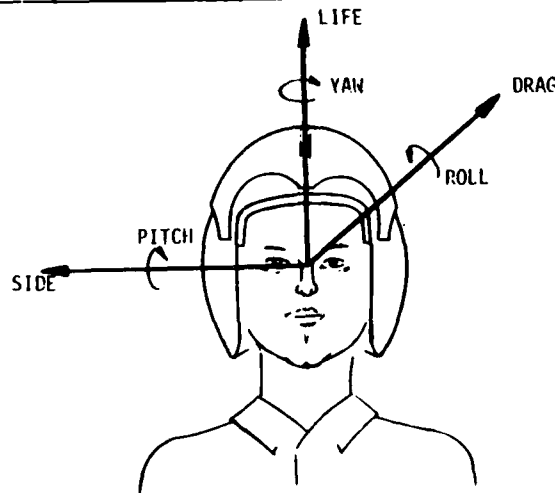


Figure 3. LRE Conceptual Design Assembly

TABLE 4. MAXIMUM ESTIMATED HELMET FORCES AND MOMENTS

VELOCITY KEAS	LIFT/LBS	DRAG/LBS	SIDE FORCE LBS	PITCH MOMENT LB-INCHES	YAW MOMENT LB-INCHES	ROLL MOMENT LB-INCHES
500	450	360	360	4900	2160	2160
600	680	610	610	7750	3700	3700
700	970	960	960	11600	5760	5760



Conceptual Mechanical Design

Using the results obtained and conclusions drawn during the initial investigation of the acceleration environment, aerodynamic loadings, required simulation of body components and motions, and state of the art of anthropomorphic dummy design, a conceptual design of a system to be used for evaluating limb restraint systems was developed. An overall cut-away view of the resulting design is presented in Figure 3. The design includes the following features:

- Maximum use of existing components from a commercially available dummy
- Limb joint rotations to human limits

The maximum forces and moments estimated for the helmet at three different airspeeds are listed in Table 4. Payne, Inc. (1975b), presented some data for helmet forces and moments at low speeds. Also, the lift and drag coefficients for the helmet were presented in Newhouse, Payne, and Brown (1980). These data document the effects of Mach number as well as the interference effects of the aircraft fuselage on the helmet loads during the ejection sequence. The appropriate Mach number associated with the various values of the free stream dynamic pressure were used to estimate the maximum lift and drag coefficients for the helmet that were measured for the basic model configuration. The estimated maximum side force was assumed to be the same as the maximum drag force. The estimated maximum yaw and roll moments were obtained by assuming the side force was located at the edge of a 12-inch diameter helmet. The maximum pitching moment was calculated assuming that the lift force was at the front of the 12-inch diameter helmet and the drag force was at the top of the helmet.

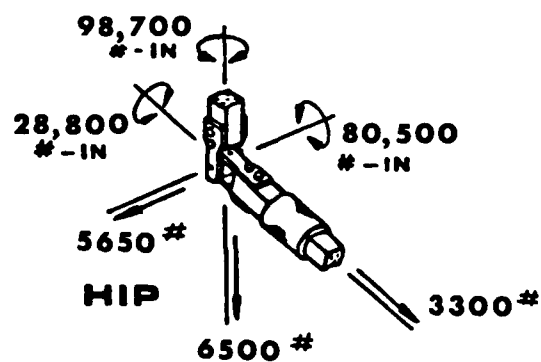
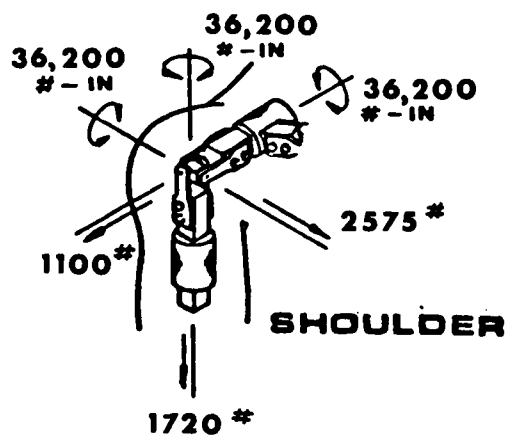
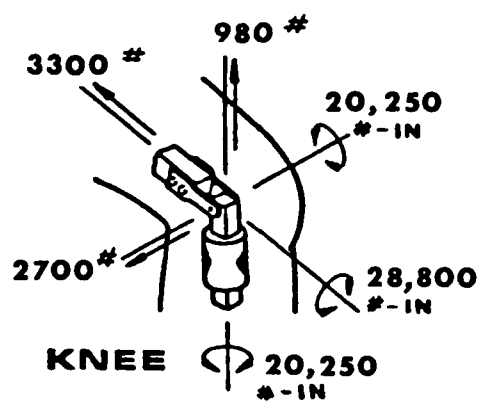
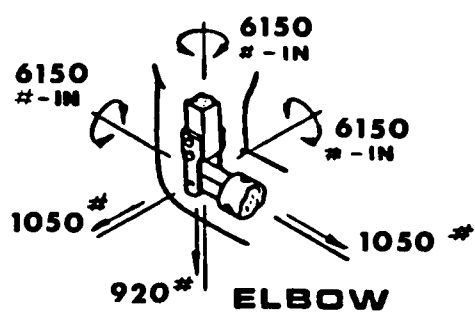
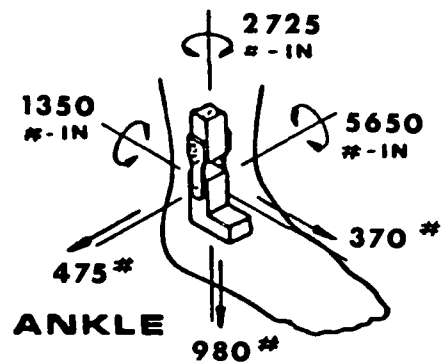
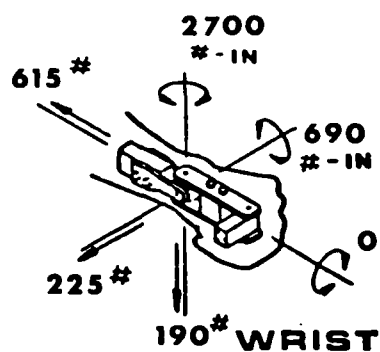
It is believed that the conservative assumptions utilized in estimating the forces and moments developed by the helmet during ejection from a high-speed aircraft provide a reasonable envelope of loadings to design a neck balance system.

The loads presented in Figure 2 and Table 4 were utilized for the design of the limbs and balance system. The inertial forces due to the accelerations associated with ejection were not considered in the design as they are considerably smaller than the aerodynamic loading and would be in a direction that would tend to relieve the aerodynamic loadings. For example, for an acceleration of 20 Gs, the inertia moment at the shoulder due to the arm is approximately 2000 inch-pounds as compared to 36,000 inch-pounds due to the aerodynamic forces. It was also believed that if the joints were designed to carry the static aerodynamic forces and moments, they would be more than capable of resisting the acceleration inertial loadings associated with joint lock-up.

The forces and moments estimated for the elbow resulted from the same loading positions at which the shoulder loads were computed.

The loads at the hip were estimated assuming the lower leg had flailed and locked the knee joint so that the entire leg was a continuous circular cylinder having a straight centerline. The moment about the vertical hip axis was estimated assuming the hip joint had reached its limit of abduction and the seat had yawed 30 degrees. The moment about the lateral axis was estimated assuming maximum hip flexion and 90 degrees of seat pitch. The reason the moment about the lateral axis does not equal that about the vertical axis was due to the assumption that the shadow effect of the seat pan would reduce the loading on the upper leg to one-half of the value it would develop in the free stream. The moment about the longitudinal hip axis was estimated assuming the long bone of the lower leg was at 90 degrees to the upper leg bone, the limits of hip medial rotation had been reached, and the seat yawed 90 degrees and rolled 13 degrees. While it is believed that all of the hip moments could be obtained with unrestrained flail in an unstable seat, it is believed that the moment about the longitudinal hip axis has the highest probability of being realized during ejection from a high-speed aircraft. The maximum moments estimated at the knee joint were also the result of the leg/seat positioning used to estimate the loads at the hip joint.

The previously discussed estimated maximum joint loads were based on the assumption that the limbs were at fixed positions. In unrestrained flailing motion of the limbs, the energy build-up in the limbs due to the flailing velocity must also be absorbed when the joint reaches its motion limits. A detailed study of the dynamic loads that will be experienced when the joint reaches its motion limits was not undertaken during the conceptual design studies. On the basis of the studies that were conducted, however, it is believed that the maximum dynamic impact loads at joint lock-up will occur at the shoulder joints. The use of simple snubbing devices to limit the joint dynamic lock-up loads to reasonable values was briefly investigated, and it was concluded that the use of these or similar devices can successfully limit the dynamic lock-up loads at the joints.



(c) 700 KEAS

Figure 2. Maximum Joint Loads (continued)

The use of existing 95th percentile flesh coverings for the LRE may require more modification than any of the other existing components. The reasons for this belief are associated with processes by which the flesh coverings are molded, and the requirement for access to the instrumentation at the joints and on the long bones. The desire to utilize existing molds to manufacture the flesh coverings for the LRE determined the selection of the 95th percentile dummy. The cost of developing molds for a 97th or 99th percentile dummy, or a specialized size, were believed to be prohibitive for the benefits that might be obtained.

It is believed that the process by which the present flesh coverings are manufactured will have to be modified to meet the requirements of the LRE. Presently, the long bones are placed at appropriate locations in the mold, and the inner and outer vinyl skins are molded. After a given time at 375°F to 400°F, an expandable foam slush is poured in between the inner and outer skins and cured at 375°F to provide the proper limb volume. At the completion of the molding process, the complete limb, from joint to joint, has been manufactured with the long bone bonded to the inner skin. The present process is obviously not compatible with using instrumented joints and limbs because of the curing temperature and the fact that the completed limb does not permit access to the instrumentation at the joints and along the long bone. In discussions with the manufacturers, it was found that the process and techniques can be modified for the manufacture of suitable LRE flesh coverings. The major modification required would be to insert a dummy long bone/joint unit having the correct volumetric shape in the mold and covering the insert with a parting agent.

After the molded limb is removed, it would be cut and removed from the dummy limbs. The flesh covering would then be placed over the instrumented limb, and a heavy zipper would be used to provide closure along the cut. This technique would also allow the flesh covering to be removed at will to gain access to the joints and associated instrumentation. Figure 9 indicates how the flesh covering would be developed for the LRE. The torso covering would be a standard covering except that the zipper would be moved from the back to the front in order to provide access to the instrumentation packages. Each of the long bone segments would be split as shown to provide access to

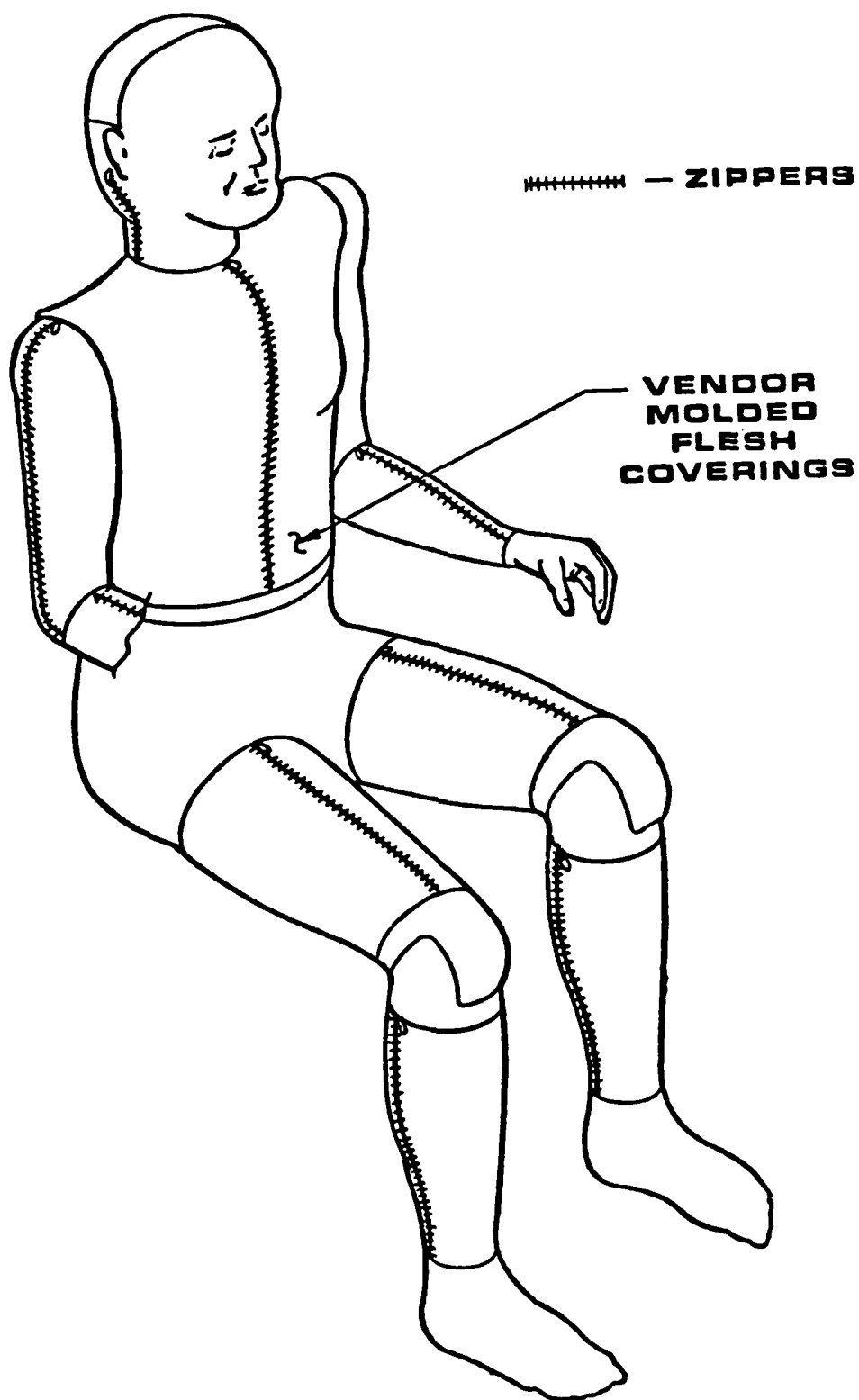


Figure 9. Flesh Covering

all of the instrumentation at the joints and on the long bones. While some details of this approach remain to be worked out, it is anticipated that a successful LRE flesh covering can be manufactured.

An existing 95th percentile hand will be modified to provide a means of obtaining a specified hand breakaway force. Figure 10 illustrates the concept that has been developed. A forward-acting force can be applied to the upper arm after the canopy leaves and prior to pilot ejection from the cockpit; therefore, the breakaway hand concept must resist compressive loadings without failure and then fail at a prescribed tension loading. The concept illustrated in Figure 10 will meet these requirements. The breakaway mechanism will be assembled by opening the strap, placing it around the D ring, inserting the two metal pieces between the strap and D ring, and inserting the connecting rod into the holes of the mechanism. The opposite pitch threads in each end of the rod will screw the rod into the wrist nut and tighten the breakaway strap around the D ring when the rod is turned. While the breakaway section of the strap will be designed to fail at a prescribed force, the final sizing will be accomplished in conjunction with tests conducted on a tensile test machine.

The primary modifications to an existing hand to incorporate the break mechanism will involve placing a threaded nut at the wrist joint and making a hole through the vinyl for the connecting rod.

Head/Neck Balance System

As noted in the discussion of the loading developed by various body components during ejection, the estimated loads developed by the head/helmet are rather large (Table 1) and, if present, could possibly break the neck. Since the estimates of the maximum loads presented in Table 1 were developed from the steady-state, one-half scale wind tunnel model data provided in Newhouse, Payne, and Brown (1980) and Payne, Inc. (1980), it is desirable to obtain dynamic loads data during ejection for comparison with wind tunnel data.

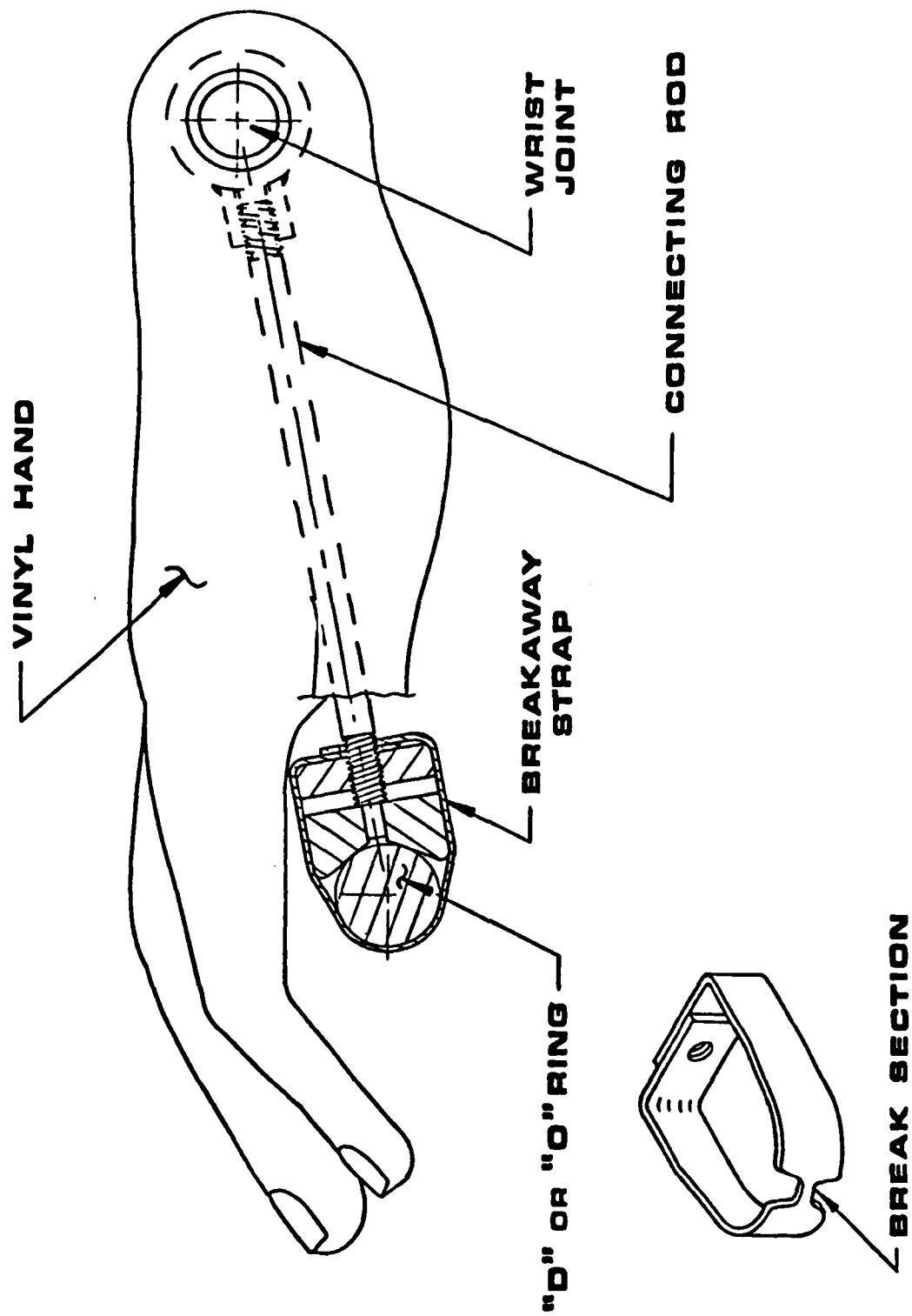


Figure 10. Breakaway Hand Concept

During the initial development of the conceptual design for a suitable balance, the following guidelines were established:

1. The balance should be as simple as possible.
2. The balance should have small deflection and withstand three times the design load without failure.
3. The balance readings should be repeatable and have a 1 to 3 percent accuracy.
4. The balance should be reliable for repeated usage.

It is believed the balance concept shown in Figure 11 meets these guidelines. As indicated in the sketch presented in Figure 11, the balance is a force ring integrally machined into a rectangular beam with retention flanges which attach to the existing skull and upper thorax assemblies. The balance is instrumented with strain gauges which measure the strains developed by forces and moments along and about three orthogonal axes. The manner in which these gauges will measure the strains associated with the various forces and moments is presented in Figure 12. The strain gauges at each of the locations indicated will be four arm bridges in which two arms will be wired so that their signals subtract. For example, at the location where ϵ_B is to be measured, the signal from the gauge at the bottom of the beam will be subtracted from the gauge at the top of the beam. Thus, when a bending moment (pitching moment) is applied, the signals from the gauges will add since the top gauge will measure a negative strain (compression) while the bottom gauge will read a positive strain (tension). When an axial force is applied (lift force), the strain signals will be of opposite sign from the two gauges and the sum of the signals will be zero.

Using this technique in wiring the gauges, the strain force relationships that would result from the noted gauge locations are presented in the middle of Figure 12. As noted from these relationships, the strain signals at B and C would be obtained if either a drag force (DF) or a pitching moment (PM) were applied at the balance reference location. Similarly, strain

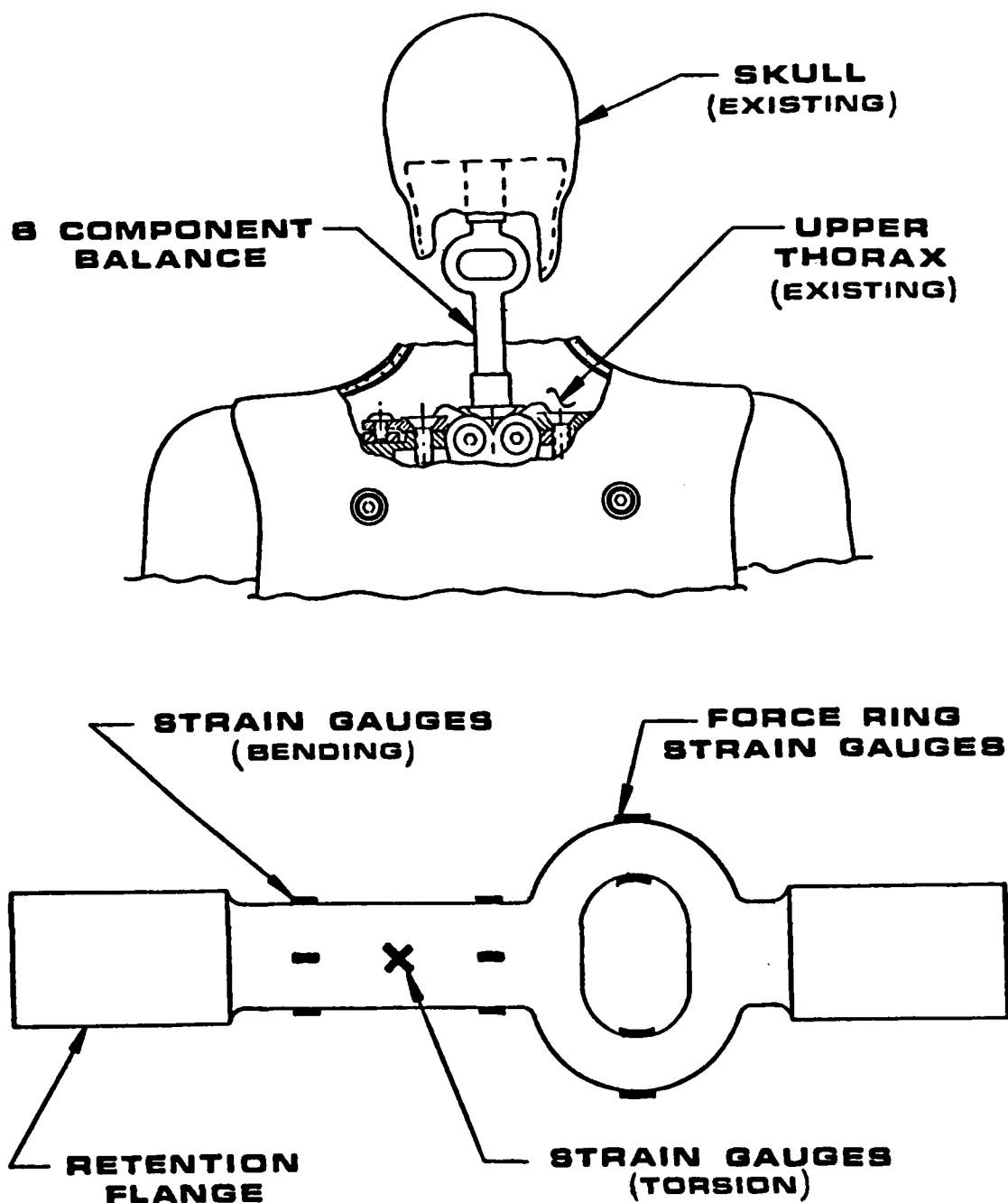
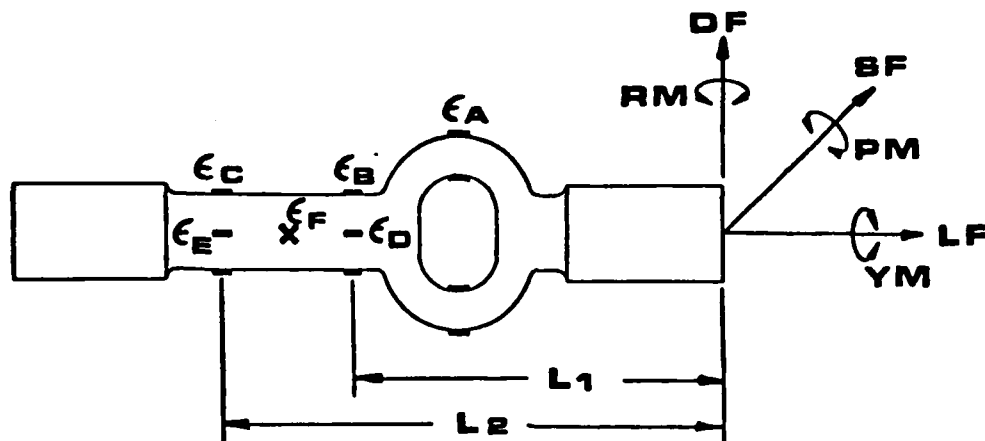


Figure 11. Six-Component Head/Neck Balance



$$\epsilon_A = LF$$

$$\epsilon_B = DF + PM$$

$$\epsilon_C = DF + PM$$

$$\epsilon_D = SF + RM$$

$$\epsilon_E = SF + RM$$

$$\epsilon_F = YM$$

STRAIN/FORCE RELATIONSHIPS

MATRIX RELATIONSHIP

$$\begin{bmatrix} \epsilon_A \\ \epsilon_B \\ \epsilon_C \\ \epsilon_D \\ \epsilon_E \\ \epsilon_F \end{bmatrix} = \begin{bmatrix} \times & 0 & 0 & 0 & 0 & 0 \\ 0 & \times & 0 & \times & 0 & 0 \\ 0 & \times & 0 & \times & 0 & 0 \\ 0 & 0 & \times & 0 & \times & 0 \\ 0 & 0 & \times & 0 & \times & 0 \\ 0 & 0 & 0 & 0 & 0 & \times \end{bmatrix} \times \begin{bmatrix} LF \\ DF \\ SF \\ PM \\ RM \\ YM \end{bmatrix}$$

DIAGONAL

Figure 12. Coupled Balance Matrix

signals at D and E would be obtained if a side force (SF) or a rolling moment (RM) were applied at the balance center. Since the gauges on the force ring are decoupled along with the torsion gauge on the beam, there is a unique relationship between the strain signals at A and the lift force (LF) as well as between the yawing moment (YM) and the signals developed by the torsion gauges. The matrix relationship between the strains and the applied loads at the bottom of Figure 12 show clearly the lack of uniqueness in the strain signals. A unique relationship between a strain signal and an applied force or moment can be developed using the various strain signals when it is recognized that the strain signals are a measure of the local moment. Thus, if a pure pitching moment were applied at the balance reference point, the moment would be the same over the beam and ϵ_B and ϵ_C would be the same. If a pure drag force were applied at the balance center, the moment along the beam and, thus, the strain would be proportional to the distance from the balance reference point. Using this information, the relationship between a strain signal and an applied force or moment can be obtained as indicated by the diagonal matrix at the bottom of Figure 13. The relationship between a new set of six strain signals and the original set is presented at the top of Figure 13.

Since K_1 and K_2 are based on geometrical relationships and do not change, the unique strain signals needed to diagonalize the balance matrix can be obtained through simple circuit manipulations.

LRE Load Measurement System

The initial load measurement system was aimed at measuring only the loads developed at the knee joint during ejection. Figure 14 illustrates the placement of the load transducers that will be utilized to measure the loads applied to the knee. The two load cells on the rotary joint below the knee will measure the torsional moments applied to the knee by the lower leg and foot. The load cells on the rotary joint at the hip will measure the loads applied to the knee when the limits of hip rotation are reached. The load cells at the knee joint will measure the loads applied at the knee when the limits of knee flexion are reached. Since the calf of the lower leg can interact with the seat pan during ejection, the reaction of the moment

$$\epsilon_1 = \epsilon_A$$

$$\epsilon_2 = \frac{\epsilon_C - \epsilon_B}{K_1}$$

$$\epsilon_3 = \frac{\epsilon_B - \epsilon_D}{K_1}$$

$$K_1 = Q_2 - Q_1$$

$$\epsilon_4 = \frac{(K_2 \epsilon_B - \epsilon_C)}{K_2 - 1}$$

$$K_2 = \frac{Q_2}{Q_1}$$

$$\epsilon_5 = \frac{K_2 \epsilon_D - \epsilon_B}{K_2 - 1}$$

$$\epsilon_6 = \epsilon_F$$

$$\begin{bmatrix} LF \\ DF \\ SF \\ PM \\ RM \\ YM \end{bmatrix} = \begin{bmatrix} x & 0 & 0 & 0 & 0 & 0 \\ 0 & x & 0 & 0 & 0 & 0 \\ 0 & 0 & x & 0 & 0 & 0 \\ 0 & 0 & 0 & x & 0 & 0 \\ 0 & 0 & 0 & 0 & x & 0 \\ 0 & 0 & 0 & 0 & 0 & x \end{bmatrix} \times \begin{bmatrix} \epsilon_1 \\ \epsilon_2 \\ \epsilon_3 \\ \epsilon_4 \\ \epsilon_5 \\ \epsilon_6 \end{bmatrix}$$

Figure 13. Uncoupled Balance Matrix

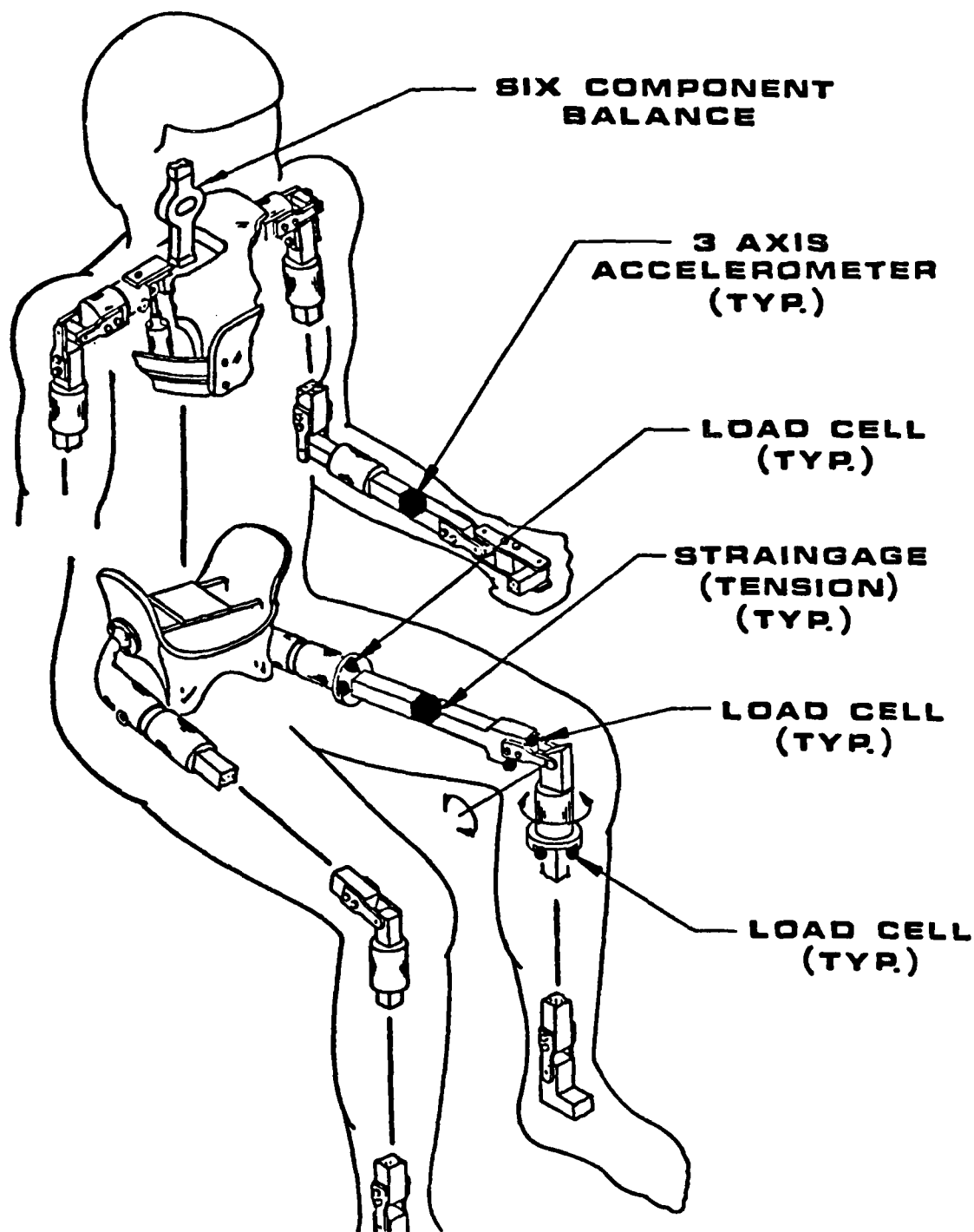


Figure 14. Instrumentation for Load Measurement

developed by the foot drag force around the calf/seat interaction point is a tension force in the upper leg long bone. To measure this force, which will tend to pull the knee joint apart, strain gauges will be attached to the upper leg long bone to measure the tension force.

In addition to the instrumentation to measure the forces applied to the knee, the six-component neck balance system described previously will be used to measure the forces and moments developed by the helmet and head. A triaxial accelerometer will also be installed in each forearm to measure the acceleration loads that could be developed by an oscillatory flailing motion.

While the instrumentation has been limited at the present time to measure the forces and moments at the noted locations, the LRE will have the capability of having similar instrumentation at any of the body joints. A detailed sketch of the manner in which the instrumentation will be utilized to measure the loads developed at the knee joint after the limits of free motion are reached is presented in Figure 15. The sketch at the top of Figure 15 indicates how the compression load cells will act as a motion limiting stop and a load measuring device for a universal joint. The load cells are protected for impact loadings much greater than those that might be anticipated during ejection; therefore, the structural integrity of the units should be satisfactory.

The sketch at the lower part of Figure 15 indicates the manner by which the compression load cells will be used to limit the motions in a rotary joint and measure the loads after the limits of free motion are reached. Since it is desired that all joints, universal and rotary, have the capability of incorporating load cells, removable spacers will be utilized to provide the proper limiting rotations when the load cells are not incorporated at a given joint.

Data Acquisition System

While the data acquisition system will be discussed in detail in the following section, the incorporation of the physical units within the LRE

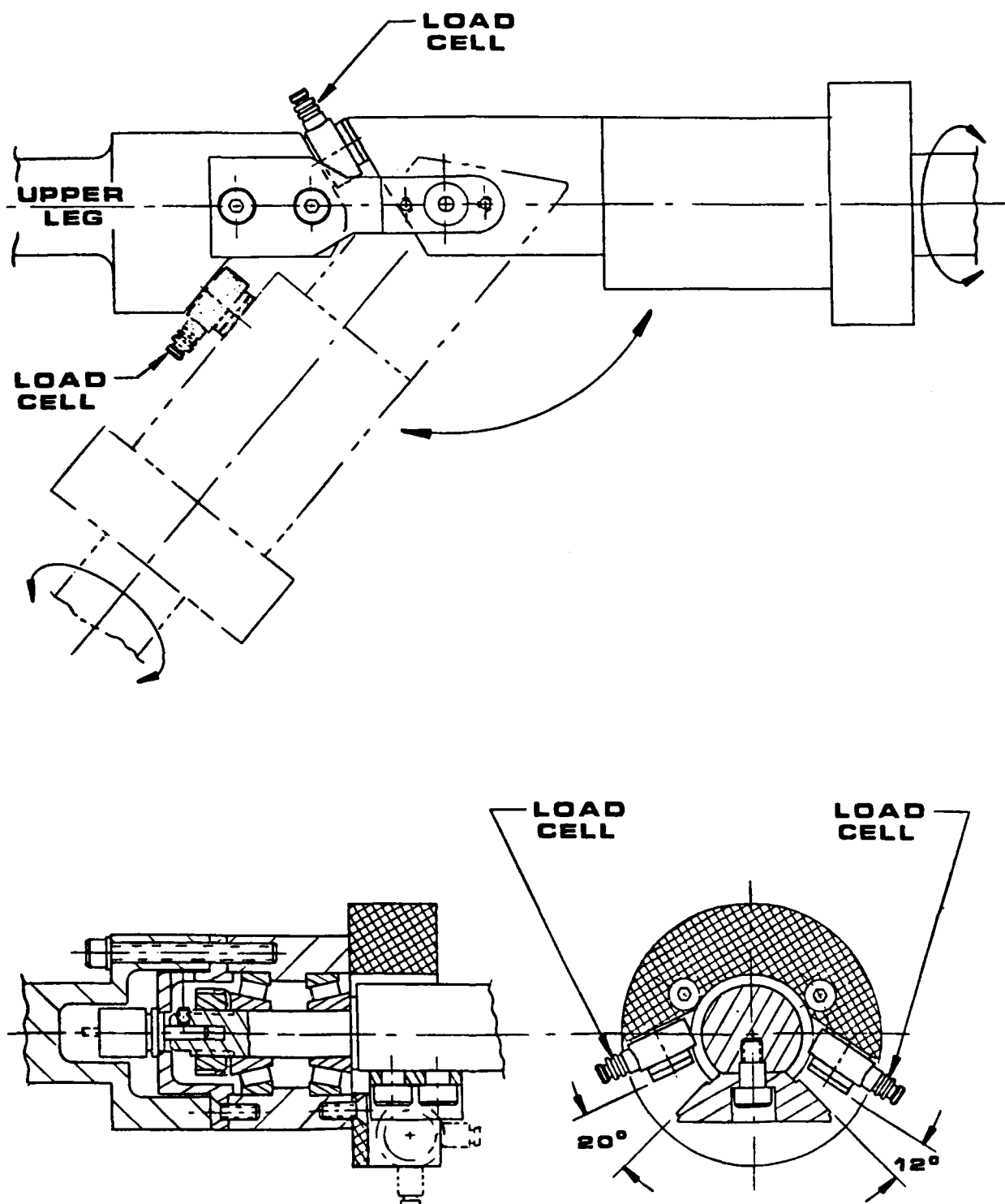


Figure 15. Load Measurement System for Knee

will be briefly noted. Table 5 lists the various parameters that will be measured, as well as the type and number transducers used. As noted at the bottom of Table 5, there will be 52 independent measurements made, recorded, and telemetered from the LRE. The placement of the instrumentation required to control the instrumentation power and receive, condition, and transmit the information from the transducers is shown in Figure 16. The locations for these units were chosen on the basis of weight and balance of the LRE, accessibility, and protection during possible body-ground contact. The transmitter will be connected to the skull antenna, as shown in Figure 3, by an instrumentation cable. The location of the quick-disconnect umbilical cord between the seat and the LRE is not shown. It is anticipated that the quick-disconnect will be located in the back of the pelvic unit to ensure compatibility with the instrumentation/power system at Holloman Air Force Base.

INSTRUMENTATION SYSTEM

The discussions of the conceptual design studies conducted for the Instrumentation and Data Collection System will be presented in three sections. The first section describes the overall system to be designed. The second section presents some background studies defining the parameters for proper data capture techniques, including a discussion of the requirements for presampling filtering. The third section presents a conceptual design of a typical system to meet the requirements of the LRE.

System Description

The purpose of this investigation is to define a practical concept for an Instrumentation and Data Collection System to measure about 50 LRE parameters associated with limb position, motion, and force, and about 26 parameters associated with the ejection seat. The system will be powered from within the LRE. The investigations conducted include studies in preparation for signal conditioning, analog-to-digital conversion processes, and digital data acquisition. The primary test environment for the LRE will be the rocket sled at Holloman Air Force Base. Secondary areas of use could include airplane drops, wind tunnel testing, and laboratory limb restraint

TABLE 5. LRE MEASUREMENT SYSTEM

Quantity Measured	Transducer	L	R
Lower Leg Torsional Moment at Knee	Load Cell	2	2
Lower Leg Roll Moment at Knee	Load Cell	2	2
Knee Loads at Flexion Stops	Load Cell	2	2
Knee Separation Force	Strain Gauge	1	1
Knee Medial and Lateral Rotation	Rotary Pot.	1	1
Knee Flexion	Rotary Pot.	1	1
Hip Medial and Lateral Rotation	Rotary Pot.	1	1
Hip Flexion	Rotary Pot.	1	1
Hip Adduction and Abduction	Rotary Pot.	1	1
Forearm Supination - Pronation	Rotary Pot.	1	1
Elbow Flexion	Rotary Pot.	1	1
Shoulder Medial and Lateral Rotation	Rotary Pot.	1	1
Shoulder Adduction and Abduction	Rotary Pot.	1	1
Shoulder Flexion - Extension	Rotary Pot.	1	1
Torso Roll	Rotary Pot.	1	
Torso Pitch	Rotary Pot.	1	
Torso Yaw	Rotary Pot.	1	
Forearm Flail Acceleration	Tri-Axis Accel.	3	3
Torso Acceleration	Tri-Axis Accel.	3	
Head Lift	Strain Gauge	1	
Head Drag Force	Strain Gauge	1	
Head Side Force	Strain Gauge	1	
Head Pitching Moment	Strain Gauge	1	
Head Roll Moment	Strain Gauge	1	
Head Yaw Moment	Strain Gauge	1	
TOTAL Independent Measurements: 52			

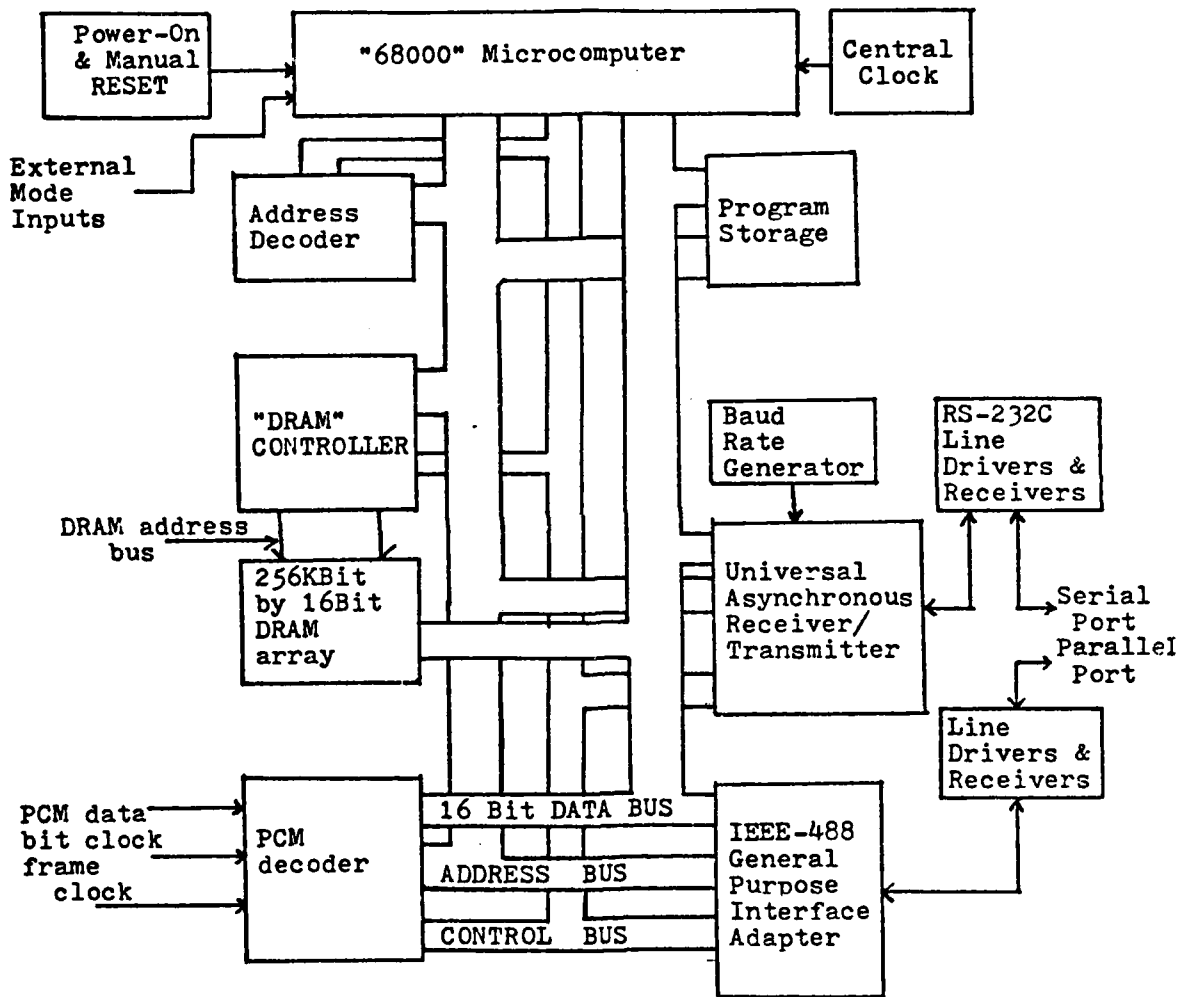


Figure 25. On-Board Computer System Block Diagram

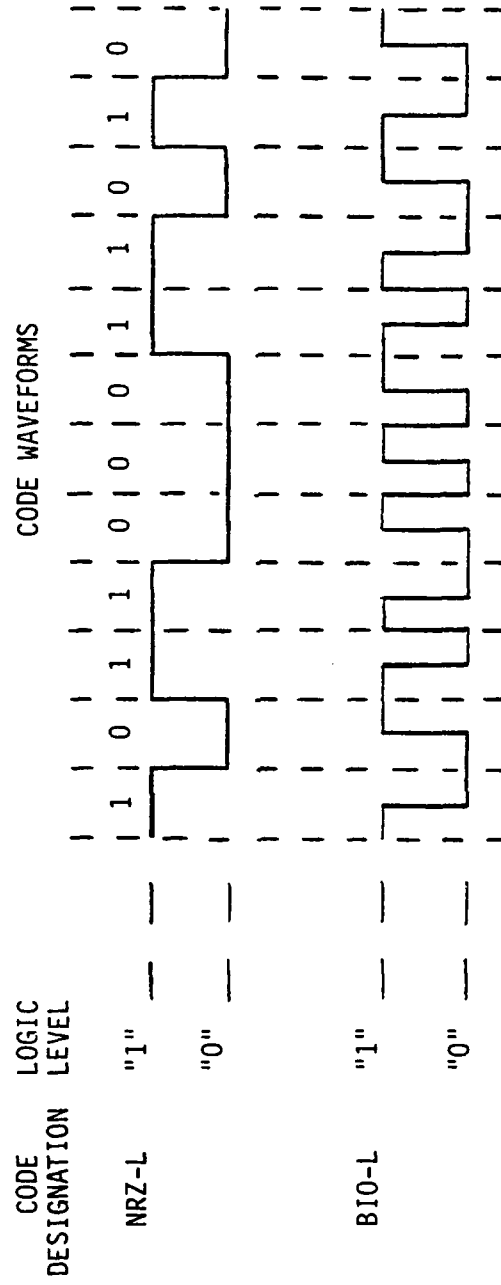


Figure 24. Typical NRZ-L and BIO-L Waveforms

NOTE: Only one of three typical Receiving/Recording stations shown.

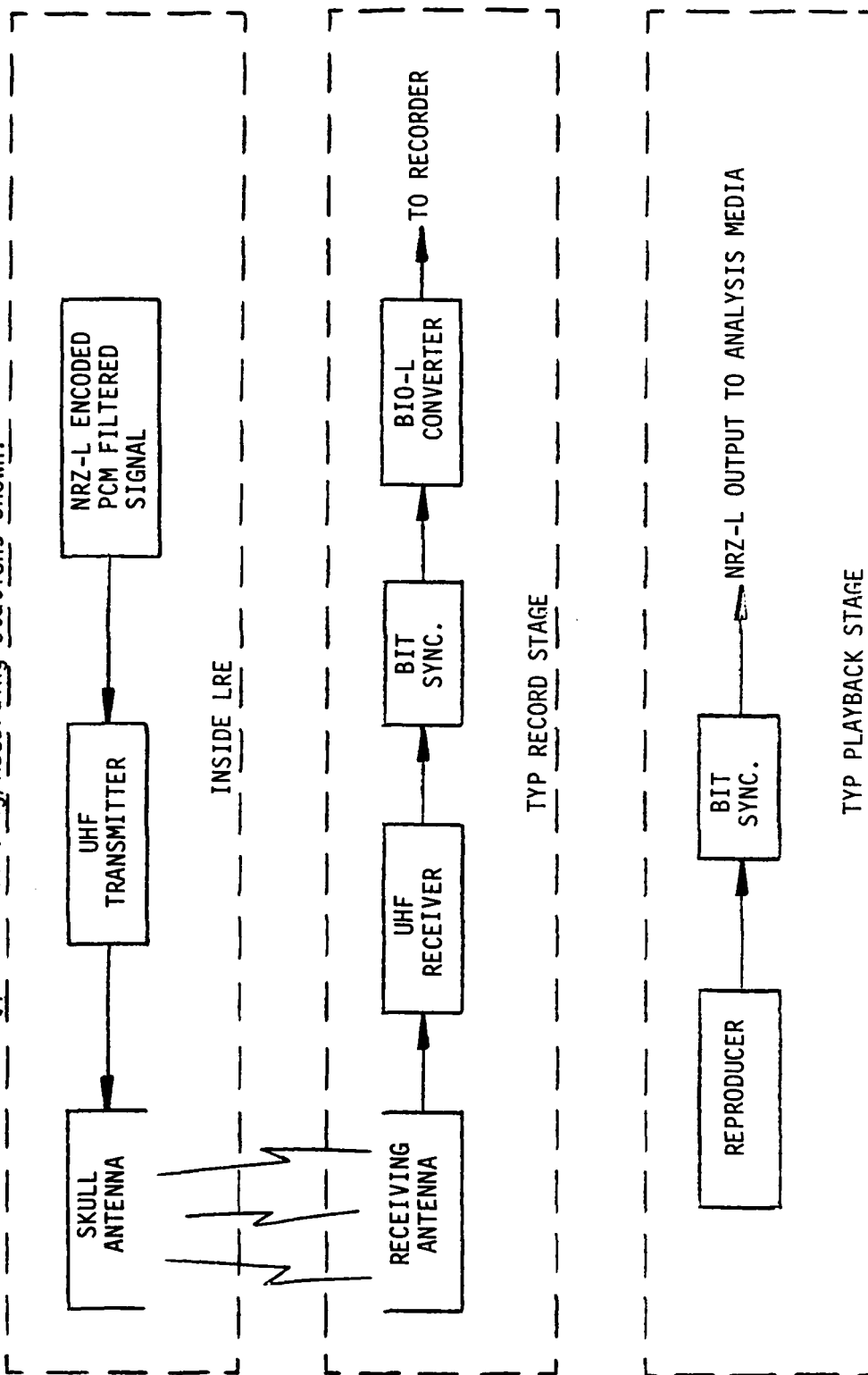
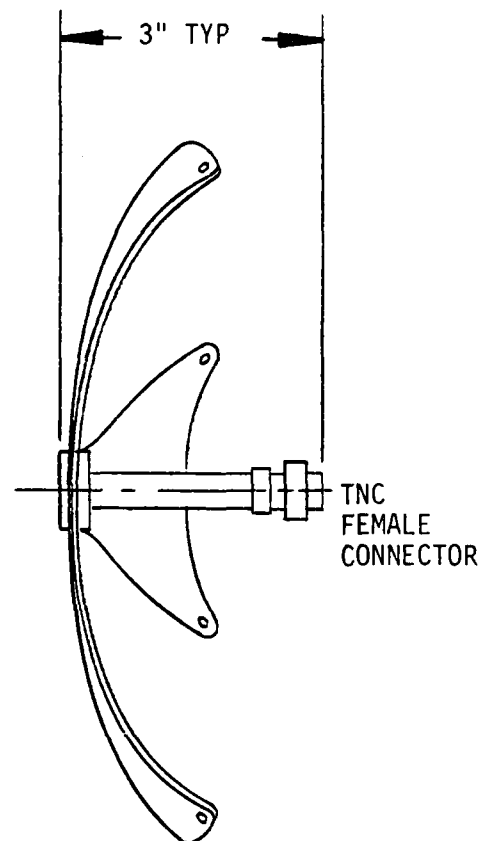
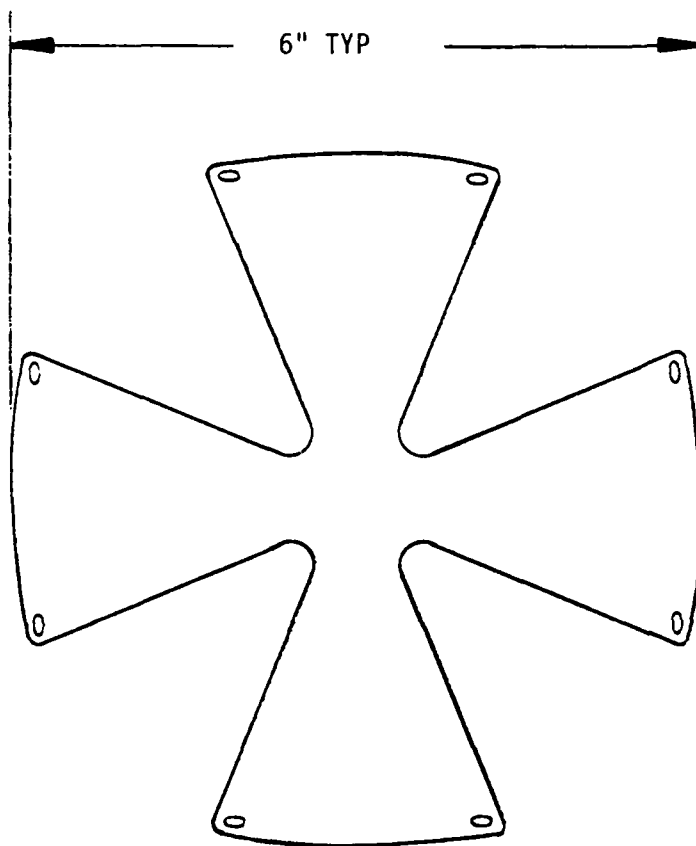


Figure 23. Typical Telemetry System (Record and Playback)

A typical telemetry system is presented in Figure 23. More details on recording techniques are presented in IRIG STANDARD 106-80. Non-Return-to-Zero-Level (NRZ-L) encoding at the PCM is defined such that "one" is represented in bit phase by one level, and a "zero" is represented in bit phase by the other level. Bi-Phase-Level (BIØ-L) encoding, sometimes called "split phase" encoding, means that a "one" is represented by a "one" level with a mid-bit period transition to the "zero" level; and a "zero" is represented by a "zero" level with a mid-bit period transition to the "one" level (see Figure 24).

The second technique for capturing the PCM encoded sensor data uses the TTL output from the PCM unit. That signal, with special PCM clock signals, is converted from a serial bit stream to a computer compatible parallel format and, depending on the test being conducted, is saved in the on-board memory array, or placed on the high-speed parallel output port. Figure 25 is a block diagram of a microcomputer system that will be used to perform this sensor data capturing technique. The system is based on the 68000 microprocessor which was selected for its ability to directly address the 512K byte memory array without segmentation or external memory management. This is crucial because the PCM data must be read and stored in memory, or transmitted out the high-speed parallel port in real time. The extra instructions required to test and readjust segment pointers would require much more time than that available. The 68000 contains sufficient internal 32-bit registers so that all limit checking and memory pointer adjustments can be done without performing time consuming memory array operations for these overhead functions.

The PCM decoder (board), using the TTL PCM data output signal with a couple of PCM generated clock signals, converts the PCM serial NRZ-L data stream to a 16-bit parallel word. Each 16-bit word represents two items of LRE or seat sensor information. When each new 16-bit word is assembled, the 68000 will acquire and save it. It will be built using small-scale (SSI) and medium scale (MSI) integration circuits utilizing, where possible, complementary metal oxide semiconductor (CMOS) logic to conserve power.



VSWR: 2.0 : 1 MAX.
 PATTERN: HEMISPHERICAL
 GAIN: ISOTROPIC
 WEIGHT: 4 OZ.
 IMPEDANCE: 50 OHMS

Figure 22. Typical Skull Antenna (for 790 MHz to 847 MHz Range)

The AFAMRL has initially proposed a 1000 sample per second rate for each channel. It is believed that since most mechanical impedances of the human/dummy body occur in the 20-30 Hz range, the type of test data anticipated would be adequately represented using this sample rate. Because there are 96,000 analog samples per second, an ultrahigh speed successive approximation type analog-to-digital converter is used in the PCM unit to develop the 8 bit digital word representation of each analog sample.

The 8-bit resolution of the PCM module was established at by default. After considering errors totaling 2 percent, introduced by the transducers, amplifiers, filters, and the PCM analog error of 0.4 percent, the addition of more bits would increase only the resolution, not the accuracy. Since this is of no significant benefit, and because an increase beyond 8 bits adds greatly to the complexity of the local storage system, 8 bits was determined to be adequate. Reducing the resolution to 7 bits only marginally degrades the system accuracy, but provides no specific advantages.

Telemetry standards, as they pertain to the encoding, filtering, and transmission of data from PCM units, are presented in IRIG STANDARD 106-80, published by the Telemetry Group of the Inter-Range Instrumentation Group, Range Commanders Council, September 1980.

Data Capture

The standard telemetry technique for encoded sensor data retrieval will be the method used primarily on the rocket sled at Holloman Air Force Base. The LRE will be delivered to Holloman Air Force Base without a transmitter installed. Mechanical mounting provisions and electrical connections will be provided for the installation of the specially modified transmitters compatible with Holloman equipment. Electrical signals connected to the transmitter unit include transmitter power, the filtered PCM encoded data input signal, and the modulated radio frequency (RF) signal output to the skull mounted antenna. A typical skull antenna is presented in Figure 22.

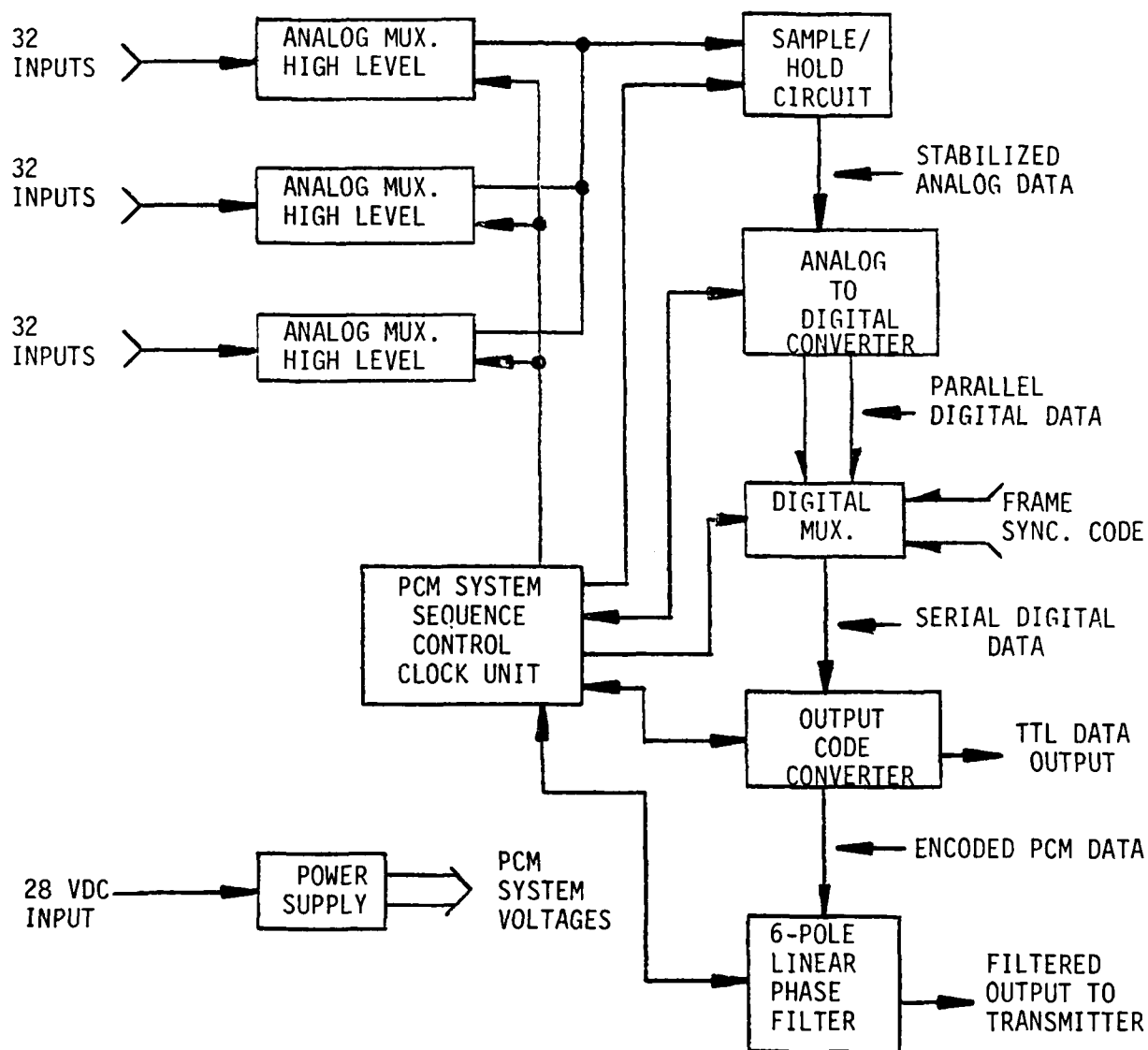


Figure 21. Typical Pulse Code Modulation System

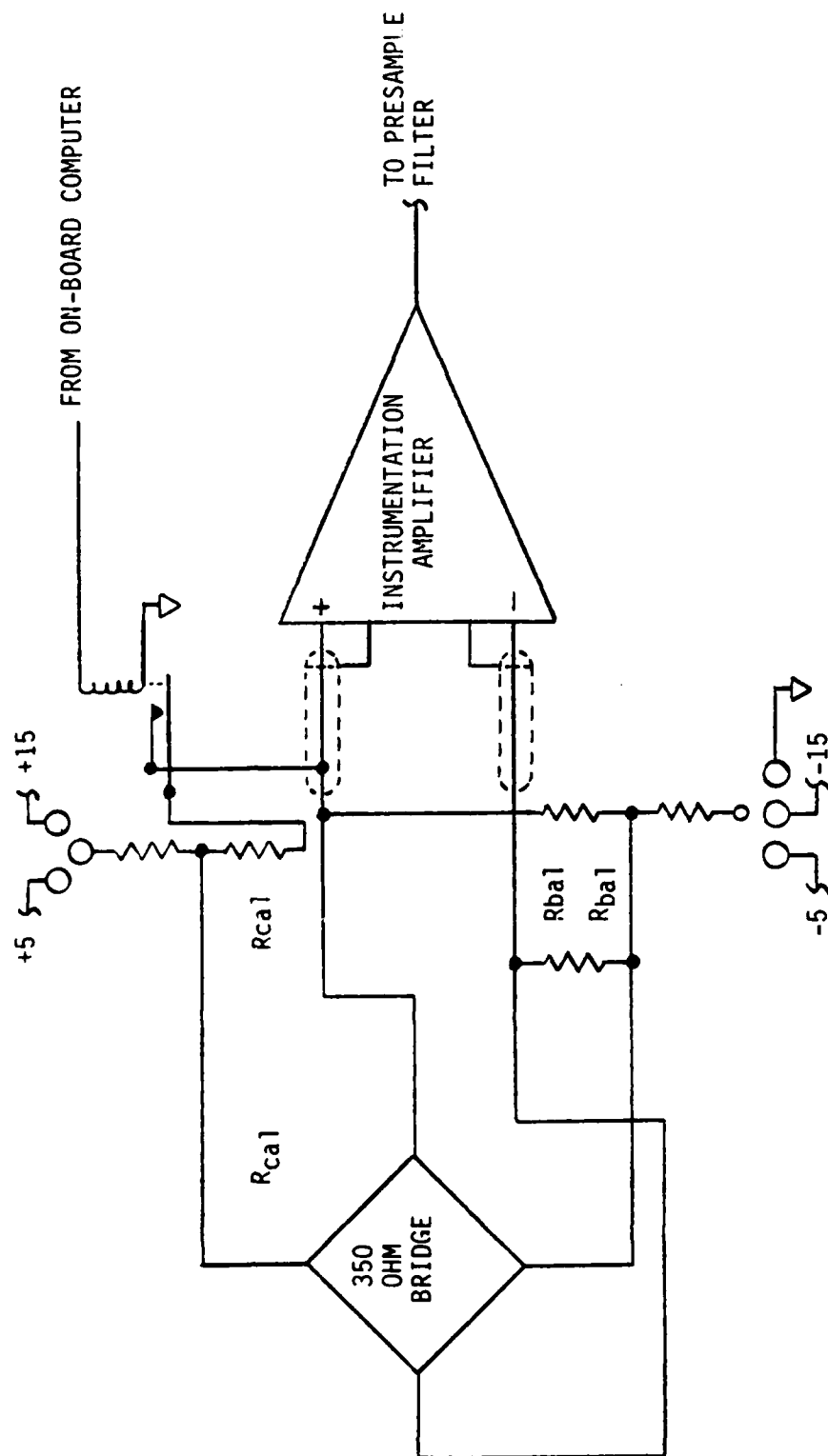


Figure 20. Typical Low-Level "Bridge" Circuit

which is a function of the excitation voltage and the amplifier gain for each channel (see Figure 20).

The presample filters are the circuits that limit the bandwidth to 100 Hz. The 100 Hz limit was established by viewing data previously recorded during ejection tests. It may well be possible to acquire good sensor data with this rate reduced significantly, but there is no practical reason for doing so at this time. Limiting the signals to a bandwidth of 100 Hz prevents aliasing errors which occur if high frequency components are present in the sampled data. Further discussion on specific filter recommendations is presented later in this report.

It is a requirement that the instrumentation system provide up to 26 channels for data originating externally to the LRE. It may be possible to package the conditioning circuits in the LRE. Otherwise, they will have to be included in the seat. In any case, transducer power and excitation sources will have to be supplied from the LRE. Connection between the LRE and the seat transducers will be made via a quick-disconnect located in the small of the back area of the LRE. The quick-disconnect can be implemented by a screw-type MS connector with the threaded coupling removed.

The central element of the instrumentation system is the PCM unit which converts the analog signals from the presampling filters to time-sliced sequential samples presented in an encoded serial bilevel bit data stream. Use of this PCM unit represents the conventional approach to the development of a telemetry system. The recommended PCM unit will be programmable with regard to sampling sequence, sampling rate, and output format. There are some nonprogrammable units available at less cost, but none that meet the present known performance requirements and space constraints. Programmability is essential for future expansion and modification capabilities (see Figure 21).

Seventy-six sensor inputs have been specified, 50 in the LRE, and 26 external to the LRE (in the seat). Reviewing technical literature from PCM manufacturers indicates that the LRE PCM system will be using a 96 high-level input PCM system. Specifying PCM inputs as all high-level type supports the goal of maintaining a capability for easy modifications.

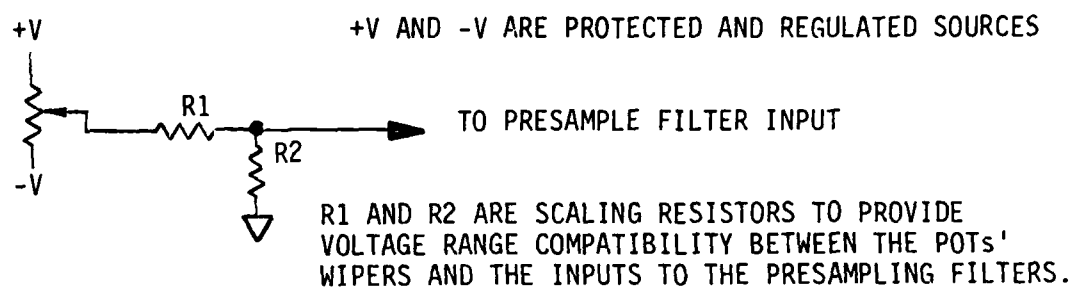


Figure 18. Typical High-Level "Potentiometer" Sensor

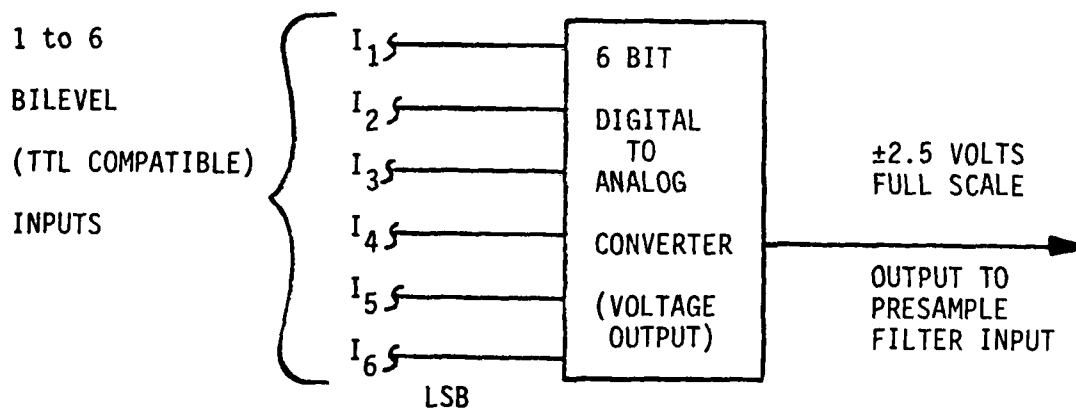


Figure 19. Typical High-Level "Bilevel" Sensor

"telemetry" channel and the on-board memory system. The data captured in the LRE memory would then be extracted after the test, using the high speed parallel port and the portable computer system. In a wind tunnel or laboratory environment, data would probably be captured using the high speed parallel port output only.

Data Sensing

All direct current (DC) type transducers within the LRE, as well as the majority of the sensors in the seat, require well regulated, current-limited voltage sources for transducer excitation. In the event that a sensor should short the excitation voltages, either to ground or to each other, there should be no effect on any other sensor's excitation sources, long term or transient.

There are two general classes of sensors which include most of the sensors within the LRE and the seat. High-level transducers, those not requiring a preamplification stage, will consist of potentiometers (POTs) for measuring joint angular positions (see Figure 18), and several digital-to-analog converters (DACs) for sensing bilevel signals (see Figure 19). Low-level transducers include 350 ohm strain bridge gauges, load cells incorporating 350 ohm strain bridges, and piezoresistive and piezoelectric single and multiaxis accelerometers.

The small signal outputs of the low-level transducers will need amplification to achieve compatibility with the input range of the PCM unit. Precision instrumentation amplifiers, featuring high common mode rejection, very low input voltage noise, and low offset voltage drift characteristics, will be used for this function. They can also have integral twin differential shield drivers to eliminate bandwidth loss due to shield capacitance, if needed. Balancing of the bridge transducers will be accomplished by fixed resistors. Each bridge conditioning circuit will also include a shunt calibration resistor that will be controlled by the on-board computer system. Using this resistor to cause a bridge imbalance will provide a calibration technique to obtain the electrical sensitivity of each transducer channel,

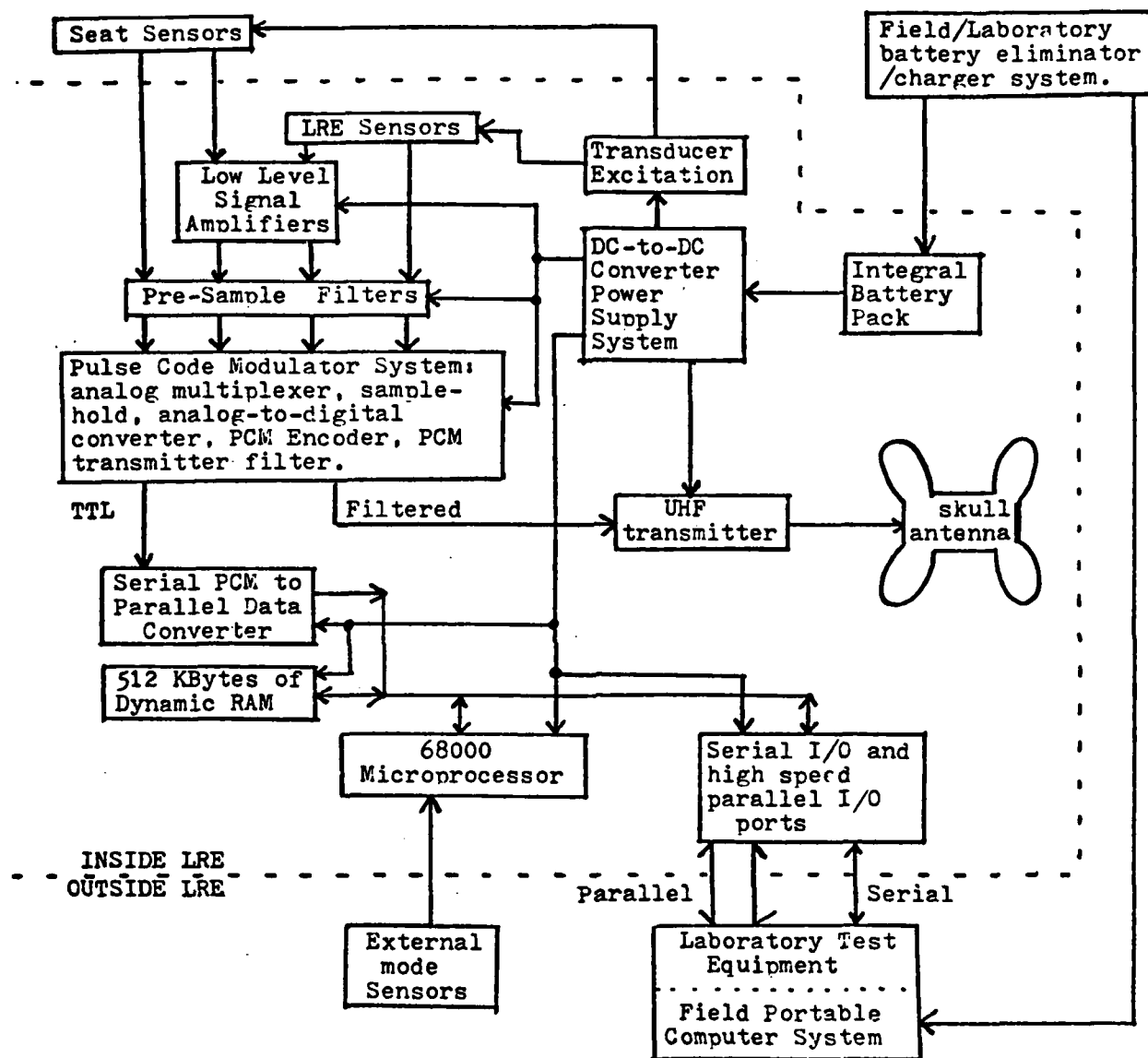


Figure 17. Block Diagram of LRE and Support Electronics Systems

systems testing. Consideration should be given to both on-board data storage and telemetry techniques of data acquisition.

A block diagram, which illustrates the basic elements of the LRE and support electronics systems, is presented in Figure 17. The two major functional sections are: (1) "data sensing," which is a physical phenomenon sensor-to-serial digital pulse train converter, and (2) "data capture," consisting of two techniques for obtaining and recording the converted sensor data. On-line and off-line support and auxiliary equipment include the internal and external power supply systems, test equipment, and the portable computer system.

The primary task of the "data sensing" section is to convert all seat and LRE physical events into a binary level bit stream using standard time-sliced sampling and conversion techniques. As shown in Figure 17, the physical sensors-to-pulse code modulated (PCM) serial data section includes transducer excitation, seat sensors, LRE sensors, low-level signal amplifiers, presample filters, and the PCM unit itself. The PCM unit contains an analog multiplexer, a sample-hold circuit, a high speed successive approximation analog-to-digital converter, a PCM data encoder, necessary timing, control and internal power supply circuits, and a transmitter low-pass filter circuit. A typical pulse code modulation system is discussed later.

The "data capture" section of the LRE is made up of two distinctive techniques of capturing and storing the PCM encoded sensor data for future analysis. One path is from the PCM unit to the transmitter via the filtered data output line and then to the skull-mounted antenna. The signal is received and recorded using conventional telemetry techniques. The other technique of recording sensor data is via the transistor-transistor-logic (TTL) level PCM signal, using a computer bus compatible PCM data to 16 bit parallel data converter, a "68000" microprocessor with nonvolatile program storage and external mode sense capabilities, a 512K byte memory array using dynamic random access memory (DRAM) integrated circuits (ICs), and serial and parallel input/output (I/O) ports to peripheral equipment for the extraction of data and general communication requirements. When the LRE is used on the rocket sled, the data will be captured using both the

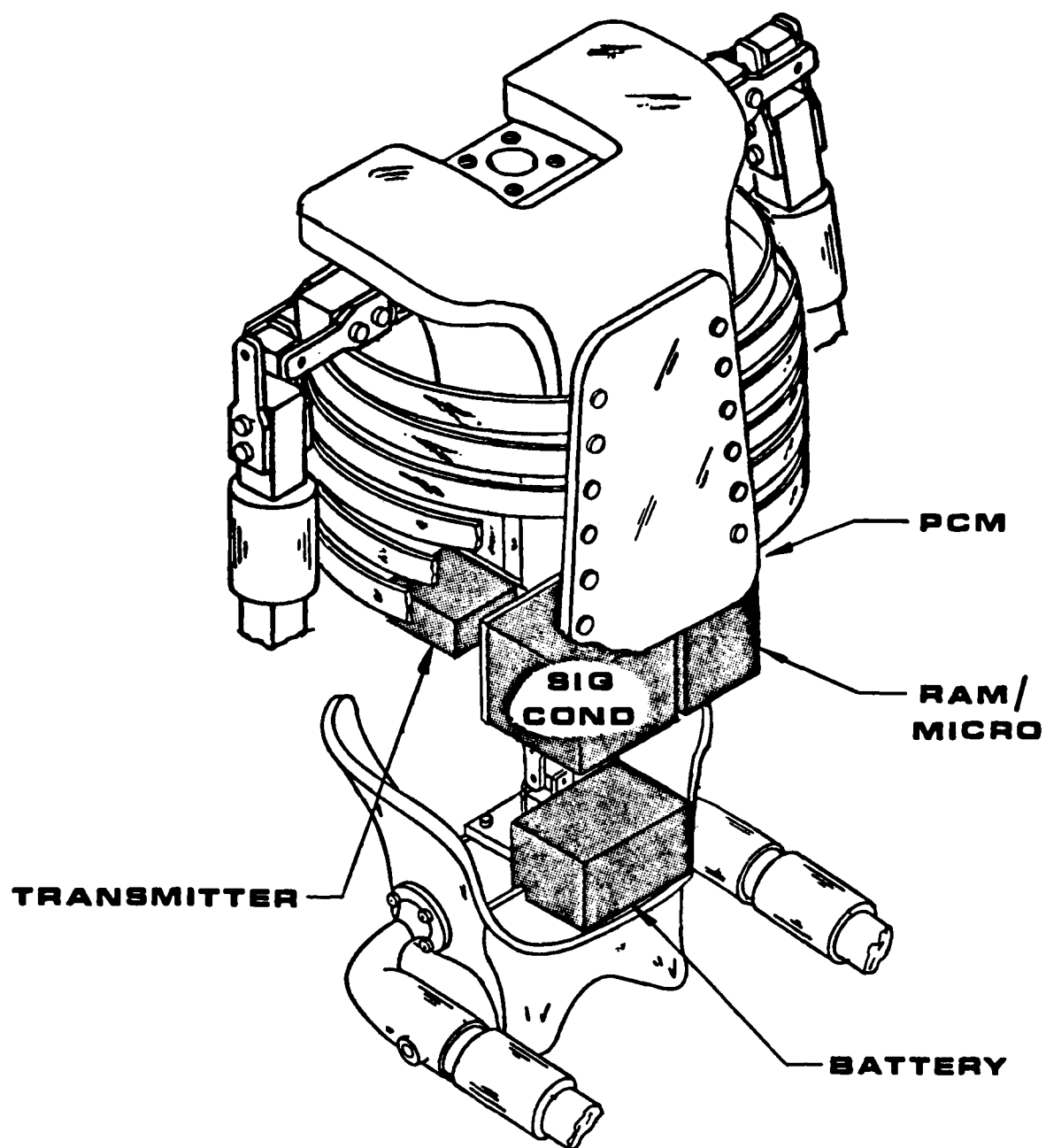


Figure 16. Instrumentation Placement

The "comm" board contains two different types of communication links between the on-board computer system and an external controller, data storage device, or portable computer system. They are designed around large-scale integration (LSI) peripheral ICs that provide all of the necessary communications protocol and computer interface logic, while special function MSI circuits provide the required electrical characteristics for the line driver and line receiver connections to the external peripheral devices. The "serial" port will use a Universal Asynchronous Receiver/Transmitter (UART) LSI device; and it will interface to the external devices using the widely accepted electrical standards of the Electrical Industry Association (EIA) Standard RS-232-C, and the Comité Consultatif International Téléphonique et Télégraphique (CCITT) Recommendation V.24, Orange Book. The "parallel" port will use LSI and MSI circuits to implement the Institute of Electrical and Electronic Engineers (IEEE) Standard 488-1978, which is a subset of the Hewlett-Packard Interface Bus (HP-IB), commonly referred to as the General Purpose Interface Bus (GPIB). It is a short haul, high speed, very versatile communications technique, widely used as the standard for parallel communications.

The 512K byte DRAM array will be a single board containing 16 256K bit DRAM ICs. These are new parts that will be available from several manufacturers in early 1983. The reasons for selecting them over mature 64K bit DRAM ICs are power savings and board space savings. There is, of course, a technical risk involved in initiating a design with new parts of such complexity. In this case, however, the similarity of the 64K bit and 256K bit packages provides an easy fall-back position, in case of technical or supply problems developing with the 256K bit parts. Using the 64K bit DRAM ICs will necessitate the use of four boards to implement the same 512K byte DRAM array.

The DRAM controller board is the interface between the 512K byte DRAM array and the 68000 microprocessor, and it consists primarily several extremely sophisticated LSI ICs that provide microprocessor bus interfacing, timing control, hidden refresh, row/column multiplexing, and capacitive load drivers. A few SSI and MSI ICs support these ICs and they will be of CMOS logic, where possible. With a possible minor modification, this DRAM

controller will satisfactorily drive either reconfiguration of the 512K byte DRAM array, using either 64K bit DRAM ICs or 256K bit DRAM ICs.

The processor board is the central element of the on-board computer system. Its primary element is the Motorola 68000 microprocessor, a high performance 16 bit (external) unit with an internal 32 bit bus structure, which is capable of directly addressing 16M bytes of memory. It has 17 multifunction 32-bit internal registers, and it is contained in a 64-pin package. Other functions on the 68000 board include a power-on reset circuit, an 8 MHz master clock derived from a 16 MHz crystal clock oscillator, a dead-man watch dog timer circuit, 4K bit by 16 bit nonvolatile memory program storage, a status/mode register which feeds one of the bilevel-to-analog DACs in the instrumentation section, address decoding and system control circuitry.

Another fairly new technology (about 3 years old) may be implemented on this board. An attempt will be made to lump together all of the SSI and MSI circuitry involved with address decoding and system control circuitry into a field programmable logic array (PLA). The advantages of attempting this will be a decrease in power, and a considerable savings in board space.

The on-board power supply system consists of a rechargeable battery and a DC-to-DC converter system. The converter gets its power from nominal 28 volts supplied externally through an LRE ankle connector, or internally from a rechargeable battery pack. Five well regulated DC outputs from the converter provide power for the transducers, data sensing (analog) section, and the computer (digital) section. The PCM, and the transmitter (when used), operate from the same supplied 28 VDC input. Figure 26 represents a typical LRE power system. Note that a separate +5 VDC regulator supplies the digital section. While the analog and digital sections do not have totally isolated ground systems, elimination of errors and noise due to "ground loops" is accomplished by using heavy conductor ground lines and a "system ground point."

The on-board computer system will have several modes of operation. The 68000 Central Processing Unit (CPU) on the processor board will poll an

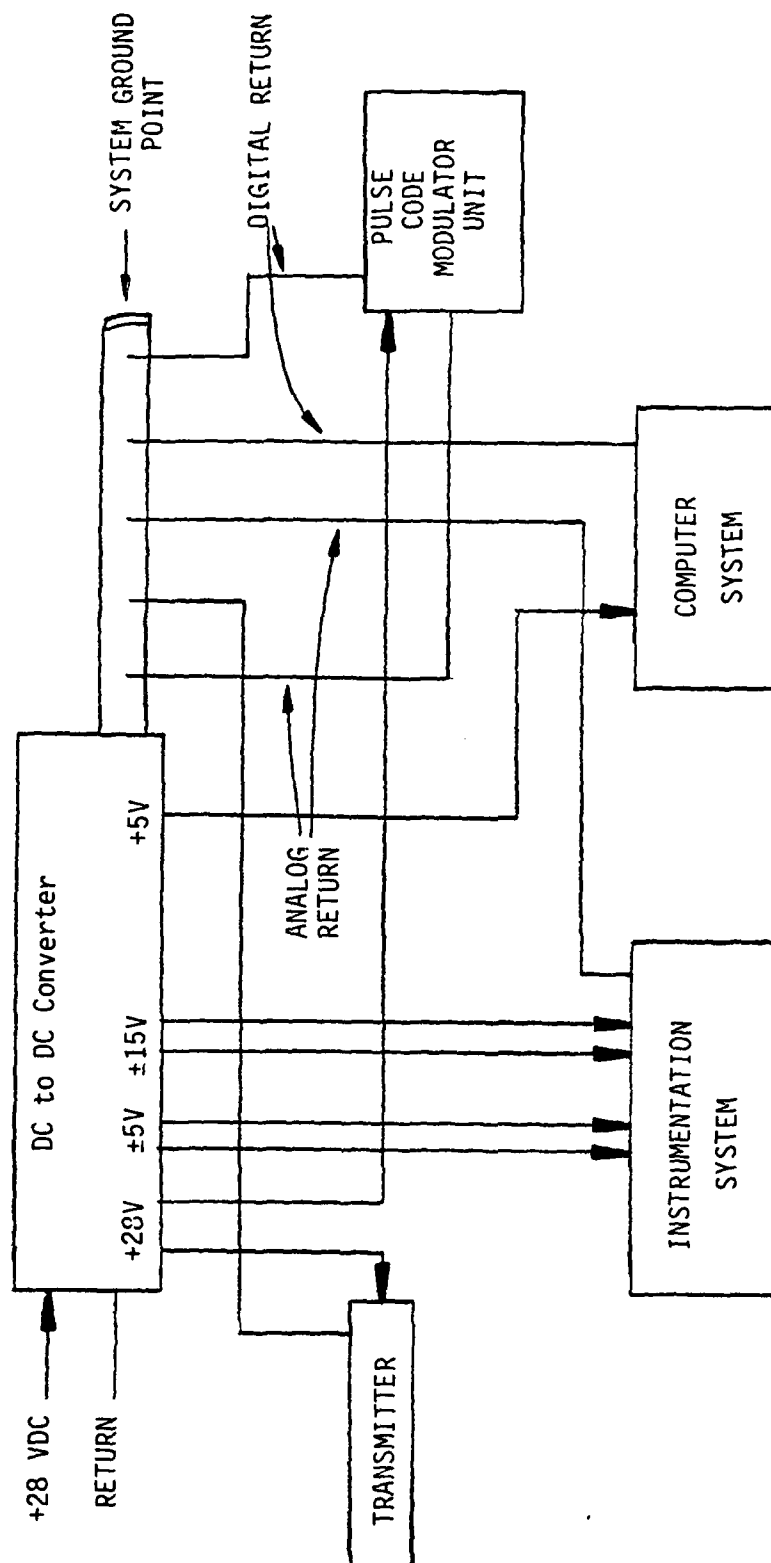


Figure 26. Typical LRE Internal Power System

external mode input, which will be called Start Data for now, after a successful power-up sequence has occurred. If the Start Data signal line is grounded (logic zero) when power is applied, the system will enter the "sled" mode of operation. A typical "sled" mode operation follows. A 1-minute timer is started, and the transmitter is turned on for unmodulated carrier tests as per IRIG 106-80. Power is applied to the transducers and the instrumentation section to allow for temperature stabilization, and a complete set of DRAM array tests will be conducted to ensure perfect on-board memory operation. At the end of the DRAM test, the mode and status will be posted in the Status Register which feeds the bilevel-to-analog DAC in the instrumentation section. When the 1-minute timer times-out, the PCM is turned on and the CPU begins reading the PCM data and storing it in the DRAM array. When the array is filled, writing continues at the beginning. During this time, the processor is concerned only with storing the PCM data and monitoring the start data signal; and no communication I/O is performed. When the Start Data signal goes high, which indicates LRE separation from the seat, it is an indication that the critical data collection period is over; and the writing of PCM data will cease. The computer will then post its current status and mode, delay about 2 seconds, and then turn off the power to the transmitter, all of the instrumentation, and the PCM module. When the LRE lands, only the on-board computer will have power applied. During this low power mode of operation, the CPU is monitoring the serial communications port, waiting for a hook-up for further instructions. When the LRE is recovered, a field battery power system will be attached to aid the on-board battery system. The portable computer system will be attached via the "serial" communications port, and the high speed parallel port will be attached to the portable computer system for the extraction of the sensor's data from the DRAM array. The transfer will begin with the oldest data, not the data in the lowest DRAM address.

If the Start Data signal is high when power is applied, the LRE is in a "non-sled" environment, and the computer monitors the serial communications port for instructions. Data can be read from the PCM and placed directly onto the high speed parallel port with no activity in the DRAM array, or selected parameters can be output through either the serial or parallel ports as needed.

Supporting Investigations

Three primary areas of concern in any data monitoring system are: data capture techniques, presample filtering, and memory errors. This section addresses these subjects.

Data Capture

One of the purposes of this study is to investigate trade-offs of local storage on-board the LRE versus radio telemetry. Telemetry is the means of data acquisition used historically for a requirement of this nature, while local storage seemed promising because of the ever-increasing density of memory and because the data of interest would occur during a 5-second period. A requirement of the instrumentation system that affected this comparison was that the data collected during the period between seat ejection and seat/LRE separation had to survive, even if the parachute failed. This, of course, imposed no requirement on the telemetry technique since the data would be safely on tape at the receiving stations at the time of impact. However, for the local storage approach, it forced consideration of only true, nonvolatile memory since it was determined that designing an electronics package to survive intact, from a high speed impact, was not a cost-effective approach. With nonvolatile memory, the data could be retrieved only if the nonvolatile memory components survived.

Four types of nonvolatile memory were evaluated: magnetic bubble memory, magnetic tape, programmable read only memory (PROM), and electrically erasable programmable read only memories (EEPROMs). All of these types of memory have a characteristic that is undesirable for this application. They cannot accept data at the LRE data rate of about 100K bytes per second. The remaining option involved writing to volatile random access memory (RAM) in real time, then transferring to the nonvolatile memory following the data collection period. This possibility was eliminated after viewing films of sled runs at Holloman Air Force Base during which the parachute failed. The total elapsed time from seat ejection to crash was less than 5 seconds, leaving no possibility of storing the data in any of the nonvolatile memory

types. For these reasons, a "local storage only" system was eliminated from further consideration.

One of the early concerns of the telemetry approach was the cost of the ground receiving equipment. When time the "local storage only" option was eliminated, it was known that the Holloman Range had all necessary receiving equipment. The only additional expense to add telemetry to the LRE was the cost of an antenna installation and the use of a Holloman Air Force Base supplied transmitter. Since these costs were relatively minor, considering the benefits of telemetry captured data, the use of telemetry became a viable option.

One of the major reasons for investigating local storage was to use this as a method of eliminating data dropouts that occur due to the relative position of the skull antenna, seat, and receiving antennas interfering with the transmission, and the atmospheric disturbances which infrequently occur. The first cause of dropouts has been largely eliminated by the use of three receiving stations placed at different locations around the track. Eliminating the second cause of dropouts is not as easy. Personnel at Holloman Air Force Base have been trying to develop a system which would use two separate transmitters and antennas placed in the LRE. The first transmitter and antenna would be used for sending the data in real time. The second transmitter and antenna would be used for sending the same data, but only after it had passed through a digital delay module, possibly a set of shift registers. This system should nearly eliminate data loss due to the atmospheric disturbances, but it has not yet been perfected. A major problem is the selection of a suitable location for the second antenna.

After telemetry was determined to be the primary data capture technique during a sled-run test, local storage was viewed as a back-up technique, rather than as an alternative technique. Of course, this description of "back-up" would apply only during sled-run tests. In test environments where telemetry is not appropriate, local storage would be the most practical method of data collection.

For example, during calibration testing of the LRE system, the on-board computer system would be used to transmit any requested channel of data through either the serial (RS-232-C) or high speed parallel (IEEE-488) interface ports. During wind tunnel tests, all channels of data can be captured in real time using the IEEE-488 port. This would permit the user to acquire, display, and store the data using standard laboratory equipment. Lastly, if the LRE were used in a test environment where the data collection period would be brief (5 seconds or less), the data could be stored on board the LRE and extracted later. With the auxiliary equipment selected for part of the LRE system, and disregarding the telemetry support needed for the sled-run tests, the user of this LRE system can be totally independent and self-sufficient.

Filtering

An unique problem in determining the accuracy of an instrumentation system arises when the system samples the data at discrete times. During signal reconstruction, it is difficult to determine what happened to the continuous input between the time-sliced samples. A widely quoted sampling theorem states that it is theoretically possible to reconstruct the input if a sample rate of two times the maximum input frequency is used.

As a practical matter, this is impossible for two reasons. First, an ideal filter cannot be built to limit the frequency to one-half the sampling rate. An ideal filter, for this application, would be a low pass filter with a flat passband response, infinite attenuation at the critical (cutoff) frequency, zero response past cutoff, and a linear phase response in the passband. However, ideal filters are mathematical constructs that are not physically realizable. In addition, an infinite order hold device needed to reconstruct the original data from discrete samples is not possible. Thus, it is reasonable to question what is a practical, achievable accuracy.

Although it is not part of the instrumentation system, the method used to interpret the sampled data after it has been collected has a significant effect on error. Probably the simplest method is to assume the input

remains constant between samples. This method introduces significant errors at even relatively high sample rates. At 10 samples per cycle, a sine wave could change from 0 degrees through 36 degrees which, of course, is over half its peak value. The first improvement over this "zero order hold" technique is to make use of two points and assume that the data fall on a straight line between them. Greater improvements can be made by including more points and defining more complex curves to pass through them. For the LRE system, it is possible to look ahead at data samples to help determine the input value between earlier samples, since the data reconstruction will not take place in real time.

In order to determine specific accuracy figures for various sample rates using different levels of interpolation, a computer program was written to simulate a steady state input and sampler. The results of the sampler were used to predict values between samples using first through ninth degree polynomials. These results were then compared to the simulated input to determine error. Figure 27 shows the results for first through ninth degree polynomials for sample rates of two through ten per cycle.

These curves show that if high frequency signals are allowed to enter the sampling process, aliasing errors (sometimes called frequency folding errors) will result. The source of the high frequency signal does not matter. Whether it is noise or insufficient sampling rates, the true dynamics of the original signal will be distorted and interpreted improperly as a lower frequency signal. Some form of filtering is necessary to attenuate potential high frequency components of the signal before it is sampled.

A low-pass filter is used to reduce man-made electrical interference noise, to reduce electronic noise, and to limit the bandwidth of the analog signal to less than half the sampling frequency in order to eliminate frequency aliasing (Datel/Intersil, 1979). According to this source, electronic noise "is random noise with noise power proportional to bandwidth and is present in transducer resistances, circuit resistances, and in amplifiers themselves. It is reduced by limiting the bandwidth of the system to the minimum required to pass desired signal components. No filter does a perfect

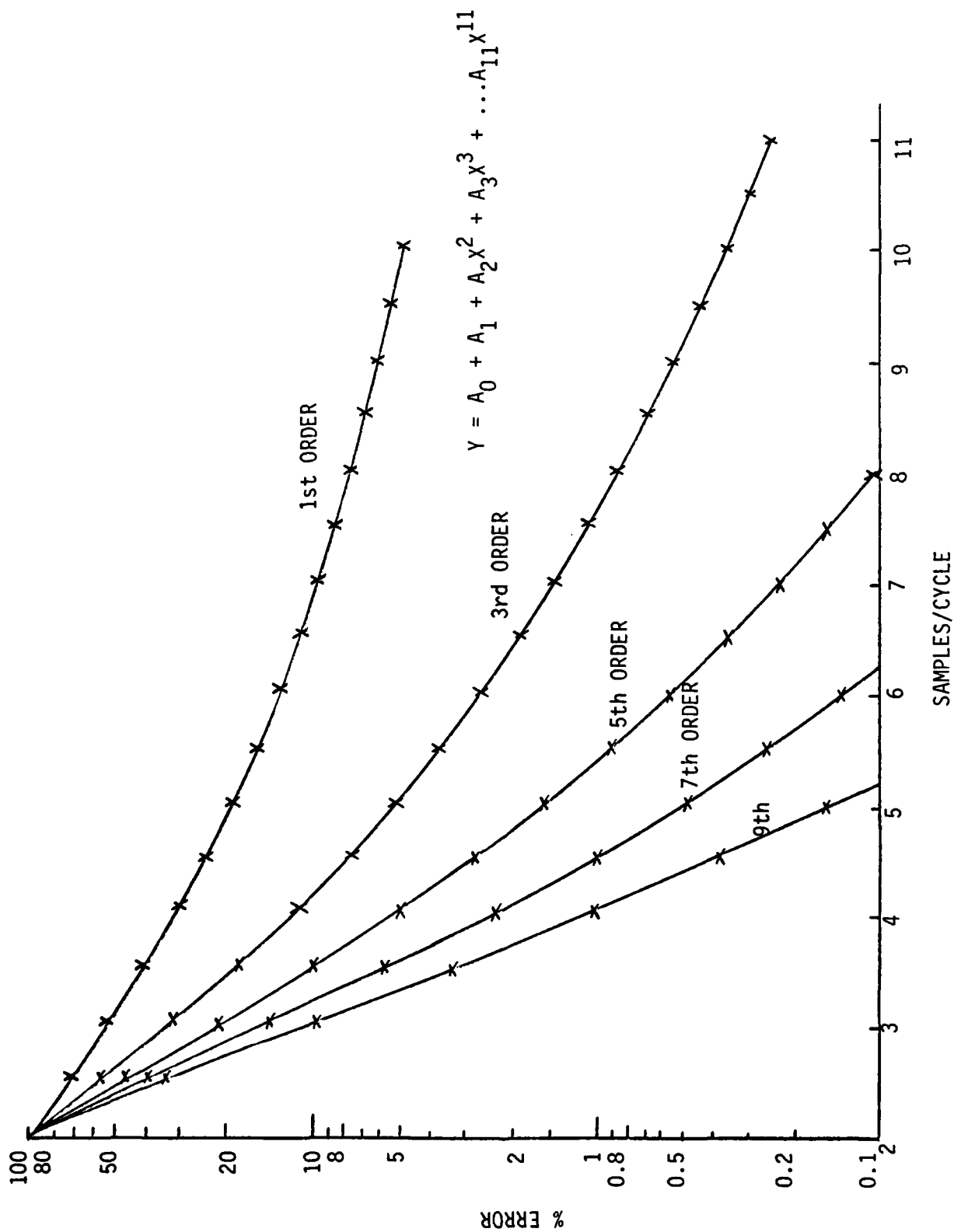


Figure 27. Aliasing Error versus Sample Rate

job of eliminating noise and other undesirable frequency components; therefore, the choice of a filter is always a compromise.

Generally speaking, a Butterworth filter should be used when the primary concern is signal amplitude accuracy, and a Bessel filter will be used when signal phase relationships are most important. The Bessel filter is a minimum-time-delay filter, whose transfer function approximates a constant time delay in the passband. The amplitude response is Gaussian, with noticeable droop at about three-tenths of the critical (cutoff) frequency, and is 3 db down at the critical frequency. The fast settling time and minimal overshoot in the step response make them desirable for pulse applications and phase-sensitive signal processing, and are often used in reconstruction of waveforms and direct frequency measurements. The Butterworth filter is a realizable approximation of the ideal filter characterized by a maximally flat amplitude response in the passband. Attenuation is 3 db down at the critical frequency and rolls off at a -6 db per octave per pole (-20 db per decade per pole) rate beyond the critical frequency. The step response displays moderate overshoot which increases with the number of poles, and it has a slightly nonlinear phase response in the bassband. It is an excellent choice for general purpose filter applications, and is particularly useful where passband gain accuracy is important, as it is in the LRE system. Therefore, the Butterworth filter is favored for use on all analog sampled channels.

Building a filter of any complexity with available components was, until recently, a delicate and expensive task. A six pole filter has the following transfer function:

$$\frac{A_0}{(s^2 + \alpha_1 s + \omega_1^2) (s^2 + \alpha_2 s + \omega_2^2) (s^2 + \alpha_3 s + \omega_3^2)}$$

This illustrates the complexity of the circuitry involved with a simple filter. By using discrete parts, there was always the danger of introducing more errors with the filter circuitry than those eliminated. As a result, many early sampled data systems used very simple filters or none at all. The users of such systems hoped that no signal frequencies would occur which

would result in erroneous interpretation. Fortunately, today's technology permits the inclusion of fairly complex filters that are well characterized, easy to use, and inexpensive.

To determine the effects on system error of several filters, differing in complexity and cut-off frequency, plots were made of the product of filter attenuation times interpolation error versus frequency, using Butterworth filters. These curves are shown in Figure 28. Filter frequencies were selected based on the goal of accurately measuring data up to 100 Hz with a sample rate of 1000 per second.

The curve obtained using a four-point, third degree polynomial, interpolation with a four-pole filter cut-off at 150 Hz shows a maximum error of about 1.5 percent at 200 Hz. This is satisfactory performance and is an easy-to-implement solution. There are some integrated six-pole filters announced that will provide an even better solution. The curve obtained using a four-point interpolation with a six-pole Butterworth filter cut-off at 138 Hz shows a maximum error of less than 1 percent, effectively eliminating error due to high frequency aliasing. These curves also indicate that a minimum of four points should be used in the reconstruction (interpolation) process.

The procedure for implementing the four-point interpolation used in the error analysis is illustrated by the following example:

Given a set of consecutive data samples, 56, 93, 104, and 76, with the requirement to determine the value of the data between samples 93 and 104.

If a two-point interpolation were used, only the 93 and 104 samples would be needed. The equation could be written by inspection: $Y = 93 + 11t$, where $t = 0$ to 1.

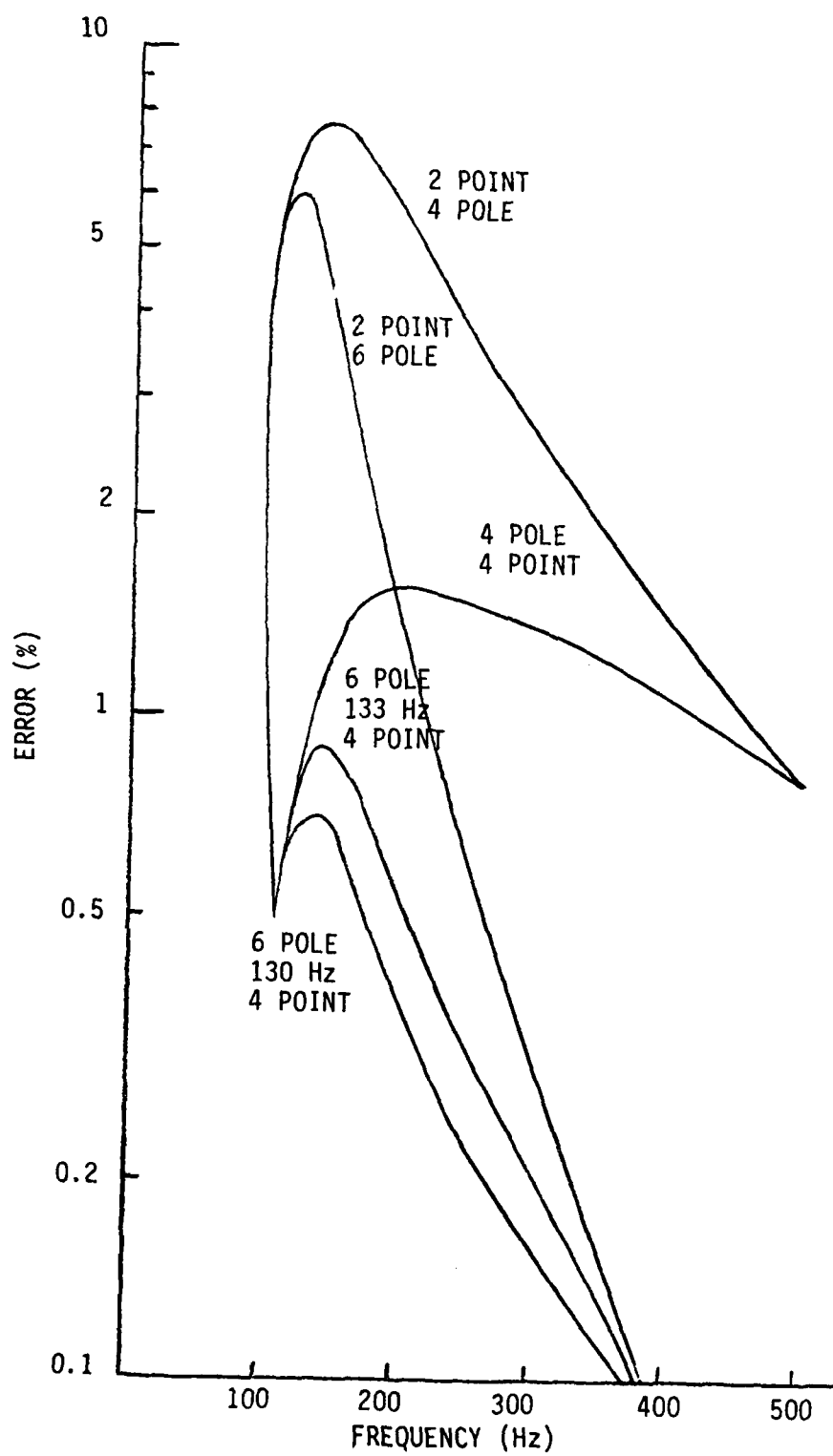


Figure 28. Percent Error versus Frequency

For the four-point interpolation, the samples 56 and 76 are also required. An equation which, in general, passes through these four points is of the form:

$$Y = A_0 + A_1t + A_2t^2 + A_3t^3$$

The four data samples are used to determine the A coefficients. Letting $t = 0$ at the first sample ($Y = 56$), the four equations for $t = 0, 1, 2$, and 3 are:

$$Y_0 = A_0 \quad (t = 0)$$

$$Y_1 = A_0 + A_1 + A_2 + A_3 \quad (t = 1)$$

$$Y_2 = A_0 + 2A_1 + 4A_2 + 8A_3 \quad (t = 2)$$

$$Y_3 = A_0 + 3A_1 + 9A_2 + 27A_3 \quad (t = 3)$$

Inverting the matrix to solve for the A terms yields:

$$A_0 = Y_0$$

$$A_1 = (-22Y_0 + 36Y_1 - 18Y_2 + 4Y_3)/12$$

$$A_2 = (12Y_0 - 30Y_1 + 24Y_2 - 6Y_3)/12$$

$$A_3 = (-2Y_0 + 6Y_1 - 6Y_2 + 2Y_3)/12$$

Substituting the samples 56, 93, 104, and 76 for Y_0, Y_1, Y_2 , and Y_3 , respectively, gives:

$$A_0 = 56, A_1 = 45.6\overline{66}, A_2 = -6.5, A_3 = -2.16\overline{66}$$

The data between the points 93 and 104 are given by:

$$Y = 56 + 45.67t - 6.5t^2 - 2.167t^3 \text{ for } t = 1 \text{ to } 2.$$

See Figure 29 for a graphic representation of this example.

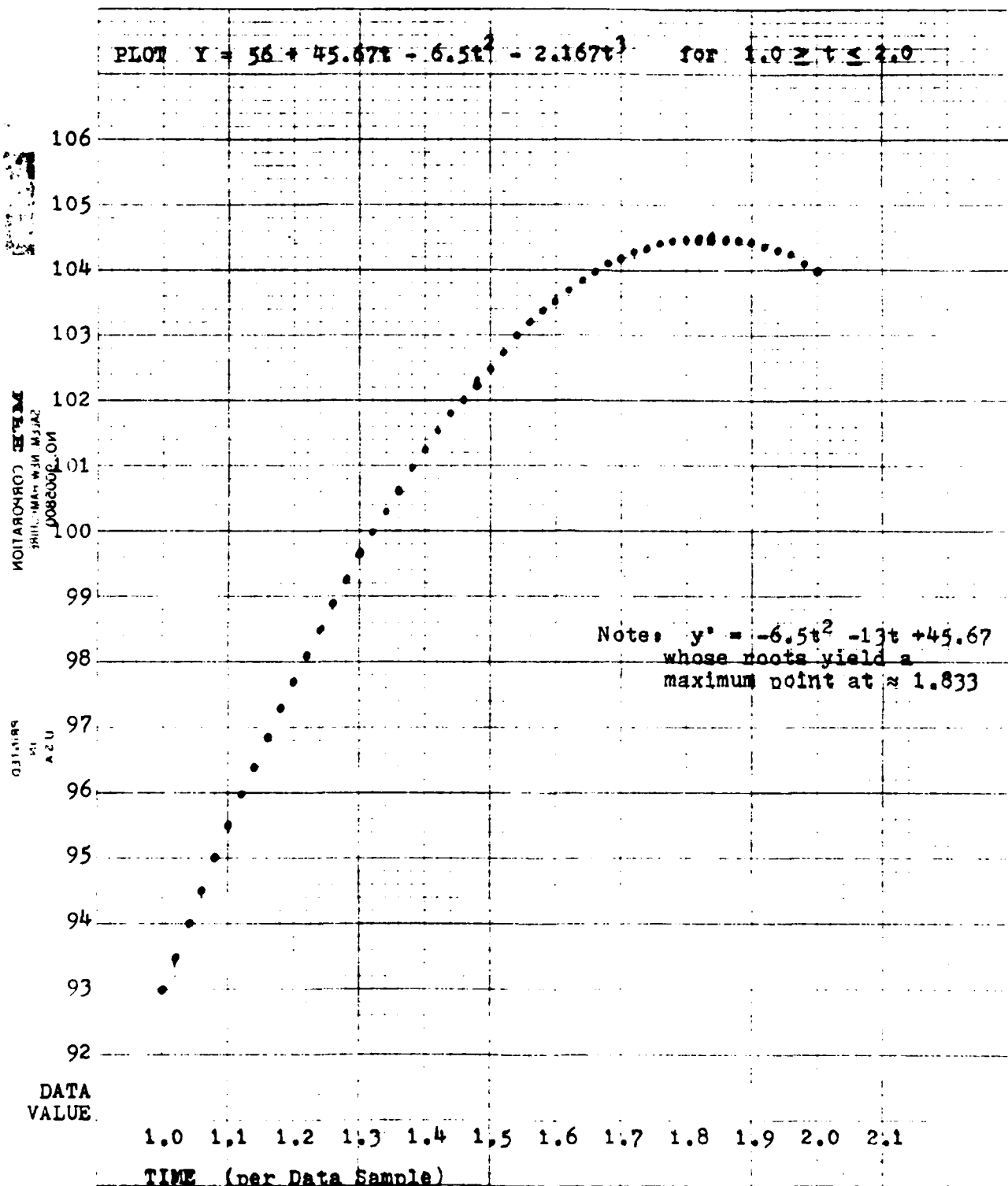


Figure 29. Four-Point Interpolation Example

AD-A151 749

PRELIMINARY DESIGN OF A LIMB RESTRAINT EVALUATOR(U)
SYSTEMS RESEARCH LABS INC DAYTON OH R P WHITE ET AL.
DEC 84 AFAMRL-TR-84-042 F33615-81-C-0500

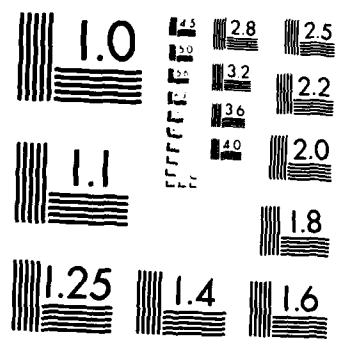
2/2

UNCLASSIFIED

F/G 6/7

NL

										END			
										FORMED			
										DTIC			



MICROCOPY RESOLUTION TEST CHART
NATIONAL BUREAU OF STANDARDS-1963-A

Memory Errors

The two general classes of DRAM array system errors are "hard" and "soft" types of errors. The hard error will be evident as a permanent failure, appearing either as a fixed logic one or a fixed logic zero. Sources of hard errors include a stuck memory bit, memory chip failure, and interface circuit failures. Hard errors will be detected in the LRE, and flagged as errors, during the power-up DRAM diagnostics. A soft error is a temporary error, and it may be overwritten with a low probability of repetition. The sources of soft errors include Alpha particles, system noise, and power glitches. Use of error detection and error correction circuitry takes care of the majority of the recoverable soft errors. Some of the new complex VLSI circuit devices include error checkers and error correctors for memory systems. One DRAM manufacturer's general rule of thumb is that if the memory system cannot tolerate any memory error at all and the system's total memory capacity is 512K bytes or more, then double bit error detection and single bit error correction is recommended. The advantage of such a system is obvious, but the price to be paid is more than the LRE system can tolerate. An additional six bits, called check bits, are needed for each 16-bit word in the DRAM array. This represents a 38 percent increase in memory size and power requirements, which corresponds to another memory board when using 256K bit DRAM ICs, or another two memory boards when using the 64K bit DRAM ICs. The error detection and error correction circuitry also increase the memory access delay times to a point of critical conflict, since the information contained in the check bits must be analyzed in each read operation; and they must be generated for each write operation.

In the LRE system, soft errors will be detected as single data points completely off a continuous curve and can be discarded when detected. Soft errors generated by power glitches can be eliminated by careful DRAM array board layout techniques, as per DRAM manufacturers' recommendations. Another technique for flagging "soft" errors involves saving a Longitudinal Redundancy Check or a Major Frame Checksum value for each Major Frame of data captured for later analysis.

System Conceptual Design

In order to develop a practical design concept for the LRE instrumentation, it was necessary to determine the commercial availability of components and systems that could be used. This section presents the results of these efforts, listing specific parts that are thought to be the best device available for the application. Although many design details are presented, there is no intent to represent a completely detailed design. Design was pursued to the extent necessary to establish parts compatibility and obtain reasonable estimates of cost, power and size requirements, performance, and risk areas.

Data Sensing

- Transducers

The types of transducers identified include potentiometers, load cells, strain gauges, accelerometers, and bilevel inputs. In addition, there are 26 seat sensor inputs from unknown sources.

Potentiometers. Potentiometers were selected for measurement of the angular joint positions. Units were found that could be accommodated in the joint mechanical design and provide the desired accuracy. The signal conditioning requirements for potentiometers are simple, and the units themselves are relatively inexpensive. Spectrol Model 142 potentiometers having the features listed below were selected.

- Servo mount
- One-half inch diameter
- Continuous rotation
- Single turn
- Center tapped
- One percent linearity

Load Cells. A load cell-type transducer was required to measure the resulting forces when a joint is pushed beyond its normal limits. The

primary requirement was to find a unit small enough to be accommodated in the joint mechanical design and cover the desired ranges. Secondary considerations were ease of electrical interface, calibration, and cost. A transducer manufactured by A. L. Design of Tonawanda, New York, provided a reasonable solution to all these goals.

Their Model ALD-MINI-T is one-half inch in diameter, cylindrically shaped, and one quarter of an inch high. It incorporates a full 350 ohm bonded strain gauge bridge and is a static device. This DC response characteristic is desirable for this application and eases calibration procedures. It is available in ranges of 200, 500, 1000, 2000, and 3000 pounds, full scale.

Accelerometers. A reasonably small triaxial accelerometer with DC response was required for the LRE torso center of gravity acceleration measurement. A piezoresistive transducer, manufactured by Entran Devices, Inc., of Fairchild, New Jersey, meets the requirements. Their Model EGA3-1 is a three-axis unit using active semiconductor gauges fully compensated for temperature changes. It is available in ten ranges from ± 5 Gs to ± 5000 Gs. Mounting and orientation are simplified by two 10-32 tapped holes. Other characteristics are:

- Size = 0.8 by 0.8 by 0.65 inches
- Weight = 20 grams, nonlinearity = 1 percent
- Transverse sensitivity = 3 percent maximum

A more demanding accelerometer requirement resulted from the specification to measure acceleration in each forearm of the LRE. Because of the location, the primary characteristics of a suitable device were small size and weight. A piezoresistive triaxial accelerometer (DC responding) meeting these requirements could not be found. An acceptable unit was found in an Endevco Corp. Model 23 triaxial, piezoelectric accelerometer. It is not a DC responding transducer; its lower frequency limit is about 5 Hz. Because of this characteristic, the calibration procedure will require a shake table rather than the more simple rate table. However, it will be capable of measuring the accelerations occurring during limb flail. This relatively

expensive transducer measures only 0.2 by 0.25 by 0.3 inch, and weighs less than 1 gram.

Bilevel Signals. Bilevel signals generated from within the LRE will be TTL Compatible signals. Any seat bilevel signals will be input as, or converted to, TTL levels before application to the bilevel-to-analog converters.

- Signal Conditioning

The actual printed circuit boards will be approximately 4 inches high and 5 inches wide, and will plug into a rigid card cage, obtaining power and control bus signals from a motherboard. The final number of boards will depend on the IC packing density and on the configuration of the 26 seat parameters. Assuming half the input signals are high level and half the signals are low level, and assuming that the MF-6 filter is not available, the board population described as follows results. Six 14-pin DIPs will be instrumentation amplifiers. Three 14-pin DIPs will be analog switches. Twelve 20-pin DIPs will be the Reticon multipole filters. The remaining room on the board will be mostly resistors and straps, with some decoupling capacitors where needed. Since this board can only handle 12 analog signals, the LRE system will need at least eight of these boards to satisfy the instrumentation system requirements. If the MF-6 filters are used, it might be possible to instrument 16 analog channels per board, reducing the total board count to six.

High temperature conditions within the LRE due to the greenhouse effect of the canopy of the rocket sled and the internal power usage of the device are a potential problem, but the severity cannot be predicted. Therefore, it is suggested that some form of temperature measurement be included in the instrumentation section, at least for the prototype systems. The circuit shown in Figure 30 will provide to the analog sampling system a reading of 1.491V at 25°C. The output of the temperature sensing circuit increases 5 millivolts per 1°C increase. This would yield a signal of 1.866V at 100°C. The sensor itself is very small and can be mounted nearly anywhere. It probably should be mounted in either the computer section or the

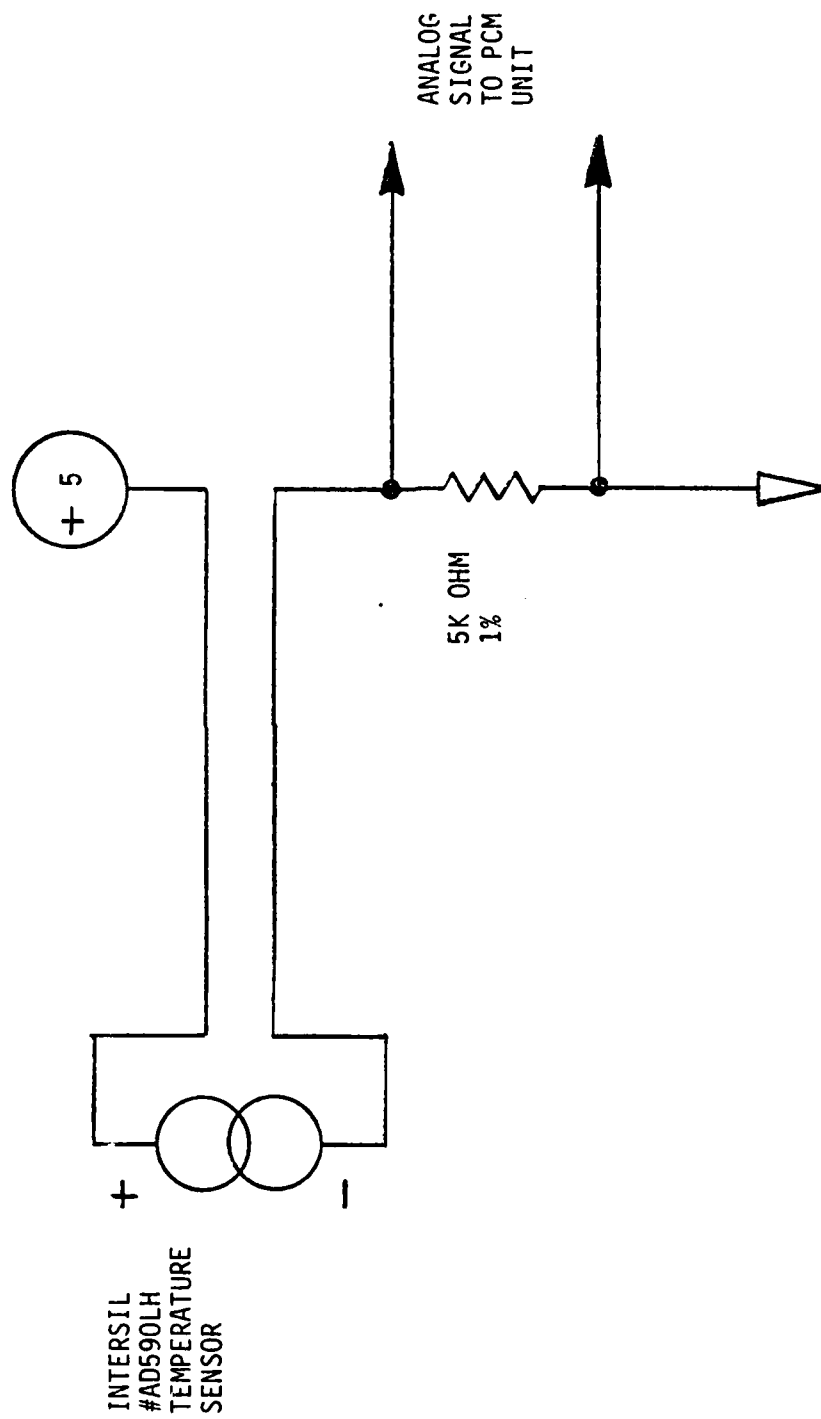


Figure 30. Temperature Measurement Circuit

instrumentation section since these are the two main heat sources and are most apt to experience high temperature conditions.

High Level Signal Conditioning.

Potentiometers. The potentiometer (POTs) require the simplest signal conditioning. A typical schematic is shown in Figure 31. Excitation voltage will be connected to the fixed taps of the POT with the wiper going to the filter. Since the POTs will be used to measure angular positions with full-scale ranges from 27 to 199 degrees, several excitation voltages will be used. These voltages, some of which are tabulated on Figure 31, will be connected to the pots through 200 ohm resistors that will protect the power to the other circuits if a short should occur. The Spectrol Model 142 POT has an effective range of 300 degrees with a center tap at 150 degrees. All POTs will have an end-to-end resistance of 10K ohms.

Bilevel Inputs. Figure 32 represents a typical bilevel digital-to-analog converter (DAC). It converts six TTL compatible signals to an analog signal, which is then fed to a presampling filter. Using a 6-bit DAC in the LRE is recommended to maintain a good safe drift and noise margin. The approximate state separation is 78 millivolts and is considered more than sufficient to successfully sense, capture, and analyze the system's bilevel inputs. The hierarchy of "hook-up" should be such that the most important bilevel input signals should be attached to the most significant bit DAC inputs.

Low Level Signal Conditioning. Figure 33 shows the circuit to be used to perform the signal conditioning function for all low-level transducers and bridge circuits. It is designed so that a single printed circuit board layout can accommodate a variety of excitation voltage and amplifier gain requirements with only resistor value and strap option changes. The resistors in series with the excitation voltages are included to protect against a possible short circuit affecting other channels. The analog switch will be activated by the computer during calibration procedures. The instrumentation amplifier shown is a National Semiconductor Model LM163. It is a monolithic unit, with pin programmable gains of 10, 100, and 1000, and

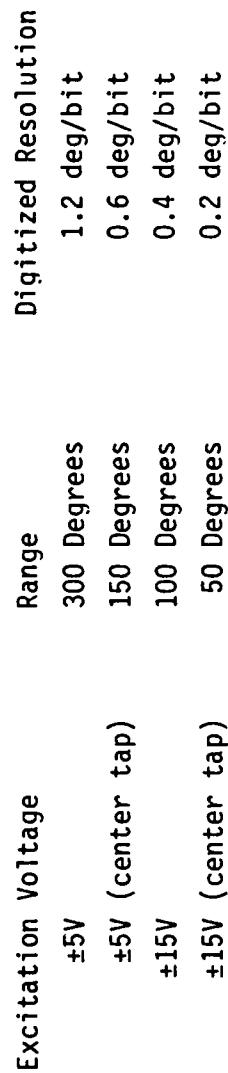


Figure 31. Typical Potentiometer Signal Conditioning

Device shown is a
Precision Monolithics'
DAC-01 or DAC-206

BILEVEL INPUTS

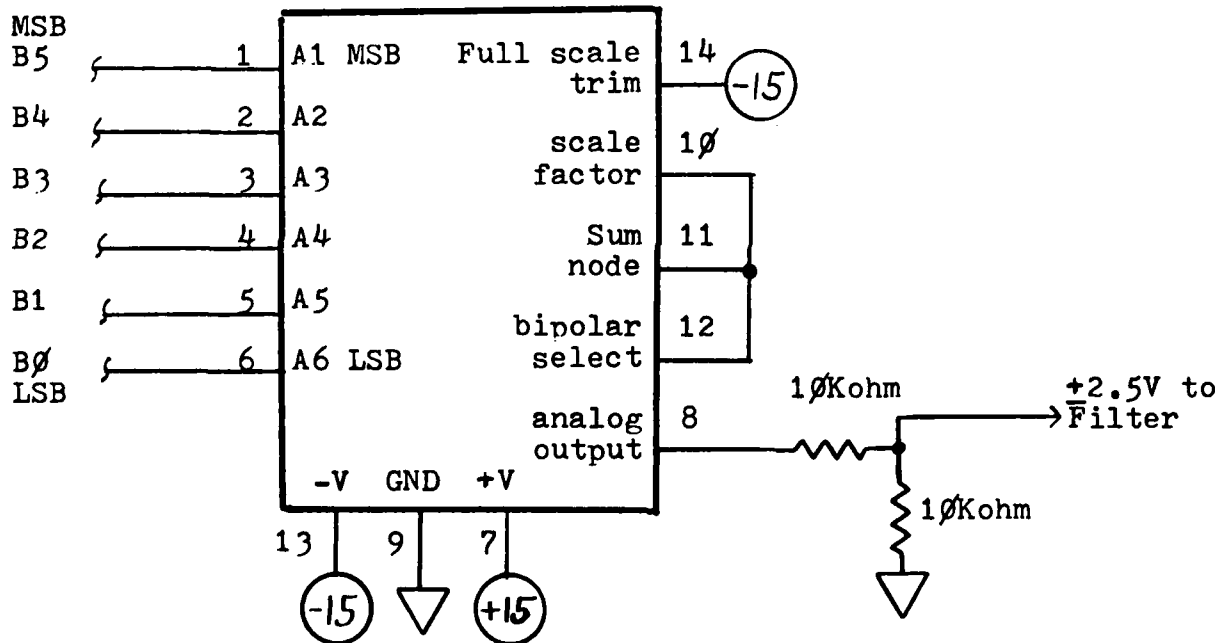


Figure 32. Typical Bilevel-to-Analog Converter

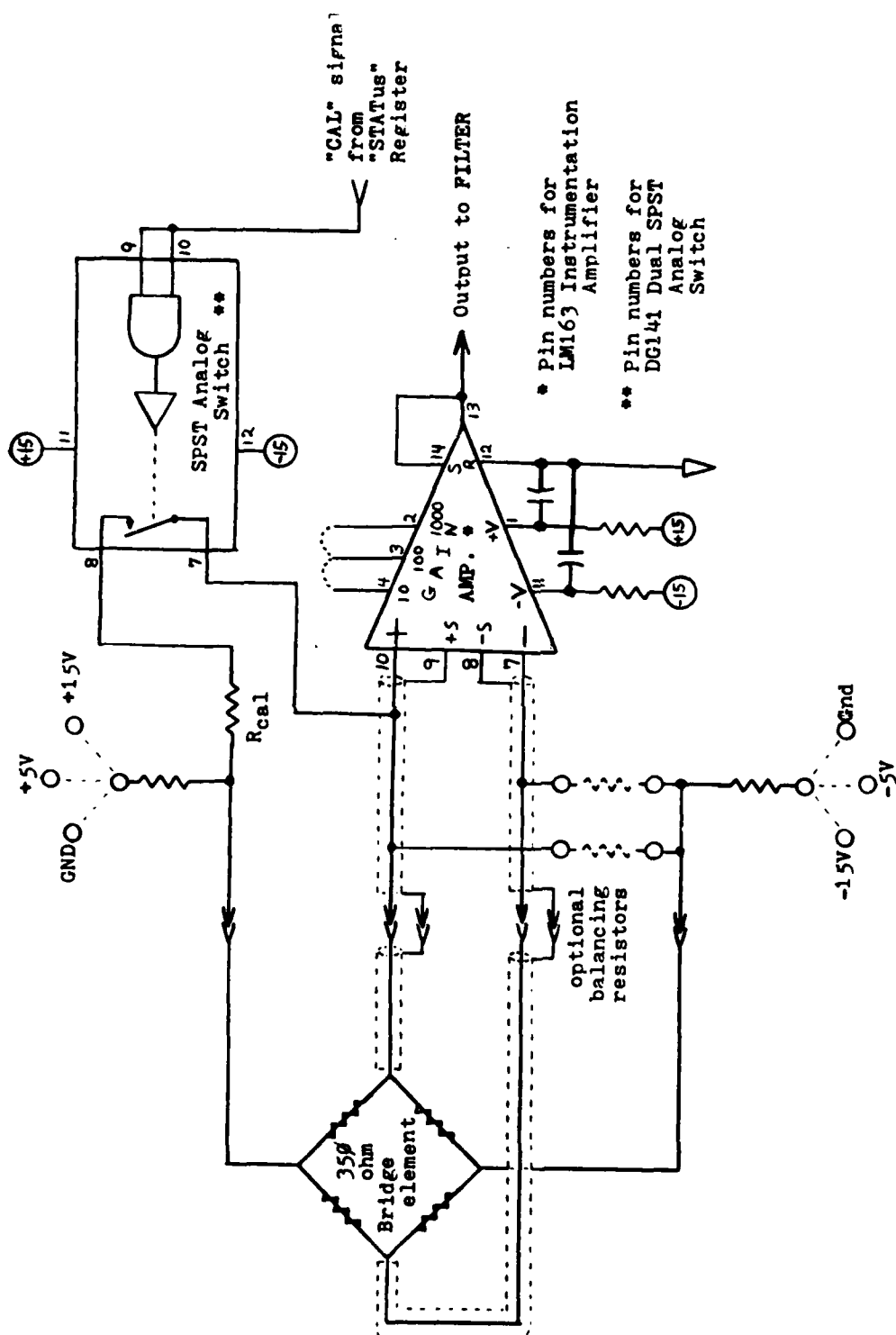


Figure 33. Typical Low-Level Signal Conditioning Circuit

intermediate values obtained by using external resistors. Its features are listed as follows:

- Low nonlinearity: 0.005 percent ($G = 10$ & 100), 0.007 percent ($G = 1000$)
- High CMMR: 130 db ($G = 1000$)
- Low offset voltage: $25\mu V$ ($G = 1000$)
- Low offset voltage drift: $0.5\mu V/^{\circ}C$ ($G = 1000$)

The features could be obtained only recently, with larger and more costly hybrid amplifiers. Analog Devices' AD524 and Burr Brown's INA101 are instrumentation amplifiers with similar excellent specifications that should be considered before finalizing this circuit design.

Signal Filtering. The presample filtering previously discussed will be used on every channel. This filter function will be implemented by National Semiconductor MF-6 ICs. These are single 6-pole Butterworth filters packaged in 14-pin dual-inline-packages (DIPs). The only external components required are two resistors to adjust the offset voltage to zero. Each filter also requires an external clock with a frequency that sets the filter cut-off (3 db down) frequency point. Since all the filters will have the same characteristics, only one external clock source will be required. This is a convenient feature if it is ever desired to change the cut-off frequency of the filters; one change of the clock source changes all the filters simultaneously. At this time, the MF-6 ICs are expected to be available in the first quarter of 1983. Several contingency devices are currently available. Using one or two 20-pin National Semiconductor MF-10 ICs or by using one 20-pin Reticon R5622 IC, two, four, six, and eight pole low-pass filters can be implemented.

• Pulse Code Modulator (PCM) System

Three manufacturers of PCM modules were found whose products have very similar specifications, prices, and delivery. They are all field programmable, expandable, and can output the desired NRZ-L format. Table 6 lists some specifications of the representative PCM modules. After examining the

TABLE 6. PULSE CODE MODULATION SYSTEMS, GENERAL SPECIFICATIONS

Operating Temperature	-10°C to +70°C
Storage Temperature	-54°C to +100°C
Humidity	0 to 95 percent nonconditional
Altitude	No limit
Shock	1000 Gs, 11 msec duration
Vibration	10 Gs, 50 Hz to 2K Hz
Acceleration	50 Gs, 5 minutes
Volume	10 to 20 inches cubed
Delivery	6 months
Cost (each)	\$12K to \$14.5K
Bit Rate	1 MBPS
Accuracy	0.4 percent

Note: All three representative systems met the electrical specifications as set forth in the System Description portion of this report.

specifications, it was not possible to select a clearly superior or most cost-effective system. In an attempt to resolve the situation, each of the vendors were requested to submit a list of names of users to be contacted so actual field performance information could be evaluated. All three vendors responded and four users of each manufacturer's equipment were contacted. The results of this survey are summarized below:

- No significant negative remarks were received on the performance. All could be expected to perform as specified.
- No consensus on a favored manufacturer.
- No manufacturer (except the three used in the survey) were mentioned favorably.
- The only negative comments received regarded delivery times with all three manufacturers receiving about equal shares.

Although the survey did not single out a preferred PCM source, it did provide assurance that any selection will provide acceptable hardware. The recommended course of action is to issue a request for quotation (RFQ) and select the best source based on delivery and price. The RFQ should include the specific number and type of inputs (96 high level channels) and the environmental specifications listed in Table 6. It should also include a request for specific data regarding the unit's capability to include a major frame count in the output data stream. This last feature will provide a direct means of synchronizing data acquired at separate telemetry receivers.

Data Capture

- Telemetry

The NRZ-L encoded PCM output will be the input to a modified UHF transmitter. The PCM output signal must be linear-phase filtered, and it must be amplitude adjustable for in-the-field transmitter matching purposes. The output of the transmitter will be connected to a skull mounted antenna. One such antenna is the Tecom Industries Model 109006 or 109007.

When operating under the "telemetry" conditions, it is imperative that all guidelines as set forth by IRIG Standard 106-80 are strictly followed. This will insure proper operation, at minimum expense, of the LRE system at the rocket sled range.

- LRE Memory

The LRE memory, simply stated, is the on-board computer system. This local storage function will be accomplished by a typical microprocessor system having the normal architecture of CPU, program memory, data memory, and input/output (I/O) interfaces, all communicating over a common bus controlled exclusively by the CPU. This system will be contained in a rigid card cage. The printed circuit boards will be approximately 4 inches wide by 5 1/2 inches high, and will implement all board interconnections via a motherboard with "Eurocard" standard 96-pin DIN connectors.

- g. 8111 FTA EMI Output Terminal Module
- h. 4400 BPK Enclosure

The overall efficiency of this power will be 40 percent, requiring 50 watts of power from the battery to supply 20 output watts. The size of this converter is 4.05 x 5.05 x 1.55 inches. The total current demanded of the LRE battery is:

RAM/Sig. Cond.	1.8 amps
Transmitter	1.0 amps
PCM	0.2 amps
3-Axis Gyro	0.9 amps

The gyro package will be mounted in the seat, but will be powered from the LRE. A 20-minute capacity would provide sufficient operating time from 1 or 2 minutes before sled blast off until the safety crew gets to the LRE after ejection. This sets the battery capacity at 1.2 amp hours. However, this goal is not met by a 1.2 amp/hour Ni-Cad battery because capacity is lost at higher discharge rates and at elevated temperatures. A 2.2 amp/hour Ni-Cad loses 15 percent capacity at the 3.9 amp discharge rate and 40 percent if operated at 120°F. The result is an effective 1.1 amp/hour battery which is close to the desired goal. A Gould, Inc., Model MP608 modular pack meets this requirement. This nominal 28.8 volt battery measures 7.1 x 7.2 x 1.9 inches and weighs 90 ounces.

Auxiliary Equipment

The LRE instrumentation requires external support to be an effective system. A means to display selected channels after conversion in the PCM module must be provided. This capability permits calibration of transducers when installed on the LRE, which is mandatory for the potentiometers measuring joint positions. It would also be valuable to be able to perform a quick check of all parameters before a sled run test. Since the LRE contains a rechargeable battery, some means of recharging is required. Also, since the instrumentation contains on-board data, some means of retrieving and storing is necessary. Two additional pieces of equipment will be

LRE Power Supply

An estimate of power required for the signal conditioning and local circuit storage is shown in Table 7.

TABLE 7. POWER REQUIREMENTS

Component	Required Voltage			
	+5	-5	+12	-12
Local Storage	1350 ma	--	12 ma	12 ma
Potentiometers	4 ma	36 ma	116 ma	84 ma
Filters (96)	768 ma	768 ma	--	--
Amplifiers (32)	--	--	64 ma	64 ma
Digital Sum	1.35 amps	--	--	--
Analog Sum	0.77 amps	0.8 amps	0.19 amps	0.16 amps

Since the power source will be a 28 volt battery, a DC-DC converter is necessary to supply these regulated voltages. No single converter was found that could meet these requirements. Further complicating the effort is the fact that the battery is only nominally 28 volts; its output will vary between 24 and 32 volts. Most DC-DC converters have an input voltage specification of 28 ± 2 volts which is not satisfactory. A custom modular power supply manufactured by Powercube Corporation was found to meet all requirements. It is made up of submodules that can be selected for specific applications. The items listed below are those required to form a complete DC-DC converter to supply all the power needs of the signal conditioning and local storage circuits.

- a. 20SP50/S1-S2 Switching Preregulator 23-36 volts inch
- b. 20G90W 40 High Frequency Generator
- c. 5TR30 ± 5 Volt Output Regulator (Digital)
- d. 4TRC10 ± 5 Volt Output Regulator (Analog)
- e. 15TRC10 ± 15 Volt Output Regulator (Analog)
- f. 2100 FTA EMI Input Terminal Module

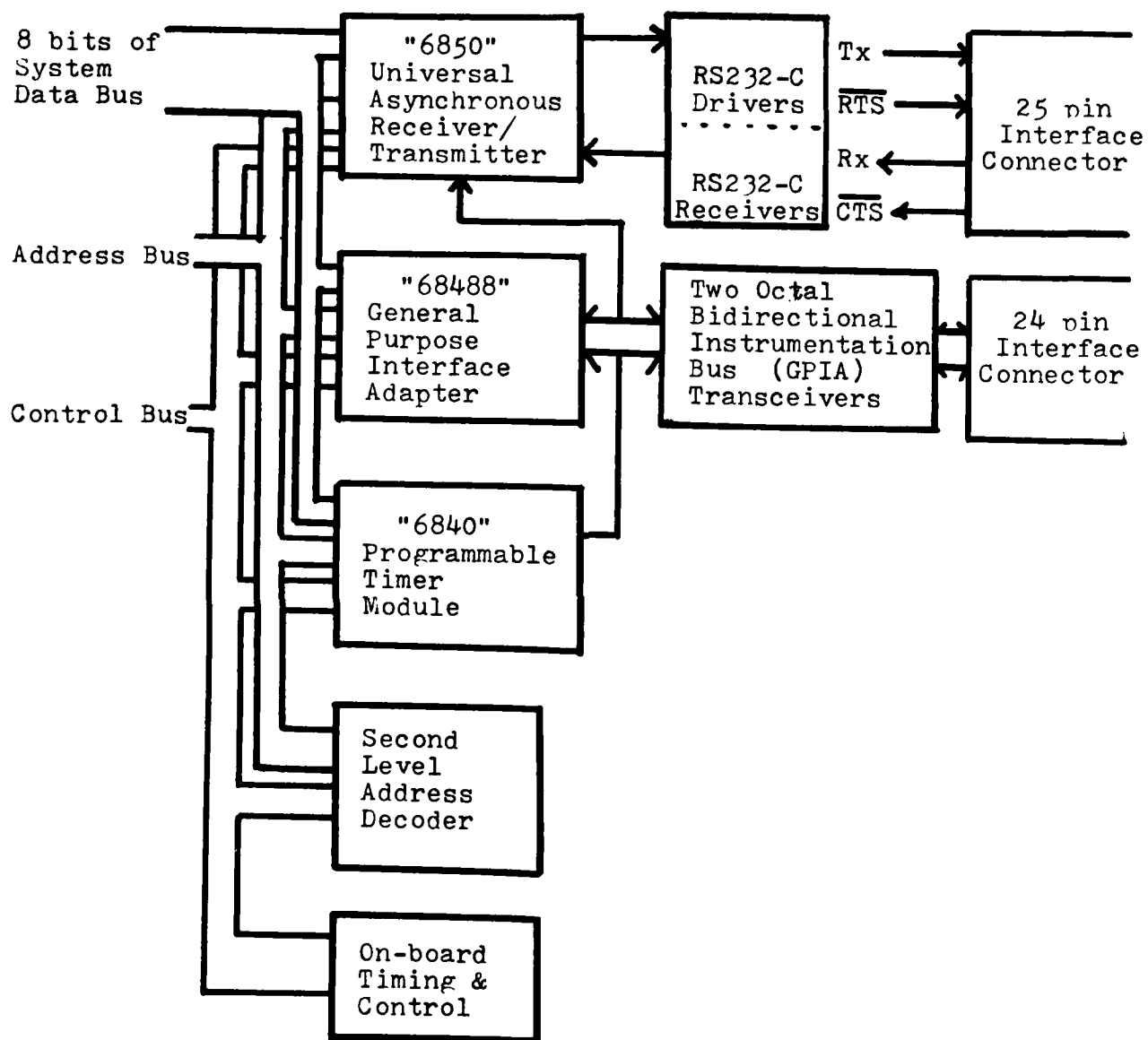


Figure 39. Typical COMMunications Board

the "start data" signal, "frame" and "bit" clocks, and other external mode and system status inputs. Timing and control circuitry, located on the processor board in the address decoder and interface controller section, assert the DTACK signal for the input status register.

The 16 bit output status register consists of two octal latches which are written into when in the write mode and when the STATCS is asserted. Timing and control circuitry, located on the processor board in the address decoder and interface controller section, assert the DTACK signal for the output status register. Four of the output status register signals are tied to one of the bilevel-to-analog converters to provide status information to the PCM. This status information will be used primarily during the "Rocket Sled" tests, where the status will be transmitted, via telemetry, for system status analysis prior to a "launch."

The other eight bilevel inputs to the two bilevel-to-analog converters receive their data from bilevel sensors within the LRE and in the seat. More bilevel-to-analog converters can be added as required.

Communications Board. Figure 39 presents a block diagram for the communications (COMM) board showing principal elements and support circuitry for nontelemetry communications between the LRE on-board computer system and all external systems. The key devices are a universal asynchronous receiver/transmitter (UART) for serial communications, and the general purpose interface adapter (GPPIA) which implements the high speed IEEE 488 parallel port communications. These two 6800 family devices, with the "6840" programmable timer module (PTM), require some special control and bus circuitry. The 6800 devices on this board have 8 bit data bus structures, and are synchronous bus compatible. The 68000 CPU bus, on the other hand, is an asynchronous bus system and it has a 16 bit data bus. The 6840 PTM contains three software controllable 16 bit counters which have numerous functions. A few purposes for the PTM in this system include the baud rate generator for the 6850 UART, the power-up 1-minute timer, and serving as a timekeeper during initialization diagnostics. All devices used on this board are industry standard parts and are readily available.

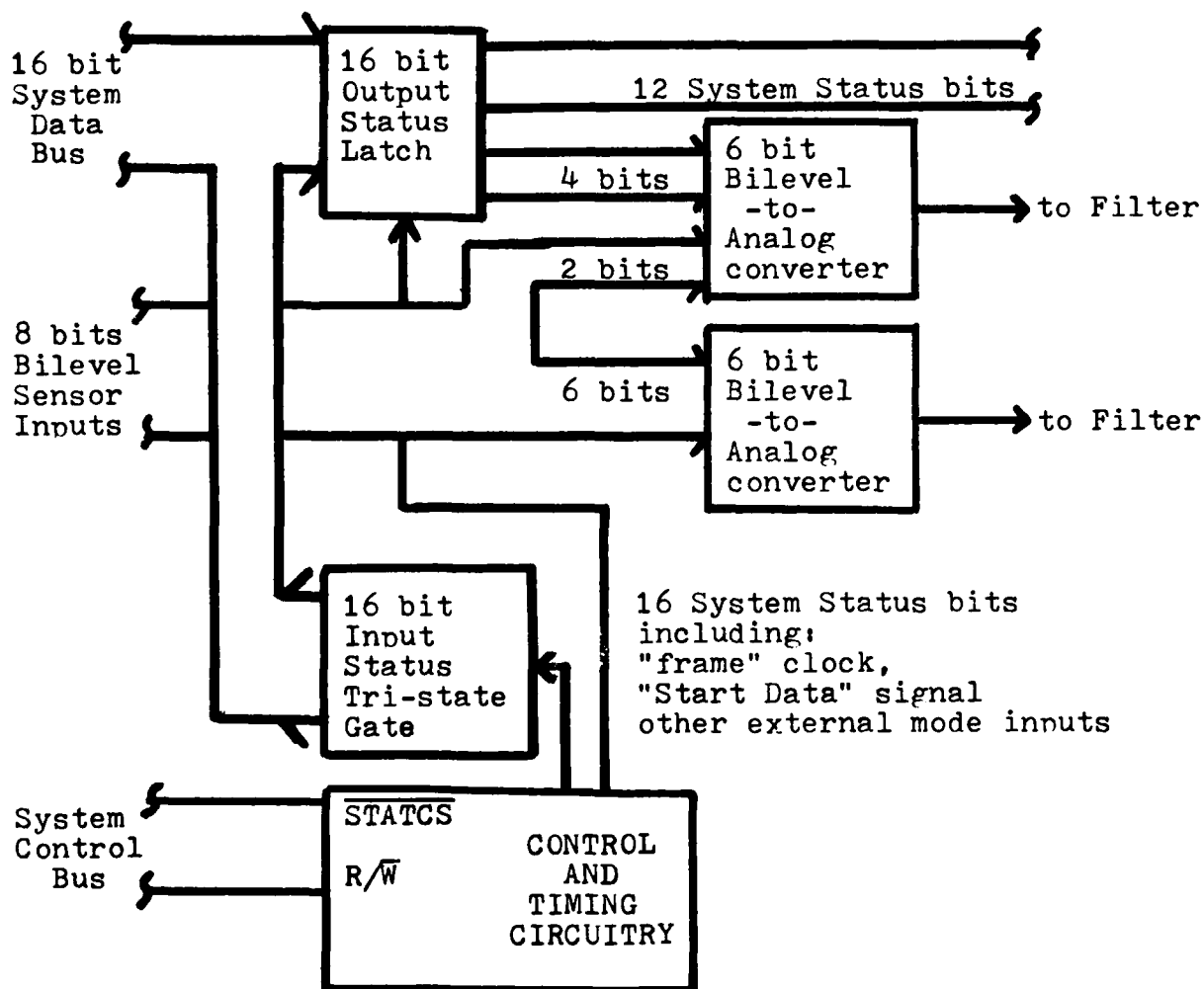


Figure 38. PCM Decoder, Status Registers

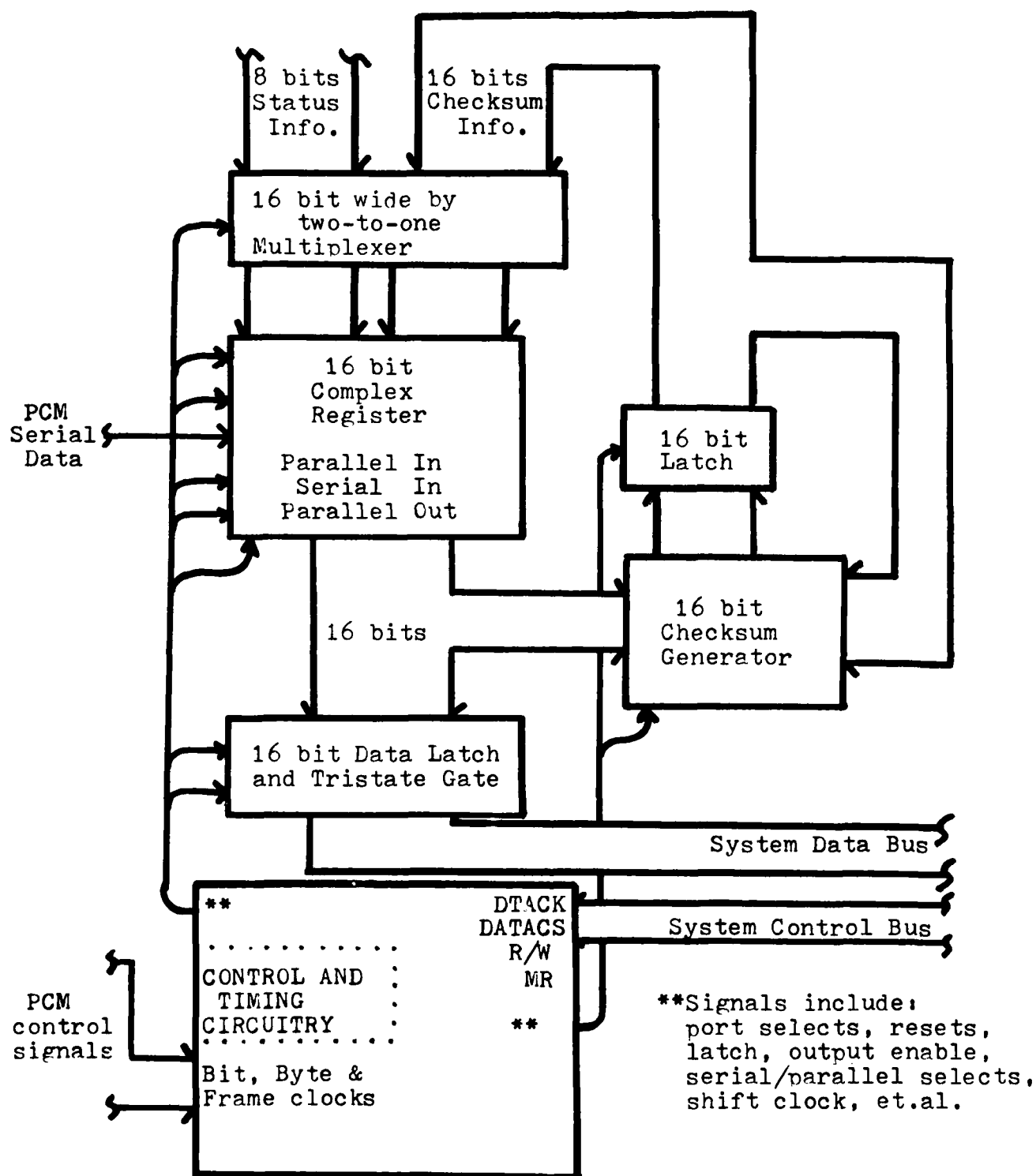


Figure 37. PCM Decoder, Serial-to-Parallel Converter

parallel data words. Other functions found on this board include input and output status registers, a status bilevel-to-analog converter, a bilevel sensor signals to analog converter, a checksum generator, and associated control and timing circuitry. Because the PCM unit has not yet been selected, the actual form of the signals and control lines is unknown. Therefore, this board is presented in block diagram form only. Most of the board circuitry can be implemented using CMOS logic.

Serial to parallel converter operation is depicted in Figure 37. During sensor data reception (96 eight-bit bytes), the "complex" register clocks in PCM serial data using the PCM provided "bit" clock. When two "byte" clocks have been received, the data is latched. If the incoming DATACS is asserted and a read attempt is in progress, then the latch outputs are bus enabled, placing PCM data on the system data bus, and DTACK is asserted. Each time PCM data are latched, the checksum value is updated.

When the frame clock signal is received, the 8 bit frame count and the first byte of the "Barker" synchronization code are serial shifted in from the PCM unit. At this time, the "Barker" code byte is overwritten with one byte of system status information. The 16 bits of frame count and status information are then latched without updating the checksum value. It is then sent to the CPU in the same manner as the sensor data discussed above. Note that the "frame" clock is also used to synchronize the pairs of "byte" clocks being received from the PCM unit.

The next two byte clocks indicate that the last two of the three "Barker" code synchronization bytes have been serially clocked into the complex register. At this time, both bytes of the "Barker" code are overwritten with 16 bits of sensor data checksum information. When it is latched, the checksum generator will be cleared to zero for the next frame of PCM data, and the checksum value will be sent to the CPU in the same manner as the sensor data discussed above.

Status register operation is depicted on Figure 38. The 16 bit input status register consists of two octal tri-state gates which are read when in the read mode and when STATCS is asserted. Typical inputs to the CPU include



DP8409 based upon the current state of the 68000 CPU, and it generates \overline{DTACK} signal for the DRAM to CPU handshaking. It also develops the upper and lower byte column-address strobe output signals (\overline{CASL}) & (\overline{CASU}).

When using the 64 pieces of the 64K bit DRAM ICs, \overline{CASL} & \overline{CASU} are buffered by the 20-pin DP84244 octal Tri-state MOS drivers. If only one board of the 256K bit DRAM ICs is used (256K word array), then the DP84244 can be eliminated, if so desired, and the \overline{CASL} & \overline{CASU} lines from the DP84322 can directly drive the DRAM ICs.

The 20-pin DP84300 is a programmable refresh timer. As shown, it generates a refresh command once every 15.5 μ sec, derived from the system's 8 MHz clock. As shown, the DRAM controller board can drive a DRAM array board(s) populated with either the 64K bit or the 256K bit DRAM ICs with no changes necessary. The DP84300 can be replaced with a fixed count divider network, if it will save room and power, after the system design is tested.

DRAM Array Board. The DRAM array schematic shown in Figure 36 represents a "generic" DRAM array board for the LRE on-board computer system data memory. It can be populated with either 64K bit DRAM ICs or the future 256K bit DRAM ICs. The pin numbers shown are for the Motorola MCM6256 (256K bit DRAM) or the Mostek MK4564 (64K bit DRAM) parts for this particular example. If the 64K bit DRAMs are used, there is no A8 line, and pin #1 is left unconnected. $\overline{RAS0}$, from the DRAM controller board, is used for the first 256K words of DRAM memory. For future expansions, there is additional DRAM controller capability to drive up to a one-M word array with no wiring modifications (one $\overline{RAS\#}$ per 256K words of DRAM memory). $\overline{CAS1U}$ & $\overline{CAS1L}$ are used for the first 16 DRAM ICs, whether they are the 64K bit DRAMs or the 256K bit DRAMs. $\overline{CAS2U}$ & $\overline{CAS2L}$ would be used for the second 64K word DRAM array board and so on. The $\overline{CAS\#U}$ & $\overline{CAS\#L}$ lines would be jumper selected to pick-off the required signal from the bus.

PCM Decoder. The PCM decoder, as the name suggests, converts the NRZ-L serial data stream from the PCM unit into computer compatible 16-bit

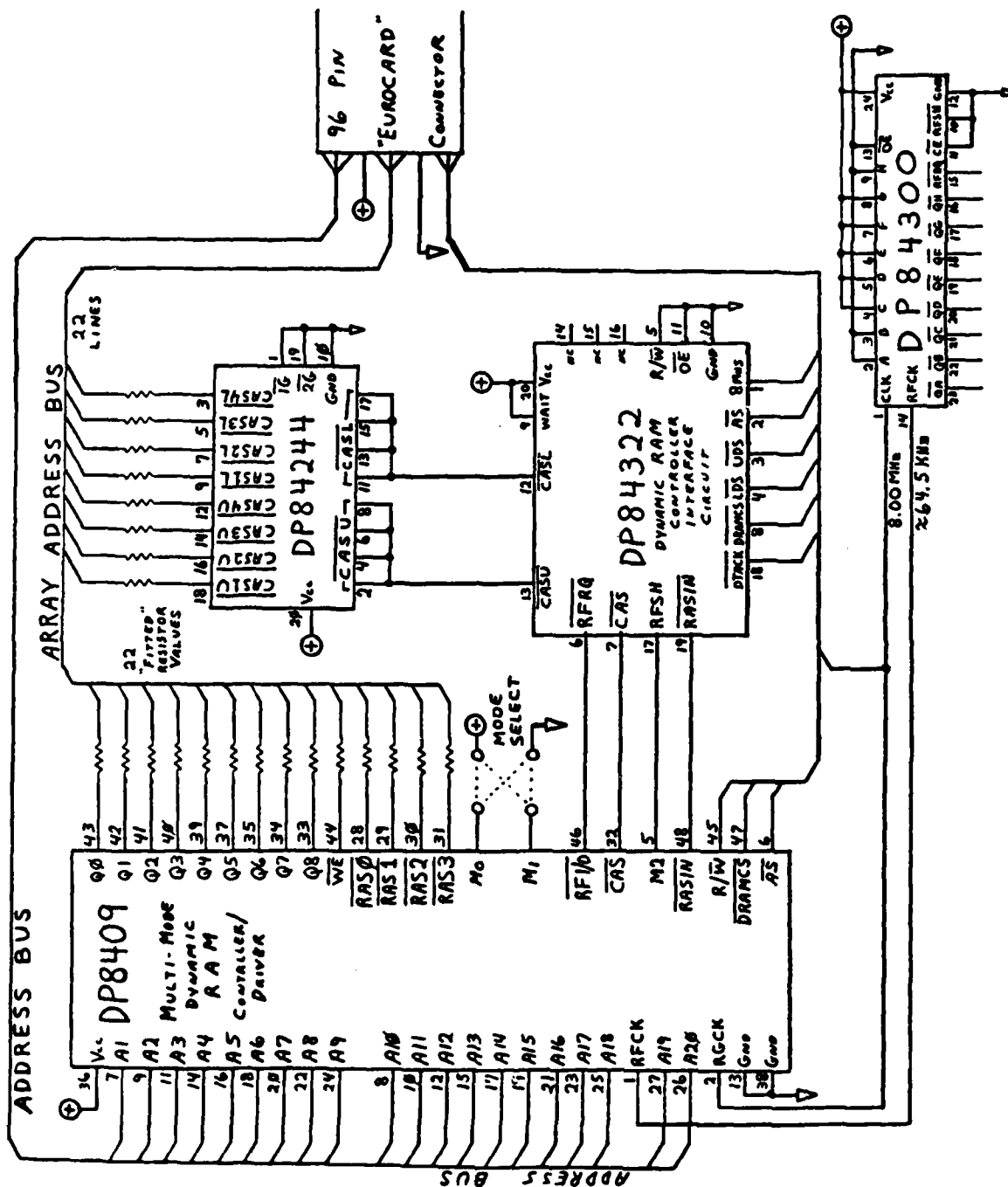


Figure 35. DRAM Controller Board

consists of three detectors which provide a master reset to the entire on-board computer system. A master reset is asserted following a successful power-up sequence, on an attempted access of an unused address, or when an apparent lack of valid bus activity is detected.

A 4K word nonvolatile memory (EPROM) contains all of the programming for all modes of operation. Depending on the "mode" of operation, a run-time program is transferred from the EPROM to the 1K word high speed static RAM cache memory for execution. In addition to the run-time program instructions, the cache memory contains "stacks," "queues," "scratch pad" memory, and other useful blocks of data. The address decoder and interface controller section develops "chip select" signals for the entire on-board computer system, as well as most of the system's handshaking control signals. Most of the signals present on the processor board are also connected to the "motherboard" via the 96-pin DIN (Eurocard) connector.

DRAM Controller Board. Figure 35 presents a typical DRAM controller board circuit. The National Semiconductor ICs reflect a four chip solution to a typical 30 IC problem. Texas Instruments, AMD, Motorola, Fairchild, and Intel also have IC sets that make it relatively easy to use dynamic RAM arrays. Simply stated, these four ICs provide all the necessary timing and control signals and the capacitive line drivers to interface any DRAM array to the 68000 CPU. The 48-pin DP8409, a multimode DRAM controller/driver, is the heart of the system. It is capable of directly driving up to 88 DRAM ICs of the 16k bit, 64K bit, and 256K bit configurations. This is beneficial in that the bench prototype system can be built using currently available 64K bit DRAM ICs, upgrading the system to 256K bit DRAM ICs when they become available, with no circuitry changes. This LSI device provides all critical timing functions, improved system performance, great reduction in the number of required ICs, lower cost, and improved reliability through the reduction of interconnections.

The 20-pin DP84322, a programmable logic array, is the specific device that allows easy interface between the DP8409 and the 68000 CPU. Among other functions, the DP84322 develops hidden and forced refresh signals for the

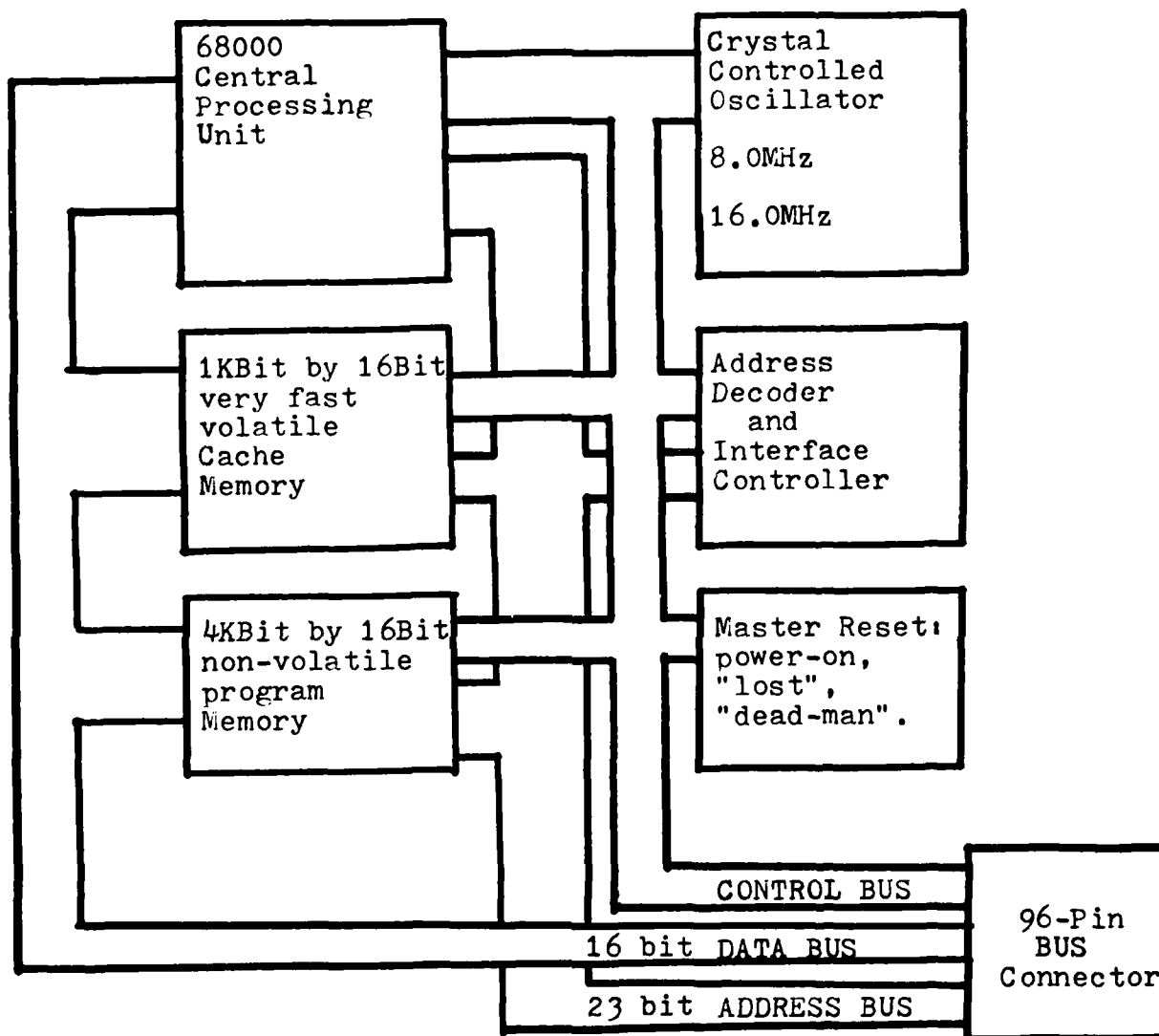


Figure 34. Typical LRE Computer System Processor Board Block Diagram

BNE	SKIP	*10	If not, skip next instruction.
MOV	A-2, A-1	*4	Reload A-1 with the first address in DRAM.
SKIP	DBF D-1, START	*10	Decrement value in D-1. If it is not zero (0), then branch back to "START."

The *(numbers) in the comment region of the above sequence are the clock cycles required to execute each instruction, which includes the single wait period inserted in each DRAM cycle. The 44 cycles at the 8 MHz clock speed yields a total execution time of 5.5 microseconds.

The 6850 and 68488 ICs that perform the serial and parallel interface functions are two of many devices available to perform these functions. The system designers should choose those with which they are most familiar. However, if the 6850 and 68488 ICs are selected, it may be desirable to increase the speed with which these peripheral chips are synchronized to the 68000 bus. This can be done by adding a few more ICs. The procedure is detailed in Motorola Applications Note 808.

The following are the conceptual (unfinished) designs for the processor board, DRAM controller board, DRAM array board(s), PCM decoder board, and the communication (COMM) board, in that order. As stated earlier, the design was carried only far enough to obtain a general idea of the scope of the task. From the design presentation, information was developed for the power and room requirements for the on-board computer system. Obviously, this information is likely to change, but any change should be minor.

Processor Board. The processor board is the heart of the on-board computer system. Figure 34 shows the primary elements of the processor board. All data manipulation, timing, control operations, and bus transfers are directly, or indirectly, controlled by the 16 bit 68000 CPU. All of the central bus activities are synchronized by the 8 MHz central clock, which is derived from a 16 MHz crystal clock oscillator. The master reset circuitry

It was stated earlier that the 68000 was selected as the CPU because of its internal architecture, which permitted the 256K word memory array to be addressed directly and without segmenting instruction. This is illustrated by the following "programming" example.

In this example, internal register A-1 contains the address of the DRAM location at which the next data sample will be stored. Initially, it could have any value between those contained in internal registers A-2 and A-3, depending on where the data was stored when the "Start Data" signal was received. Four additional internal registers are initialized with constant values prior to entry to the routine. Register A-2 would contain the first DRAM array address. Register A-3 would contain the last DRAM array address. Register A-4 would contain the address of the "DATA" register on the PCM decoder board. Register D-1 would contain a number equal to the total number of words (two 8-bit sensor bytes) to be collected. For example, if 96 sensors were being captured, with one byte of frame count information and with two bytes of checksum information, fifty 16-bit words would have to be stored per millisecond. Using the maximum DRAM array memory capacity without overwriting, 5.242 seconds worth of complete frames of information would yield a value of 262100_{10} to be loaded into register D-1.

The following five-instruction sequence is entered upon receipt of the "Start Data" signal, which occurs when the seat starts its upward movement for this example. If the "Start Data" signal is generated from the LRE separation from the seat (more like "Stop Data"), then the data collection period would be nearly over and the value in Register D-1 would be as small as that required to reflect that short period of time.

```
START  MOV    (A-4)(A-1)+  *14  Move data from the PCM port to the
                                location pointed to by A-1, then increment
                                register A-1.
```

```
      CMP    A-1, A-3      *6  Does A-1 now point past the end of
                                memory?
```

required to perform these and other tasks. The first is a portable, commercially available, personal computer. The second is a collection of power supplies, battery, and battery-charging circuits enclosed in a briefcase-size container.

- Portable Computer

An Osborne personal computer meets all the requirements for data retrieval, calibration data display, and quick testing of the data channels. It is a 32-pound briefcase-size computer that can be powered from external battery power. It includes a full ASCII keyboard, a 5-inch CRT, dual 5-inch floppy discs, and 64K byte of RAM. It also has RS-232 and GPIB ports that can be used for communication with the LRE microprocessor system.

The Osborne is easily capable of displaying any desired parameter(s) on the CRT during calibration, in raw form or in engineering units. It could check all channels quickly before a test to assure that all are in predefined limits that were earlier loaded on a disc file. Also, it could download the 1/2M byte of data from the LRE and store it on discs. Three discs would be required.

- Portable Power Unit

The auxiliary power unit will operate in two distinct modes: (1) performing different tasks when powered from a standard 110 volt line source, and (2) in a portable mode using internal battery power. When operating from standard line power, the auxiliary power unit must be able to perform the following two tasks simultaneously:

- a. Supply 28 VDC to the LRE for an extended period of time.
- b. Charge its internal battery and the LRE battery at variable rates as recommended by the manufacturer.

When operating without external power, the auxiliary unit must be able to perform the following two tasks simultaneously:

- a. From its internal battery, supply power to the LRE sufficient for 30 minutes of operation.
- b. From its internal battery, supply regulated power to the portable computer sufficient for 30 minutes of operation.

The front panel controls that will fix the mode of operation will consist of the following:

- a. An AC line power switch
- b. A three-position switch that controls power delivered to its LRE labeled AC, DC, and OFF.
- c. Two switches for selectively powering the LRE--one for the electronics, the other for the transmitter.
- d. Two position switches selecting high, medium, and low charge rates for its internal battery and the LRE batteries.
- e. A panel meter with an associated switch to select the 28 volt power supply, the charging current power supply, the LRE battery, or the internal battery.
- f. A power ON/OFF switch for the panel meter.

A simplified schematic of a preliminary design for this power unit is shown in Figure 40. The major components are listed in Table 8. The projected size is 21 x 13 x 6 1/2 inches with a total weight of 28 pounds.

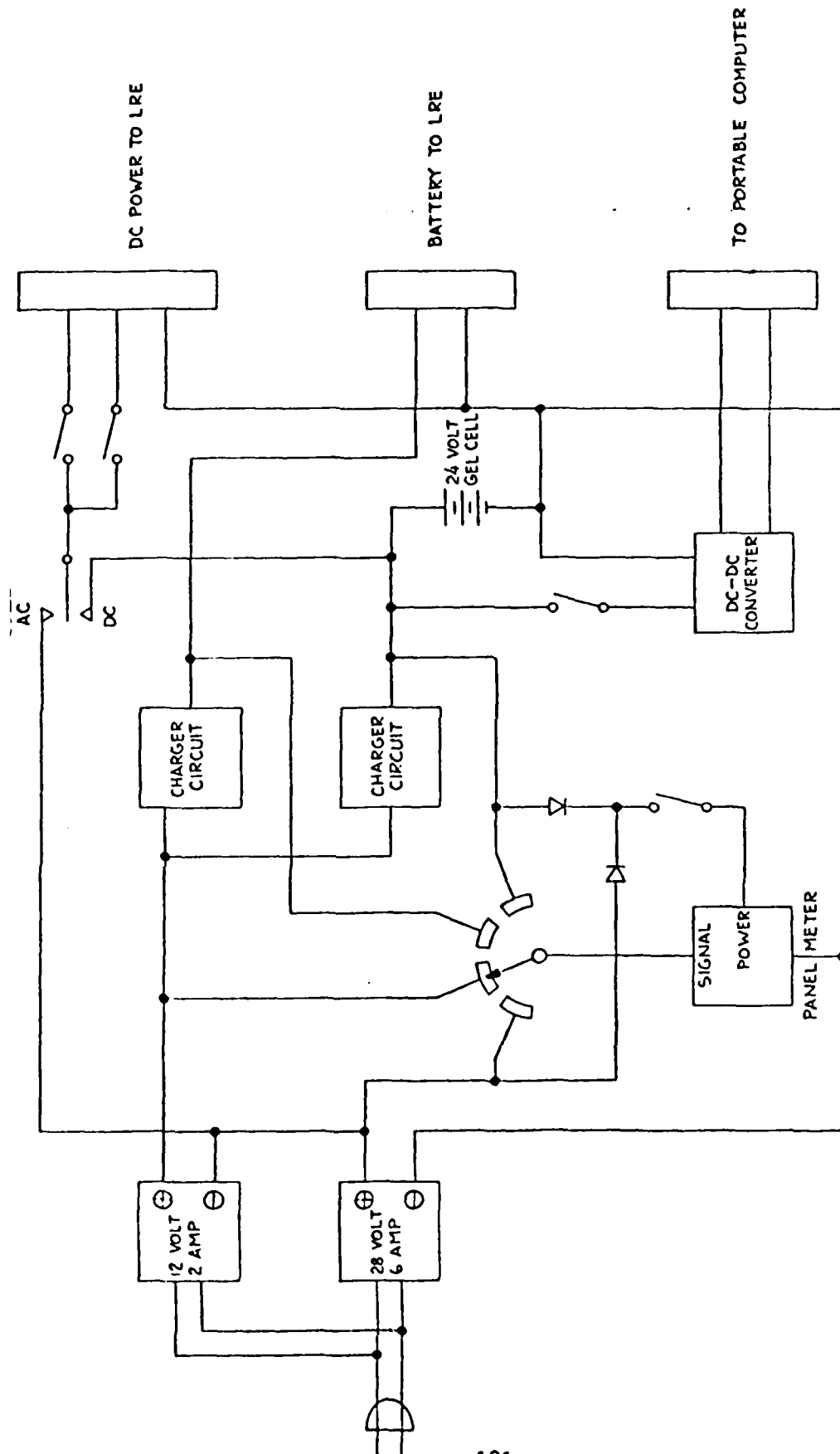


Figure 40. Schematic of Power Unit

TABLE 8. MAJOR COMPONENTS OF POWER UNIT

1	KEPCO RMK 28-B Power Supply 28 volts, 6.4 amps, 6 pounds 3.27 x 5.12 x 9.61 inches
1	KEPCO RMP 12-S Power Supply 12 volts, 2.5 amps, 3 pounds 1.38 x 5.12 x 6.38 inches
2	Gould Gelyte PBM1260 Battery 12 volts, 6.4 amps/hour, 4.6 pounds each 2.78 x 3.85 x 5.5 inches
1	Zero Case 105 4.1 pounds 13 x 21 x 6.5 inches
1	Datel Panel Meter DM 3100 U1
1	Tecnetics 3050-28-148 DC-DC converter, 2.25 pounds 4 x 4 x 1.8 inches

Section 3

CONCLUSIONS

The basic objective of the investigation was achieved through the formulation of a design approach for a system to evaluate the effectiveness of limb restraint devices to protect crewmembers during ejection from advanced aircraft. The Limb Restraint Evaluator (LRE) will survive the severe environment of an ejection and will simulate, to the degree required, the dynamic loads imparted to human limbs during the ejection. A preliminary design for a complete data acquisition system was developed to collect, sample, record, and transmit analog signals from over 50 transducers measuring loads, motions, and accelerations affecting the limbs and torso of the LRE.

The following specific conclusions were reached during the investigation:

- The LRE should represent the body characteristics of the 95th percentile male of the Air Force flying personnel.
- The LRE should utilize commercially available components for the head, upper thorax, pelvic unit, hands, and feet.
- Specialized arms and legs must be developed to properly represent the limb dynamic flail characteristics of the human body.
- A simple and reliable six-component balance system can be designed to measure the helmet/head loads during ejection.
- A modular joint design can be developed to represent the degrees of freedom of all pertinent body joints and limit the motions in each degree of freedom to those of the corresponding human joint.
- The electronic data acquisition system should be designed to provide the capability for up to 5 seconds of on-board storage, as well as real-time telemetering for all data channels.

- A data sample rate of 1000 samples/second should be used to cover the data frequency content of interest.
- A presampling six-pole filter with a cut-off frequency of approximately 138 Hz should be used to eliminate errors due to high frequency aliasing.
- Data reconstruction during recovery should utilize a four-point interpolation to minimize the reconstruction error in the sampled data.
- A possible problem of heat build-up in the LRE, from enclosed instrumentation, can be solved by controlled usage of the data system.
- An optimization analysis should be conducted to maximize the power usage/battery size once the complete data system requirements have been established.
- All transducers and instrumentation are state of the art and are readily available, or can be replaced with acceptable and available substitutes.

REFERENCES

- Bibbero, Robert J., 1977, Microprocessors in Instruments and Control, John Wiley & Sons, New York.
- Brand, John R., 1979, Handbook of Electronic Formulas, Symbols and Definitions, Van Nostrand Reinhold Co., New York.
- Burstein, A. H., Currey, J. D., Frankel, V. H., and Reilly, D. T., 1972, The Ultimate Properties of Bone Tissue: The Effects of Yielding, Journal of Biomechanics, Vol. 5, pp. 35-44.
- Buchsbaum, Walter H., 1973/1982, Buchsbaum's Complete Handbook of Practical Electronic Reference Data, Prentice-Hall, Inc., New Jersey.
- Clauser, C. E., McConville, J. T., and Young, J. W., August 1969, Weight, Volume, and Center of Mass of Segments of the Human Body, AMRL-TR-69-70, Aerospace Medical Research Laboratory, Wright-Patterson Air Force Base, Ohio.
- Cummings, R. J. and Dasata, F. E., June 1979, Exploratory Development of Aircrew Windblast Protection Concepts, AMRL-TR-79-16, Aerospace Medical Research Laboratory, Wright-Patterson Air Force Base, Ohio.
- Datel/Intersil, 1979, Data Acquisition and Conversion Handbook, page 11.
- Douglas Aircraft Company, ACES II Advanced Concept Ejection Seat, Report No. MDC J4576A.
- Engin, A. E., May 1981, Long Bone and Joint Response to Mechanical Loading, Interim Progress Report, April 1, 1980 - March 31, 1981, Ohio State University Research Foundation.
- Engin, A. E., April 1979, Measurement of Resistive Torques in Major Human Joints, AMRL-TR-79-4, Aerospace Medical Research Laboratory, Wright-Patterson Air Force Base, Ohio.
- Evans, F. G., 1973, Excerpts from: Mechanical Properties of Bones, C. C. Thomas, Springfield, Illinois.
- Evans, F. G., 1957, Excerpts from: Stress and Strain in Bones, C. C. Thomas, Springfield, Illinois.
- Gardenhire, W., April 1964, Selecting Sample Rates, ISA Journal.
- Garrett, Patrick H., 1978, Analog Systems for Microprocessors and Minicomputers, Reston Publishing Co., Inc., Virginia.
- Garrett, Patrick H., 24 May 1977, Optimize Transducer/Computer Interfaces, Electronic Design.
- Giacoletto, L. J. (Ed.), 1977, Electronic Designer's Handbook, McGraw-Hill Book Co., New York.

Gordon, Bernard M. and Seaver, William H., Practical Sampled-Data Theory for the Instrumentation Engineer, Epsco, Inc.

Grood, E. S., Noyes, F. R., and Butler, D. L., October 1978, Knee Flail Design Limits: Background, Experimentation, and Design Criteria, AMRL-TR-78-58, Aerospace Medical Research Laboratory, Wright-Patterson Air Force Base, Ohio.

Hawker, F. W. and Fuler, A. J., June 1976, Wind Tunnel Measurements of Vertical Acting Limb Flail Forces and Torso/Seat Back Forces in an ACES II Ejection Seat, AMRL-TR-76-3, Aerospace Medical Research Laboratory, Wright-Patterson Air Force Base, Ohio.

Hawker, F. W. and Fuler, A. J., July 1975, Extended Measurements of Aerodynamic Stability and Limb Dislodgement Forces with the ACES II Ejection Seat, AMRL-TR-75-15, Aerospace Medical Research Laboratory, Wright-Patterson Air Force Base, Ohio.

Hight, T., January 1981, Long Bone Injury Criteria for Use with the Articulated Total Body Model, AFAMRL-TR-81-3, Air Force Aerospace Medical Research Laboratory, Wright-Patterson Air Force Base, Ohio.

Hoerner, S. F., 1965, Fluid Dynamic Dummy, Hoerner Fluid Dynamics, New Jersey.

Horner, T. W. and Hawker, F. W., May 1973, A Statistical Study of Grip Retention Force, AMRL-TR-72-110, Aerospace Medical Research Laboratory, Wright-Patterson Air Force Base, Ohio.

Jacob, J. Michael, 1982, Applications and Design with Analog Integrated Circuits, Reston Publishing Co., Inc., Virginia.

Jung, Walter G., 1979, IC Op-Amp Cookbook, Howard W. Sams & Co., Inc., Indiana.

McConville, J. T. and Churchill, T. D., December 1980, Anthropometric Relationships of Body and Body Segment Moments of Inertia, AFAMRL-TR-80-119, Air Force Aerospace Medical Research Laboratory, Wright-Patterson Air Force Base, Ohio.

Metzger, Daniel L., 1982, Electronics Pocket Handbook, Prentice-Hall, Inc., New Jersey.

NASA Reference Publication 1024, July 1978, Anthropometric Source Book: Volume I, Anthropometry for Designers; Volume II, Handbook of Anthropometric Data, Volume III, Annotated Bibliography of Anthropometry.

Newhouse, H. L., Payne, P. R., and Brown, J. P., December 1980, Wind Tunnel Measurements of Total Force and Extremity Flail Potential Forces on a Crewmember in Close Proximity to a Cockpit, AMRL-TR-79-110, Aerospace Medical Research Laboratory, Wright-Patterson Air Force Base, Ohio.

Oppenheim, Alan V. and Willsky, Alan S., 1983, Signal and Systems, Prentice-Hall, Inc., New Jersey.

Payne, Inc., October 1980, Sub- and Transonic-Wind Tunnel Measurements of the Forces Acting on a Crewmember and His Seat in Simulated Escape from an Aircraft, Final Report, Contract F33615-79-C-0527.

Payne, Inc., June 1976, Wind Tunnel Measurements of Vertical Acting Limb Flail Forces and Torso/Seat Back Forces in an ACES II Ejection Seat, AMRL-TR-76-3, Aerospace Medical Research Laboratory, Wright-Patterson Air Force Base, Ohio.

Payne, Inc., July 1975a, Low-Speed Aerodynamic Forces and Moments Acting on the Human Body, AMRL-TR-75-6, Aerospace Medical Research Laboratory, Wright-Patterson Air Force Base, Ohio.

Payne, Inc., July 1975b, Stability and Limb Dislodgement Force Measurements with the F-105 and ACES II Ejection Seats, AMRL-TR-75-8, Aerospace Medical Research Laboratory, Wright-Patterson Air Force Base, Ohio.

Payne, Inc., July 1975c, Extended Measurements of Aerodynamic Stability and Limb Dislodgement Forces with the ACES II Ejection Seat, AMRL-TR-75-17, Aerospace Medical Research Laboratory, Wright-Patterson Air Force Base, Ohio.

Payne, P. R., May 1974a, On the Avoidance of Limb Flail Injury by Ejection Seat Stabilization, AMRL-TR-74-9, Aerospace Medical Research Laboratory, Wright-Patterson Air Force Base, Ohio.

Payne, P. R., December 1974b, Some Studies Relating to "Limb Flailing" After an Emergency Escape from an Aircraft, AMRL-TR-73-24, Aerospace Medical Research Laboratory, Wright-Patterson Air Force Base, Ohio.

Payne, P. R. and Band, E. G. U., August 1971, Development of a Dynamic Analog Anthropomorphic Dummy for Aircraft Escape System Testing, AMRL-TR-71-10, Aerospace Medical Research Laboratory, Wright-Patterson Air Force Base, Ohio.

Payne, P. R. and Hawker, F. W., May 1974, USAF Experience of Flail Injury for Noncombat Ejections in the Period 1964-1970, AMRL-TR-72-111, Aerospace Medical Research Laboratory, Wright-Patterson Air Force Base, Ohio.

Phillips, N. S., Carr, R. W., Wittman, T. J., Scranton, R. S., December 1973, An Investigation of Automatic Restraint and Body Positioning Techniques, AMRL-TR-71-101, Aerospace Medical Research Laboratory, Wright-Patterson Air Force Base, Ohio.

Reilly, D. T. and Burstein, A. H., 1975, The Elastic and Ultimate Properties of Compact Bone Tissue, Journal of Biomechanics, Volume 8, pp. 303-405.

Rockwell International, June 1980, Aircrew Windblast Protection Concepts, Final Report.

Savant, C. J., Jr., 1964, Control System Design, McGraw-Hill Book Co., New York.

Schmitt, T. J., January 1954, Wind Tunnel Investigation of Air Loads on Human Beings, Report 892 Aero 858 (AD 491-201), Navy Department, The David Taylor Model Basin Aerodynamic Laboratory.

Schneck, D. J., 1978, Aerodynamics Forces Exerted on an Articulated Human Body Subjected to Windblast, Aviation Space and Environmental Medicine, 49(1), pp. 183-190.

Stencil Aero Engineering Corporation, May 1979, Prototype Development, Passive, Seat-Mounted, Limb Retention System, NADC-79-201-60, Naval Air Development Center, Pennsylvania.

Tow, Julius T., 1975, Digital and Sampled-Data Control Systems, McGraw-Hill Book, Co., New York.

Zuch, Eugene L., 1979, Data Acquisition and Conversion Handbook, Boston: Datel Intersil.

END

FILMED

5-85

DTIC